Water Resources and Dynamics of the Troodos Igneous Aquifer-system, Cyprus

- Balanced Groundwater Modelling -

Doctorate Thesis
submitted at the
Julius-Maximilians University of Würzburg

by

Joachim Mederer

from

Heilbronn

Würzburg 2009

Grundwasserdynamik und Ressourcen des Troodos Aquifersystems, Zypern

- Bilanzierte Grundwassermodellierung -

Dissertation zur Erlangung des
naturwissenschaftlichen Doktorgrades
der Bayerischen Julius-Maximilians Universität Würzburg

von

Joachim Mederer

aus

Heilbronn

Würzburg 2009

Abstract

The study investigates the water resources and aquifer dynamics of the igneous fractured aquifer-system of the Troodos Mountains in Cyprus, using a coupled, finite differences water balance and groundwater modelling approach. The numerical water balance modelling forms the quantitative framework by assessing groundwater recharge and evapotranspiration, which form input parameters for the groundwater flow models. High recharge areas are identified within the heavily fractured Gabbro and Sheeted Dyke formations in the upper Troodos Mountains, while the impervious Pillow Lava promontories - with low precipitation and high evapotranspiration - show unfavourable recharge conditions. Within the water balance studies, evapotranspiration is split into actual evapotranspiration and the so called secondary evapotranspiration, representing the water demand for open waters, moist and irrigated areas. By separating the evapotranspiration of open waters and moist areas from the one of irrigated areas, groundwater abstraction needs are quantified, allowing the simulation of single well abstraction rates in the groundwater flow models.

Two sets of balanced groundwater models simulate the aquifer dynamics in the presented study: First, the basic groundwater percolation system is investigated using two-dimensional vertical flow models along geological cross-sections, depicting the entire Troodos Mountains up to a depth of several thousands of metres. The deeply percolating groundwater system starts in the high recharge areas of the upper Troodos, shows quasi stratiform flow in the Gabbro and Sheeted Dyke formations, and rises to the surface in the vicinity of the impervious Pillow Lava promontories. The residence times mostly yield less than 25 years, the ones of the deepest fluxes several hundreds of years. Moreover, inter basin flow and indirect recharge of the Circum Troodos Sedimentary Succession are identified. In a second step, the upper and most productive part of the fractured igneous aquifer-system is investigated in a regional, horizontal groundwater model, including management scenarios and inter catchment flow studies. In a natural scenario without groundwater abstractions, the recovery potential of the aquifer is tested. Predicted future water demand is simulated in an increased abstraction scenario. The results show a high sensitivity to well abstraction rate changes in the Pillow Lava and Basal Group promontories. The changes in groundwater heads range from a few tens of metres up to more than one hundred metres. The sensitivity in the more productive parts of the aquifer-system is lower. Inter-catchment flow studies indicate that - besides the dominant effluent conditions in the Troodos Mountains - single reaches show influent conditions and are sub-flown by groundwater. These fluxes influence the local water balance and generate inter catchment flow.

The balanced groundwater models form thus a comprehensive modelling system, supplying future detail models with information concerning boundary conditions and inter-catchment flow, and allowing the simulation of impacts of landuse or climate change scenarios on the dynamics and water resources of the Troodos aquifer-system.

Kurzfassung (German summary)

Die vorliegende Arbeit untersucht die Grundwasserressourcen und die hydraulische Dynamik des Troodos Kluftaquifersystems in Zypern mit Hilfe gekoppelter numerischer Wasserhaushalts- und Grundwasserströmungsmodelle auf Rasterbasis. Die Wasserhaushaltsmodelle quantifizieren die hydrologischen Rahmenparameter des Untersuchungsgebietes. Grundwasserneubildung und Evapotranspiration werden als Eingangsparameter der Grundwassermodelle weiterverarbeitet. Die Grundwasserneubildung ist in den niederschlagsreichen Regionen des höheren Troodos Gebirges, im Bereich der stark geklüfteten Gabbro und Sheeted Dyke Lithologien, am höchsten, nimmt zu den Vorgebirgen ab und erreicht dort ein Minimum in den gering durchlässigen Pillow Lava Sequenzen. Die Evapotranspiration zeigt einen umgekehrten Trend. Zusätzlich zur aktuellen Evapotranspiration wird eine sogenannten Sekundär-Evapotranspiration ermittelt, die sich – unabhängig von der Bodenfeuchte – aus der Verdunstung von Wasser-, Feucht- und Bewässerungsgebieten berechnet. Dieses Konzept erlaubt die Ermittlung der Verdunstungsmenge der bewässerten Flächen und somit die Abschätzung regionaler Grundwasserentnahmeraten, die als Brunnenentnahme in die Grundwassermodelle eingearbeitet werden.

Mit zweidimensionalen, bilanzierten, vertikalen Grundwassermodellen, die entlang geologischer Schnitte durch das Untersuchungsgebiet verlaufen, wurde die Grundwasserströmung bis zu einer Tiefe von mehreren Kilometern hoch auflösend simuliert. Die generelle Strömungscharakteristik zeigt eine dominierende Vertikalkomponente in den Neubildungsgebieten des hohen Troodos, quasi stratiforme Strömung in den Mittelläufen im Bereich der Gabbros und Sheeted Dykes, und einen relativen Anstieg des Potentials und Grundwasserausfluss im Bereich der geringdurchlässigen Pillow Laven der Vorgebirge. Indirekte Neubildung durch Grundwasser aus dem Troodos kann in den überlagernden Sedimenten nachgewiesen werden, ebenso wie Lateralflüsse zwischen den Einzugsgebieten. Die Grundwasserverweildauer liegt meist bei wenigen Jahrzehnten. Ausnahmen bilden tiefe Strömungen aus dem hohen Troodos, die Verweilraten von mehreren Jahrhunderten erreichen.

Der oberflächennahe, stark geklüftete und für die Wasserwirtschaft wichtige Teil des Aquifersystems wurde in einem horizontalen, den gesamten Troodos umfassenden Grundwassermodell nachgebildet. Bewirtschaftungsszenarien ohne bzw. mit gesteigerten Entnahmeraten simulieren die Dynamik dieses Aquifers. Die Ergebnisse zeigen, dass die Sensitivität auf die Änderung der Entnahmeraten regional sehr unterschiedlich ist. In den Entnahmegebieten des hohen und mittleren Troodos liegen die Spiegelschwankungen meist bei wenigen Metern bis Zehnermetern, während die Schwankungen in den gering durchlässigen und niederschlagsarmen Vorgebirgen teilweise mehr als hundert Meter betragen können.

Das laterale Strömungsverhalten wird in einzelnen Test-Einzugsgebieten im Troodos untersucht. Während in den Untersuchungsgebieten generell effluente

Grundwasserverhältnisse vorherrschen, gibt es Seitentäler, die vom Grundwasser unterströmt werden und die Grundwasser in benachbarte Einzugsgebiete abgeben. Diese Lateralflüsse können lokal die Wasserbilanz von Einzugsgebieten im Troodos beeinflussen. Die bilanzierten Grundwassermodelle illustrieren sowohl die Tiefenströmung mit hoher Auflösung als auch den oberflächennahen, wasserwirtschaftlich interessanteren Teil des Troodos - Kluftaquifersystems und zeigen die großflächigen Auswirkungen von Änderungen der Grundwasserentnahmerate.

Die bilanzierten Grundwassermodelle stellen somit ein Übersichtsmodellsystem dar, mit Hilfe dessen Randbedingungen und Lateralflüsse für zukünftige Detailmodelle bestimmt, sowie Auswirkung künftiger Klima- bzw. Landnutzungsänderungen auf die Dynamik und die Grundwasserressourcen des Troodos Aquifersystems abgeschätzt werden können.

Acknowledgments

First of all, I wish to thank Prof. Dr. Peter Udluft for sharing his hydrogeological experience and supervising my scientific work on the semi-arid island of Cyprus for many years. Without his valuable assistance, friendly advice and ongoing motivation this study would not have been possible.

Many thanks go to Armin Dünkeloh for his encouraged technical support concerning the latest versions of MODBIL, for proof reading and numerous scientific discussions. Your work is very much appreciated!
I would like to thank the partners of the GRC-project for supporting my studies, especially, Dr. Christoph Külls for sharing his experience and for many technical advices, and Prof. Dr. Jörg Schaller and staff.
I am very grateful to the scientific personnel of the Geological Survey Department of Cyprus for supporting my work and for data supply. Special thanks go to the head of the Hydrogeological Section Dr. Maria Charalambous and Dr. Costas Constantinou for their substantial cooperation and splendid team spirit, to Christos Christophi for detailed information on the subject, to Mr. George Petridis, former Director of the GSD, for his concern and motivating thoughts and to Dr. Antonis Charalambides and staff for supporting my laboratory work.
I wish to thank all the Cypriot farmers in the Pitsilia area for supporting my field work in a very hearty and friendly way.

I am very grateful to the Faculty for Geosciences of the University of Würzburg for granting a scholarship and financing part of my scientific studies.
Many thanks to Sonja Wahler for text review and improvement of the English phrasing.
I would like to thank all my colleagues of the Department of Hydrogeology and Environment of the University of Würzburg, especially Dr. Heike Wanke, Bernhard Schäffers, Dr. Mohammad Al Farajat and Dr. Holger Mainardy for manifold scientific discussion, valuable advices and support, and enjoyable coffee breaks.
Last not least I would like to express cordial thanks to my parents for supporting me and my studies in many ways.

Table of content

Appendices

List of figures

List of tables

1 Introduction

Water is one of the most precious goods on our planet and constitutes a fundamental heritage for every generation. (…) We have, therefore, an obligation towards improving its quality, its management on a national level and its proper use.

Timis Efthimiou (Dec. 2003), Minister of Agriculture, Natural Resources and Environment of Cyprus

A highly variable semi-arid climate controls the water resources of the Eastern Mediterranean island of Cyprus, producing episodically recurring droughts (KAMPANELLAS ET AL., 2003). Mitigation measures had to be invented to face the re-occurring water shortages. Rain water storage and open conveyor systems have been used since pre-Christian times. The chain of wells (*Laoumia, Qanats*), a tapping system for underground water, allowed the diversion and extraction of groundwater and was crucial for the water supply of the major cities till the end of the Turkish rule in the 19th century (e.g. Larnaka; KAMPANELLAS ET AL., 2003). The expansion of irrigation and water supply works in the beginning of the 20th century and the introduction of diesel pumps increased the water consumption of the island. As a consequence, extensive groundwater abstractions in the lowlands depleted the first class aquifers and led to salt water intrusion in the coastal regions.

In the second half of the 20th century, the focus of water supply shifted towards the Troodos Mountains, designated as the "water tower of the island" (AFRODISIS ET AL., 1986) due to high precipitation rates. Large storage and distribution systems were constructed conveying water, stored in dams and ponds in the Mountains, to irrigation schemes. Enhanced drilling techniques allowed large-scale prospection for groundwater and hydrogeological investigations within the ophiolitic rocks.

At the end of the 20th century, water conflicts and the implementation of EU water legislation led to a systematic assessment of the water resources of Cyprus. To this end, several technical cooperation projects were implemented (e.g. WDD-FAO project, EU-LIFE project "KYPROS"). In the frame of the project "Re-evaluation of the Groundwater Resources of Cyprus" (GRC-project), the Geological Survey Department of Cyprus (GSD) and the University of Würzburg in Germany have assessed the groundwater resources quantity and quality wise for the whole island, including water balance and groundwater flow investigations in the Troodos.

Based on the results of the GRC-project (Chapter 1.2), the present study deepens the investigations of the "water tower of the island" by simulating the dynamics of the

fractured aquifer-system using a coupled groundwater flow and water balance modelling approach. For the first time, the Troodos Mountain Range as a whole is modelled as a single groundwater basin.

The geographical and geological terminology used in this study is based on the official Geological Map of Cyprus (Geological Survey Department, 1995). Coordinates are indicated in the Universal Transverse Mercator (UTM) system, Zone 36 North, based on the WGS84 ellipsoid model.

1.1 Problem statement and objectives of the study

Increasing water demand in times of decreasing precipitation rates aggravates water conflicts on the island of Cyprus. Additionally, pollution threatens (ground-)water quality in the vicinity of settlements and agricultural areas. The Troodos region, with high precipitation and comparably small human impact, becomes more and more relevant to mitigating these conflicts. Discharge of the rivers in the Troodos generates inflow to dams and ponds, supplying both local communities and large irrigated areas in the lowlands. Additionally, the Troodos rivers recharge the major gravel aquifers in the lowlands and are important for the restoration of coastal aquifers affected by salt water intrusions. Due to the manifold storage and surveyor projects and a dense network of gauging stations, the surface water system of the Troodos is being understood quite well. Discharge characteristics of important catchments and lithologies are described by UDLUFT ET AL. (2003).
Groundwater exploration and investigations of the groundwater system have been intensified since the 1980s (Chapter 1.3). Since then, groundwater has become the major source for water supply of the Troodos villages. Therefore, a systematic scientific investigation of the Troodos aquifer-system and its dynamics is crucial for a sustainable management of these resources. In this context, investigations within the GRC-project (Chapter 1.2; UDLUFT ET AL., 2003) form a landmark. In this project, hydrophysical properties of the single lithologies were determined Troodos-wide. Groundwater recharge dynamics were modelled for single catchments and for the Troodos region with a numerical water balance modelling approach. Conceptual groundwater models simulated the groundwater flow characteristics along geological cross-sections of the Troodos Mountains. BORONINA ET AL. (2003) established a groundwater model of the Kouris catchment, which is the major drain of the upper Troodos to the south.

The present study developed in the frame of the GRC-project, resumes and reworks part of the water balance and groundwater flow studies, and expands the groundwater model to the extent of the igneous Troodos aquifer-system. It forms thus a quasi holistic aquifer model including balanced in- and outflow volumes, the simulation of the deep percolating fluxes as well as the fast draining fluxes in the upper, most productive part of the aquifer-system.

The main objectives of study are the following:

- Estimation of groundwater recharge, evapotranspiration and groundwater abstraction rates by water balance modelling.
- Characterisation of the principle flow dynamics including supra-regional, deeply percolating fluxes in vertical, cross-sectional groundwater models.
- Establishing groundwater management scenarios and simulation of the lateral groundwater flow dynamics of the entire Troodos igneous aquifer-system.

1.2 Project framework

The presented study is based on the scientific-technical cooperation project "Re-evaluation of the Groundwater Resources of Cyprus" (GRC), conducted from spring 2001 to autumn 2004. The GRC-project has been financed by the Ministry of Agriculture, Natural Resources and Environment (Cyprus), performed by the Department of Hydrogeology and Environment (Prof. P. Udluft, University of Würzburg, Germany), Hydroisotop (Dr. C. Külls, Germany), Planning Bureau Prof. Dr. J. Schaller (Germany) and supervised by the Geological Survey Department (Cyprus). The project database ENVIS and the GIS database, compiled by the Planning Bureau Prof. Dr. J. Schaller, are the major sources for mapping-, meteorological-, and hydrogeological data used in this study. The water balance and part of the groundwater flow investigations are based on specific investigations within the GRC-project (UDLUFT, 2002B; UDLUFT ET AL., 2003, 2004A, 2004B, 2004C). An improved version of the water balance modelling programme MODBIL (Chapter 3.1) was used to re-estimate the water balance of the study area. The cross-sectional flow models, developed within the GRC project are re-worked using the re-estimated water balance parameters.

1.3 State of hydrogeological research in the Troodos

Although the Troodos Ophiolite has been subject of manifold geological investigations (Chapter 2.3), the importance for groundwater supply and thus for hydrogeological investigations had not been recognised till the late 1970s. BURDON (1955) describes the Troodos as a highly fractured aquifer, the UNDP project (UNITED NATIONS, 1970) in contrast, mapping for the first time the occurrence of groundwater in Cyprus in a systematic way and assessing water balances for the major aquifers, classifies the Troodos as impervious. In 1976, the Geological Survey Department started a comprehensive drilling programme for groundwater exploration in the Troodos, setting the base for further hydrogeological investigations. Hydrochemical studies were conducted in a technical cooperation programme by the German Federal Ministry of Economic Cooperation and

Development (BMZ) (BMZ project no. 1975.2019.0 and 1981.2224.4). WAGNER ET AL. (1987; 1990) and ZOMENIS ET AL. (1988) describe the groundwater quality, and the suitability of the existing groundwater resources for domestic supply and for irrigation as important results of these projects. AFRODISIS ET AL. (1986) indicates the importance of the Troodos for the water supply of the island. AFRODISIS & FISCHBACH (1988) published studies on the mineral waters in the Troodos region. Isotope investigations in the Troodos were carried out by BORONINA ET AL. (2005) and described in several technical reports of UDLUFT & KÜLLS (2003), VERHAGEN ET AL. (1991) and JACOVIDES (1979). Within the LIFE project groundwater contamination due to asbestos mining activities in the upper Troodos were assessed (CHARALAMBIDES ET AL., 1998). Water balance investigations, including a first numerical water balance model of the Kouris catchment in the Troodos, were conducted within the project Groundwater Recharge in the Eastern Mediterranean (GREM-project; KÜLLS ET AL., 1998; UDLUFT, 2002A; ZAGANA ET AL., 2007). A technical cooperation project between the Food and Agriculture Organisation of the United Nations (FAO) and the Water Development Department of Cyprus (WDD) determined ground- and surface water resources and water demand of selected Troodos catchments and the Troodos igneous aquifer (KLOHN, 2002). BORONINA ET AL. (2003) investigated the groundwater resources of the Kouris catchment using numerical groundwater modelling. In the frame of the GRC-project (Chapter 1.2) distribution and dynamics of water balance parameters of single catchments and the complete Troodos region were assessed with numerical water balance models (UDLUFT ET AL., 2003; DÜNKELOH, 2005A; MEDERER, 2005). Numerical cross-sectional groundwater models describe the principle flow dynamics of the Troodos igneous aquifer (UDLUFT ET AL., 2004B, MEDERER & UDLUFT, 2004A; MEDERER & UDLUFT, 2004B). Detailed investigations on the water balance dynamics of the Troodos are conducted by DÜNKELOH (2009).

2 Study area

The study area comprises the Troodos Mountains and the Lemesos Forest in the south-eastern part of the island of Cyprus (Fig. 4), covering the igneous lithologies of the Troodos Ophiolite surrounded by a "buffer" of the Circum Troodos Sedimentary Succession (Fig. 5, Chapter 2.3). The study area is bordered by the Mediterranean Sea to the west and the south east, by the Mesaoria plain to the north, and by foothills of the Lemesos and Pafos region to the south. It extents from 448700 m E to 545200 m E and 3839550 m N to 3894800 m N (UTM zone 36 North; WGS84). With an area of 2925 km², the study area covers nearly one third of the island.

2.1 Terrain and land cover

The Troodos Mountains reflect the ellipsoidal dome-structure of the Troodos Ophiolite with the Mount Olympos (1952 m.a.m.s.l.) as the highest elevation, both of the study area and Cyprus. The high mountainous part covers most of the study area. It is deeply dissected, so that subordinate ranges veer off at many angles forming steeply incised valleys. The mountains descend in a series of stepped foothills to the borders of the study area, except for the western Troodos, where they slope downwards steeply to the coastline.
The major streams of Cyprus rise in the Troodos forming a perennial, radial drainage system. The catchments are usually narrow with short tributaries in the study area. Gradients and turnover volumes are high. The distance from source to mouth is mostly less than 100 km. Perennial riparian vegetation in the igneous part of the Troodos indicates predominant effluent flow conditions. Downstream, within the sediments of the Circum Troodos Sedimentary Succession (Fig. 5), the flow conditions become influent. The Troodos rivers form thus an important source for indirect recharge of the gravel aquifers in the lowlands. Mostly, the infiltration length is long enough for total runoff infiltration and outflow to the sea is restricted to heavy rain events. Dry up in the lower reaches is aggravated by numerous reservoirs and ponds for surface water storage in the Troodos, and by groundwater recharge dams for the lowland gravel aquifers.

UDLUFT ET AL. (2002) describe the land use and plant cover of the study area in a very detailed way. Although deciduous trees in the floodplains are very indicative for predominant effluent groundwater conditions, they cover only small parts of the study area. Pine forest of mostly open character, maquis and garigue in the understory prevail in moderately elevated parts of the study area, especially in the western Troodos. The pines are mostly calabrian pine *(Pinus brutia)*, replaced by black pine *(Pinus nigra ssp. pallasiana)* in high mountainous regions, locally cyprus cedar *(Cedrus libani ssp. brevifolia)* or aleppo pine *(Pinus halepensis)*. In low precipitation or low temperature regions, the number of pines in the association diminishes, so that maquis dominates the

foothills and the high mountainous regions. In this areas, tall shrub communities of the endemic golden oak *(Quercus alnifolia)*, strawberry tree *(Arbutus andrachne)*, terebinth *(Pistacia terebinthus)*, kermes oak *(Quercus coccifera)* and styrax *(Styrax officinalis)* are found. Garigue of compact and open character grows mainly in the uncultivated, poor and dry parts of the lowlands of the study area, e.g. in the sedimentary foothills and on the alkaline soils of the Pillow Lava formations (Fig. 5).

The soils in the study area are typical Mediterranean soils, characterised by a deficient in humus due to retardation of chemical weathering. Undeveloped, shallow A-C profile soils (Regosols) prevail. Colluvial deposits have developed at the bottom of moderately inclined slopes, especially in the Gabbro and Sheeted Dyke regions. With exception of the calcareous, fine grained soils in the promontories, the soils are skeleton rich, coarse grained and poorly graded and show high hydraulic conductivities and low to medium field capacities.

The population density is very variable. Settlements in the form of villages are abundant in the coastal zone, the Pitsilia, Commandaria and Solea region (Fig. 4). Large areas of the western, central and eastern Troodos are populated sparsely.

Agriculture is generally bound to the villages. Depending on climate, water supply and arability, different crops are cultivated. Vegetables, citrus and olive trees are mostly irrigated and prevalent in the lowlands and coastal regions of the western Troodos and in the vicinity of the major reservoirs. To a small extent, grains and olive trees are grown in the lowlands of the north eastern part of the study area. On moderately inclined limestone hills of the Commandaria region, viticulture is the dominant land use. Secondarily, viticulture is pursued on small and isolated terraces of the Troodos. Orchards (cherry, apple, almond and walnut) are widespread in the Solea and Pitsilia region, especially on the floodplains and flat depressions of the major streams. On the slopes of the Troodos Mountains they are usually cultivated on terraces, almonds up to an elevation of 1700 m.a.m.s.l. Irrigation is common in the lower elevated regions. Animal husbandry is practised in the Solea region on the banks of the Kargotis river (Fig. 4, Fig. 6). The land cover of the uppermost Troodos region is dominated by a closed down open cast mine for asbestos. The fallow mining terraces cover an area 2.2 km² and are currently under a state of restoration.

2.2 Climate

The climate in the study area is Mediterranean semi-arid, experiencing mild wet winters and dry hot summers. Variations in temperature and rainfall are controlled by altitude and, to a lesser extent, distance from the coast. Hot, dry summers from May to September and rainy, rather changeable winters from November to March are separated by short autumn and spring seasons. Precipitation ranges from 200 to 300 mm/a in the lowlands to more than 1000 mm/a in the upper Troodos. Due to the high mountainous topography, rain events often show a small-scale distribution, especially scattered showers and

thunderstorms, which typically occur during the summer season. The mean annual temperature reaches 18 to 20 °C in the coastal region and 12 to 15 °C in the upper Troodos, where snowfall in winter is common while lowlands generally are frost-free. Due to their importance for the water resources management, evapotranspiration rates are determined within the water balance modelling process of this study and are described in detail in Chapter 4.1.3.2. The potential evapotranspiration ranges between 800 and 1800 mm/a. The actual evapotranspiration yields 200 to 600 mm/a for most parts of the study area. In open water, irrigation or moist areas, water availability exceeds precipitation and reaches the order of magnitude of the potential evapotranspiration. The seasonal variability of the actual evapotranspiration is very pronounced. Highest values do not coincide with highest precipitation or highest potential evapotranspiration amounts. They occur in the short spring season when temperatures are already elevated, and soil moisture contents are still very high.

The intra annual fluctuation is shown in the climate classification for long-term monthly mean temperature and precipitation according to WANG & JÄTZOLD (1969) in Fig. 3. For the meteorological station Agros (Nr. 377-91; 1015 m.a.m.s.l.; time period: 10/1987 to 09/1997) situated in the upper Troodos, most “winter” months group in the humid, and most “summer” months in the arid category. This classification illustrates the briefness of the transition seasons, typically for the Mediterranean climate. Additionally, the intra-annual variability is visualized in two Walter climate charts for the coastal and high mountainous regions respectively (Fig. 1 and Fig. 2).

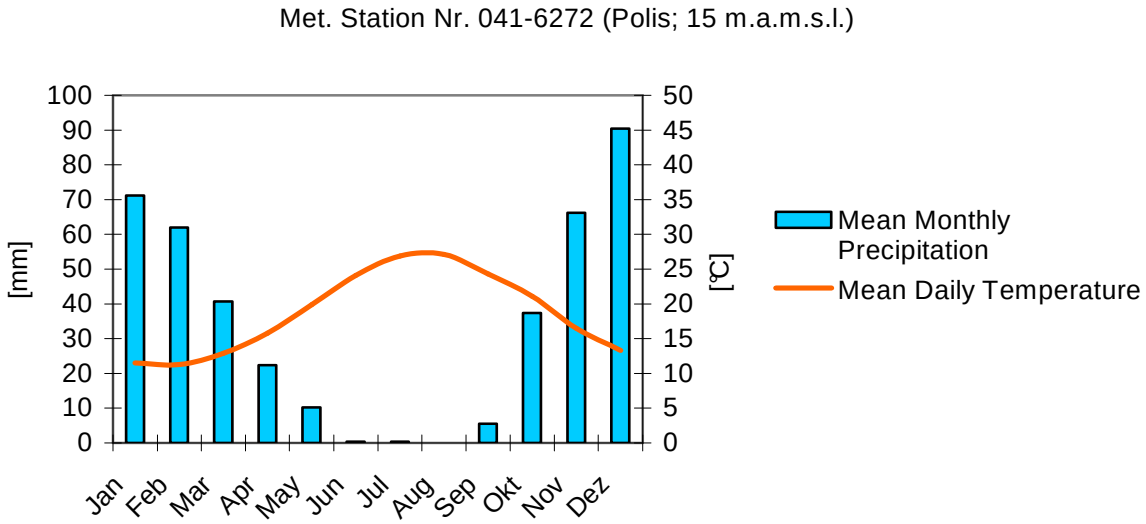

Fig. 1: Walter climatic chart for the coastal region in the western Troodos (time period: 10/1987 to 09/1997).

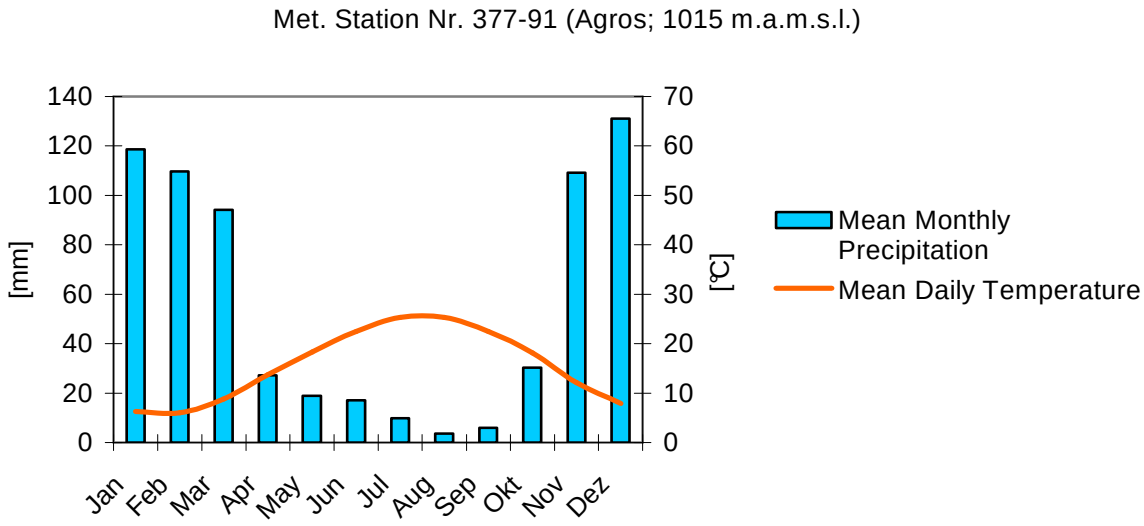

Fig. 2: Walter climatic chart for the high mountainous Pitsilia region in the central Troodos (time period: 10/1987 to 09/1997.

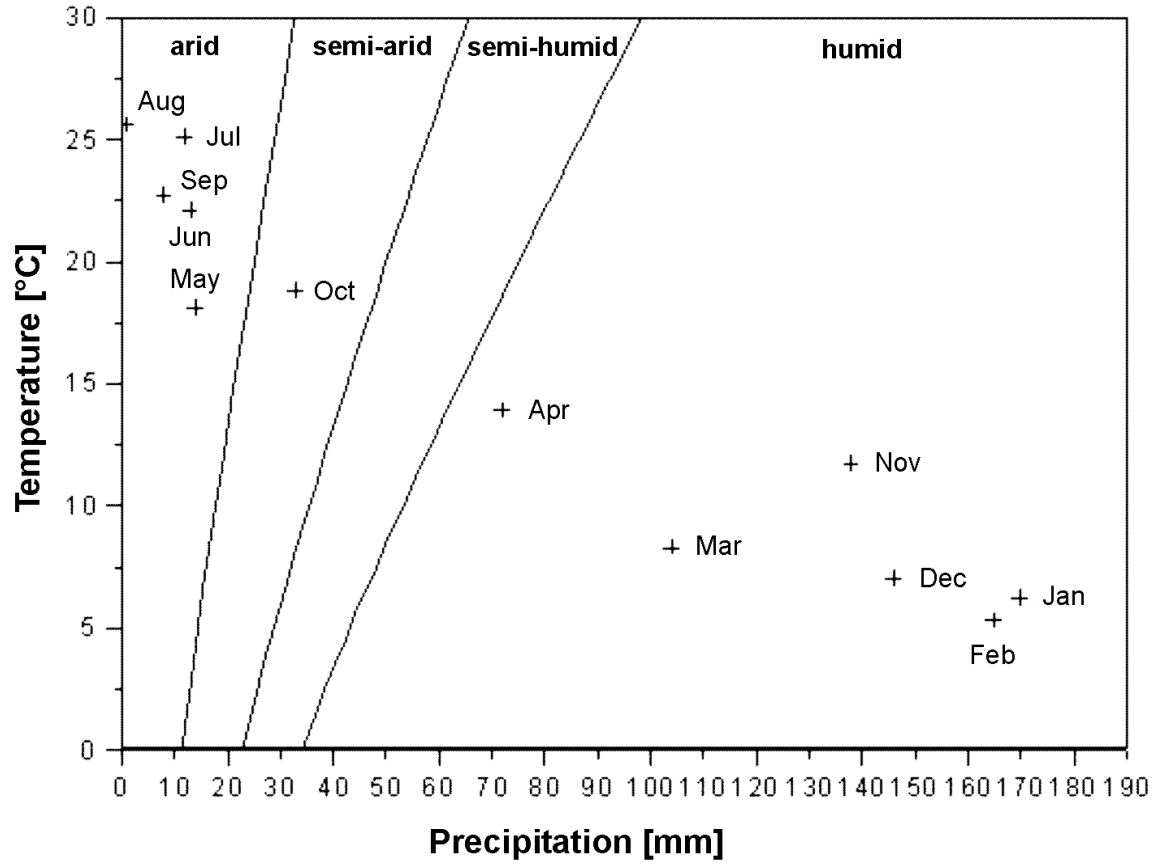

Fig. 3: Climate classification according to WANG & JÄTZOLD (1969) for long-term monthly mean values of the station Agros (377-91; 1015 m.a.m.s.l.; time period: 10/1987 to 09/1997).

2.3 Geology and hydrogeology

Cyprus is situated in a complex tectonic environment close to the boundaries of the African, the Arabian and the Anatolian plates. The island itself is part of the Anatolian plate, while the converging African-Anatolian boundary parallels closely the southern coast in the Mediterranean Sea, elongating the East Anatolian Fault (McCALLUM & ROBERTSON, 1990). Within this tectonic setting, Cyprus has formed above an intra-oceanic subduction zone as an assemblage of welded terranes (ROBERTSON, 1990). The study area comprises the Troodos Terrane and parts of the Mamonia Terrane, welded in the Palaeogene, uplifted and covered with Tertiary and Quaternary sediments of the Circum Troodos Sedimentary Succession (Fig. 5). The Troodos Terrane comprises Upper Cretaceous ophiolite complexes and is lithologically subdivided into the Olympos and Arakapas Sequence. The Mamonia Terrane consists of Middle Triassic to Upper Cretaceous marine sediments, metamorphics and volcanic series. Due to its „chaotic" internal structure, this assemblage is interpreted as an accretionary wedge (ROBERTSON, 1990).

The Olympos Sequence of the Troodos Terrane forms the so called Troodos Ophiolite, covering approx. 80 % of the study area and containing a complete, undisturbed ophiolitic sequence, being subject of many scientific publications (MALPAS ET AL., 1990; GASS ET AL., 1994; VARGA ET AL., 1999). Uplift and erosion processes have formed an elliptic dome structure, uncovering tectonised and serpentinised Harzburgites of the Mantle Sequences in the highest parts of the Troodos Mountains (Fig. 5 and Fig. 23). They are overlain by Wehrlites, Pyroxenites and Gabbros of the Plutonic Sequence and Sheeted Dykes (Intrusive Sequence), showing the largest areal share of the Troodos. Volcanic Sequences are exposed in the foothills.

The Arakapas Sequence comprises a second ophiolite complex (Anti-Troodos) of different origin but similar lithology, and a fault zone (Arakapas fossil transform) separating the two.

In the lowlands, close to the border of the study area, the terranes are overlain by Tertiary limestones, chalks and marls and Quaternary arenites, gravels, sands and silts of the Circum Troodos Sedimentary Succession (Fig. 5).

The lithologies in the study area exhibit different hydrogeological properties: The igneous lithologies and consolidated sediments show low effective porosities (UDLUFT ET AL., 2003; BORONINA ET AL., 2003). They form fractured aquifers or aquifer-systems, where the density of open fractures and joints is high. This is especially the case with the Gabbros in the Pitsilia area. Vulnerability to weathering has increased the fracture density and produced comparably smooth landforms, favourable for agricultural use and, due to high precipitation rates, favourable for groundwater recharge. Springs are common. As a consequence, high population density and intensive agricultural use are typical for the high mountainous Pitsilia region. The surrounding Sheeted Dykes are more resistant to weathering, showing a rugged topography with steep slopes unfavourable for agricultural use. Thus, most part of the Sheeted Dykes, especially in the western Troodos, are covered

with forests or scrubland. Hydrogeological investigations of the Harzburgites in the uppermost Troodos indicate a higher effective porosity but very low hydraulic conductivities (UDLUFT ET AL., 2003). Sepentinisation of the Harzburgites has decreased the volume of open fractures and fissures and thus the hydraulic conductivity. As a consequence, a large part of the high precipitation amount forms surface runoff and interflow (Chapter 4.1.3.4). The Pillow Lavas show low permeabilites as well, and high total but small effective porosities.
Compared to the Olympos Sequence, the Ultramafics and Pillow Lava series of the Arakapas Sequence contain more favourable hydraulic properties as they are affected by heavy faulting and fracturing in the vicinity of the Arakapas Fossil Transform zone.
The Mamonia lithologies are generally classified as low permeable due to a high content of fine-grained, impervious sediments.
The Tertiary consolidated calcareous sediments of the Circum Troodos Sedimentary Succession show medium to low conductivities. Especially, where the limestones are interbedded with marls, permeabilites are reduced. Sandy, interstratified beds form local aquifers. Generally, the groundwater level is very low as low precipitation quantities produce small recharge. Additional recharge occurs through riverbed infiltration and through indirect recharge from the igneous lithologies as isotope investigations postulate (UDLUFT & KÜLLS, 2003, 2004; BORONINA ET AL., 2005).
The unconsolidated alluvial and colluvial sediments form the only porous aquifers of the study area. Their areal extent is very limited, but for local water supply of the coastal region and in the Kargotis valley they play an important role.

Hydraulic conductivities and effective porosities decrease with depth. Borehole records indicate that favourable aquiferous conditions decrease rapidly below a depth of 150 to 200 m below surface (UDLUFT ET AL., 2003) leading to a fast draining system with high turnover rates, especially in the high mountainous regions. Deep percolating systems might exist and are part of the investigations carried out in this study (Chapter 4.2.1).

Groundwater in the study area has a low to moderate content of dissolved solids, Chloride is mostly below 25 mg/l, especially in the high mountainous parts where groundwater recharge rates are high (UDLUFT & KÜLLS, 2004). Large areas of sea water intrusions have not been identified in the study area (Chapter 4.2.2.3). AFRODISIS & FISCHBACH (1988) describe groundwaters with elevated salinity, high alkalinity and elevated temperatures in the Troodos. Sulphate rich alkaline to hyperalkaline springs discharge from a Gabbro aquifer in the upper Troodos, in the Arakapas Fault Zone and in the eastern Troodos. The elevated Sulphate content (> 1000 mg/l) might be the result of weathering of sulphidic ores. The high pH is attributed to the serpentinisation of ultrabasic rocks by meteoric water (AFRODISIS & FISCHBACH, 1988).
Groundwater in the Pillow Lavas is enriched in salts that probably derive from connate water, in general seawater, trapped in the voids of the lavas. Elevated Boron contents of 1 to 5 mg/l, locally greater than 5 mg/l, and thus exceeding the limit of 1 mg/l of the EU drinking water guideline (EU Directive 98/83/EC) are common in the groundwaters of the

Pillow Lavas. According to previous studies of AFRODISIS ET AL. (1986), Boron is enriched and released from volcanic glasses and from dissolution of mineral phases in former hydrothermal vents. Anthropogenic sources for Boron (Borax) are found in the vicinity of the major cities of Cyprus, but they are unlikely the main sources for elevated Boron contents in the study area.

Sodium enriched groundwater - as a result of ion exchanging processes - occurs occasionally in the Circum Troodos Sedimentary Succession and rarely in the igneous lithologies.

Nitrate deteriorates the groundwater quality locally, especially in the intensely cultivated regions like the Pitsilia, the Kargotis valley and the coastline of the western Troodos, where Nitrate contents exceed 100 mg/l (limit of the EU Directive: 50 mg/l).

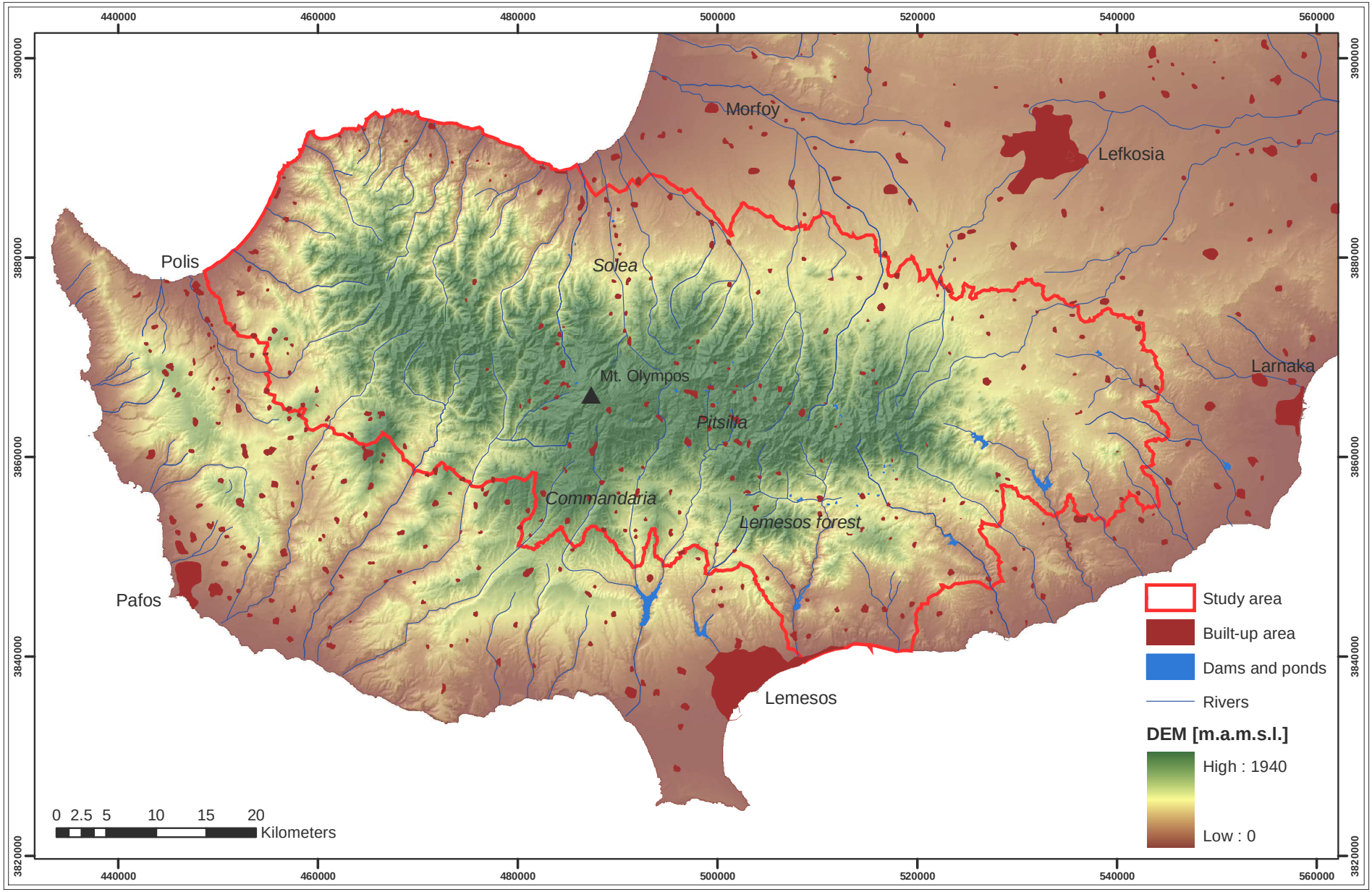

Fig. 4: Terrain model, major cities, villages, regions and drainage system of the study area.

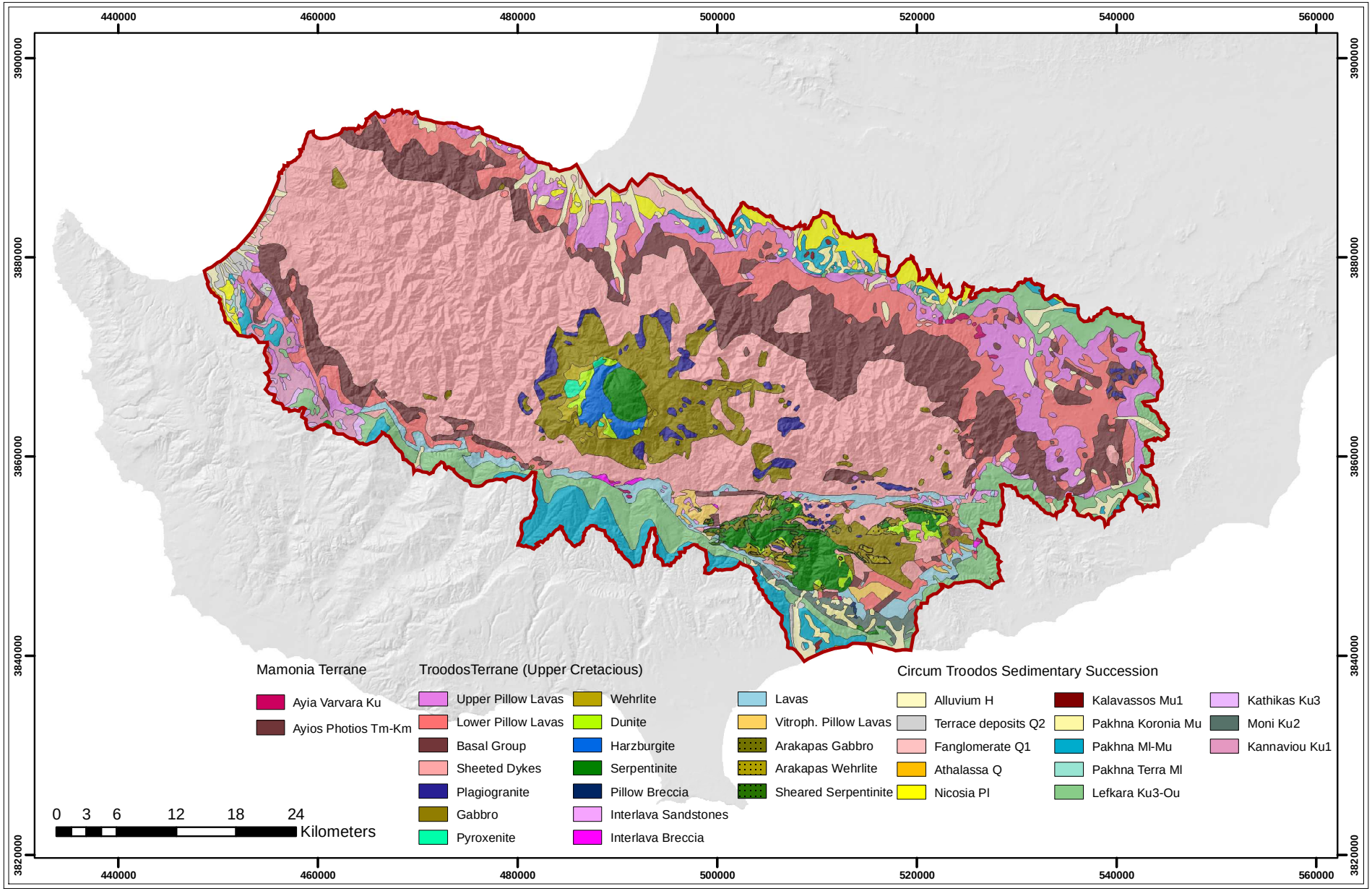

Fig. 5: Simplified geological map of the study area (for details see Chapter 2.3; abbreviations indicate geological epochs/periods).

2.4 Pilot catchment areas

For computational efficiency, calibration and validation of single parameters - both of the water balance and the groundwater flow models (Chapter 3) - is carried out in selected catchment areas. These so called “pilot catchment areas” cover all relevant hydrogeological regions with characteristic lithologies, landuse and exposition types. Important criteria for selection were the availability of high quality meteorological and runoff data and effluent flow conditions of the catchments’ rivers. These conditions minimise the difference between actual and measured total runoff. The catchments of the Upper Diarizos up to the gauging station Philousa (1-2-4-95), the Limnatis (gauging station U/S Kouris dam, 9-6-7-70), the Pyrgos (Phlevas, 2-7-2-75) and the Kargotis rivers (Skouriotissa, 3-3-4-95) (Fig. 6) meet these criteria.

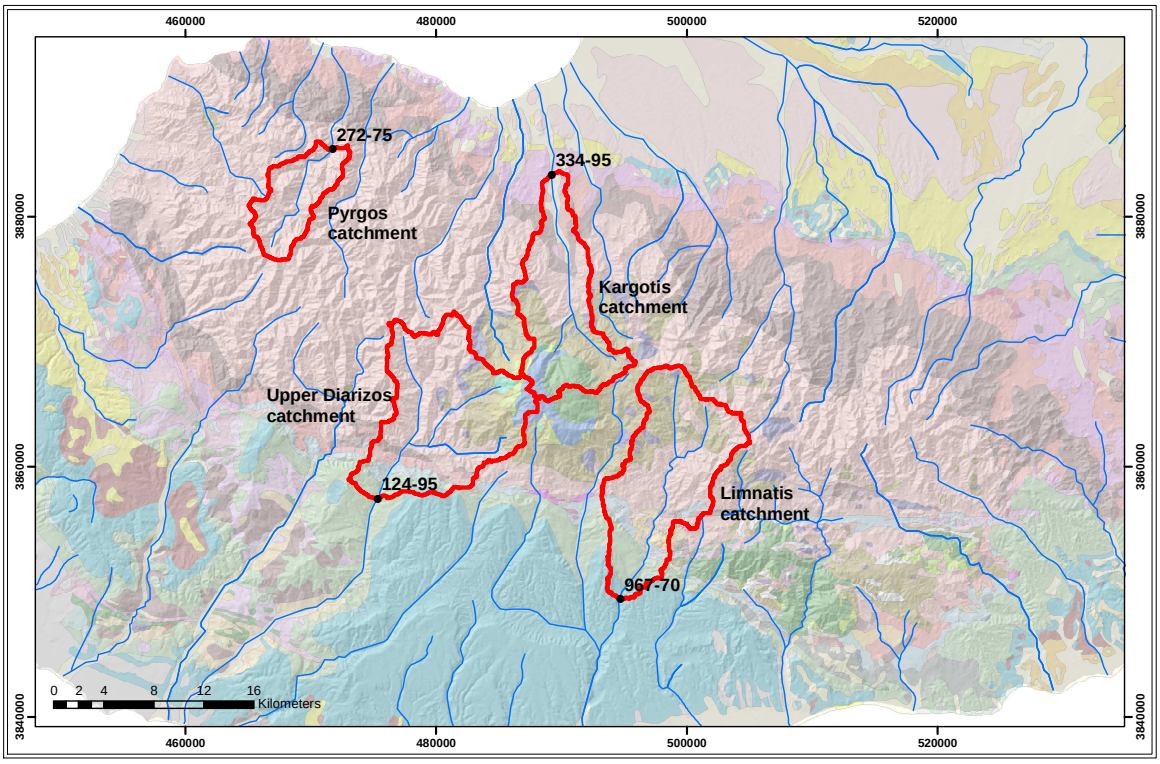

Fig. 6: Location of the pilot catchment areas and the corresponding gauging stations.

3 Methods and data

The dynamics of the Troodos fractured aquifer are simulated using groundwater flow models, whose in- and output fluxes are quantified by numerical water balance models. In detail, the methodology comprises a succession of numerical modelling procedures within different levels of the hydrologic cycle. Vertical fluxes between (sub-)soil, vegetation and atmosphere are being simulated and balanced with water balance models (Chapter 3.1 and 4.1). They form the quantitative framework of the presented study with a special emphasis on groundwater recharge, evapotranspiration (Chapter 4.1.3) and the quantification of groundwater abstraction needs for irrigation.
The balanced groundwater models simulate fluxes in the bedrock and interactions with the surface drainage system. In a first step, two-dimensional vertical models along geological cross-sections identify the general flow characteristics (Chapter 4.2.1). The one-layer models simulate vertical fluxes up to a depth of more than 1500 m. They allow the analysis of the fast draining “near-surface” groundwater system with high turnover rates, as well as the deep percolating “slow flow” system. In a third modelling step, a regional horizontal flow model is being constructed covering the whole Troodos Mountains up to a depth of 300 m. This large scale modelling approach is chosen to eliminate lateral fluxes between single catchments (inter-catchment flow). This model simulates the fast draining and high turnover system, and is used to develop water management scenarios and inter-catchment flow studies.

The water balance and groundwater flow models are raster based, combining a high spatial resolution with computational efficiency and thus allowing large scale modelling within one modelling frame.

The first part of this chapter describes the water balance modelling methodology and the programs used. The groundwater modelling methods and programs are outlined in the second part. The last part of this chapter deals with base data and data processing.

3.1 Water balance modelling with MODBIL

The water balance of the Troodos is determined with the module version Mbd48 of the numerical water balance modelling program MODBIL (UDLUFT & DÜNKELOH, 2005) developed at the Department of Hydrogeology and Environment (Prof. P. Udluft, University of Würzburg, Germany). DÜNKELOH (2009) describes the latest MODBIL program modifications and gives a detailed description of the program code. An overview is presented hereafter.

MODBIL has been applied and tested mainly in arid and semi-arid regions, among others in Brazil, Greece, Cyprus, Israel, Jordan, Namibia, Central African Republic and Germany (ROSA FILHO, 1991; KÖNIG, 1993; ALBERT, 1994; UDLUFT & ZAGANA, 1994; KÜLLS ET AL., 1998; AL-ALAMI, 1999; MAINARDY, 1999; ZAGANA & UDLUFT, 1999; ZAGANA ET AL., 1999; KÜLLS ET AL., 2000A; KÜLLS ET AL., 2000B; UDLUFT & KÜLLS, 2000; OBEIDAT, 2001; WEIGAND, 2001; ZAGANA, 2001; UDLUFT, 2002A; WIJNEN, 2002; AL-FARAJAT, 2003; DÜNKELOH ET AL., 2003; MEDERER, 2003; UDLUFT ET AL., 2003; BORGSTEDT, 2004; DÜNKELOH & UDLUFT, 2004A; DÜNKELOH & UDLUFT, 2004B; DÜNKELOH ET AL., 2004; UDLUFT & DÜNKELOH, 2004A; UDLUFT & DÜNKELOH, 2004B; DÜNKELOH, 2005A; DÜNKELOH, 2005B; MEDERER, 2005; DÜNKELOH, 2009).

The distributed, GIS-based, process-oriented, physical water balance model MODBIL considers the major water balance components: precipitation, groundwater recharge, surface runoff and interflow, and evapotranspiration on the base of the water balance formula (Equ. 1). A spatially differentiated water balance is calculated by simulating water fluxes and storages at temporal and spatial resolutions - based on meteorological, topographic, soil physical, landuse (land cover), and geological input parameters.

For a vertical soil column, the discrete form of the water balance formula is defined as:

$$R(t) = P(t) - ET(t) - Q(t) + \Delta S \qquad \text{Equ. 1}$$

with $R(t)$ as recharge for a given time step t, $P(t)$ as precipitation, $ET(t)$ as evapotranspiration, $Q(t)$ as runoff and ΔS representing change in water storage.

Fig. 7 shows the modelling concept of MODBIL. The model handles the temporal and spatial variations of the water balance components in different process steps. In the first step, daily meteorological data are interpolated for each active raster cell depending on topographic parameters. Snow storage is simulated using precipitation and temperature. Landuse dependent interception storage controls the interception loss. Effective precipitation (precipitation that reaches the soil surface) is then calculated allowing for snow and interception storage status.

The second model step simulates soil water storage, evapotranspiration, surface runoff, interflow and groundwater recharge based on soil, subsoil and landuse parameters. A one layer soil model is used for the simulation of soil moisture conditions and relevant fluxes into and out of the soil system for each time step. Surface runoff and infiltration are calculated depending on effective precipitation, hydraulic conductivity of surface, soil and landuse data. The infiltrating part is added to the soil water storage. Surface runoff occurs, when the infiltration amount exceeds the maximum capacity or when the soil moisture storage reaches saturated conditions.
In addition, soil water is lost in every time step due to actual evapotranspiration calculated with a modified method after SPONAGEL (1980) and RENGER ET AL. (1974), based on

potential evapotranspiration, soil water content and landuse. Potential evapotranspiration is calculated according to Penman-Monteith (MONTEITH, 1965; ALLEN ET AL., 1998), Haude (HAUDE, 1959) or PanA (ALLEN ET AL., 1998). Deep percolation (groundwater recharge) occurs when soil water content exceeds effective field capacity. The amount of groundwater recharge is driven by the soil percolation amount, and by hydraulic conductivity of both soil and subsoil. Bypass effects can create additional groundwater recharge through macropore flow before effective field capacity is reached. Interflow is generated as soon as the percolation exceeds the maximum infiltration capacity of the subsoil.

The integrated *secondary evapotranspiration* concept is developed for water balance models in arid or semi-arid regions, where flood plains, natural moist and irrigated areas yield higher actual evapotranspiration rates, due to additional water availability through rivers, lakes, springs, capillary rise or irrigation. In MODBIL, the secondary evapotranspiration is simulated for specific landuse types (e.g. moist and irrigated areas, open waters) and might be adjusted by entering irrigation time periods for different crop types into the model. The secondary evapotranspiration *(Etsec)* for a given time step *t* is calculated according to Equ.2:

$$ET\,\mathrm{sec}(t) = ETc(t) - ETa(t) \qquad \text{Equ. 2}$$

With:

ETc = potential evapotranspiration for a specific landuse (under well watered soil conditions without water stresses)

ETa = actual evapotranspiration for a specific landuse under actual soil water conditions (with or without water stresses)

The model is preferably calibrated in clearly delimitable catchments with reliable gauging station data. First, the total runoff - comprising interflow and groundwater recharge - is calibrated by adjusting the parameters influencing the actual evapotranspiration. In a second step, the modelled groundwater recharge rate is adapted to the base flow content, derived from hydrograph separation techniques as proposed e.g. by NATERMANN (1951), WUNDT (1953), RUTLEDGE (1998) or WITTENBERG (1999), by customising soil and subsoil conductivities. Additional fine calibration is achieved by adjusting a modelled hydrograph, generated by a simple storage outflow regression according to MAILLET (1905), to a measured hydrograph.
The results can be verified by additional indirect groundwater recharge estimation methods based on chloride mass-balance or isotope investigations (MAINARDY, 1999; BORONINA, 2003; UDLUFT & KÜLLS, 2003). As the Pillow Lava lithologies in the Troodos promontories contain seawater inclusions, the chloride mass-balance method is restricted to non-influenced catchments in Cyprus.

Precipitation, effective precipitation, potential evapotranspiration, actual evapotranspiration, soil water content, groundwater recharge and interflow are the output parameters of the model at daily resolution. Interflow in MODBIL comprises surface runoff and interflow.

Previous investigations indicate that an uncertainty for the water balance model of less than 10 % is reasonable (UDLUFT ET AL., 2003). Density and distribution of the meteorological stations and data quality play an important role concerning model quality. Compared to the water balance investigations of the GRC-project (UDLUFT ET AL., 2003) the improved MODBIL version Mbd48 allows the separate processing and interpolation of meteorological input parameters. It enhances the number of selectable stations and thus the accuracy of the meteorological input raster data.

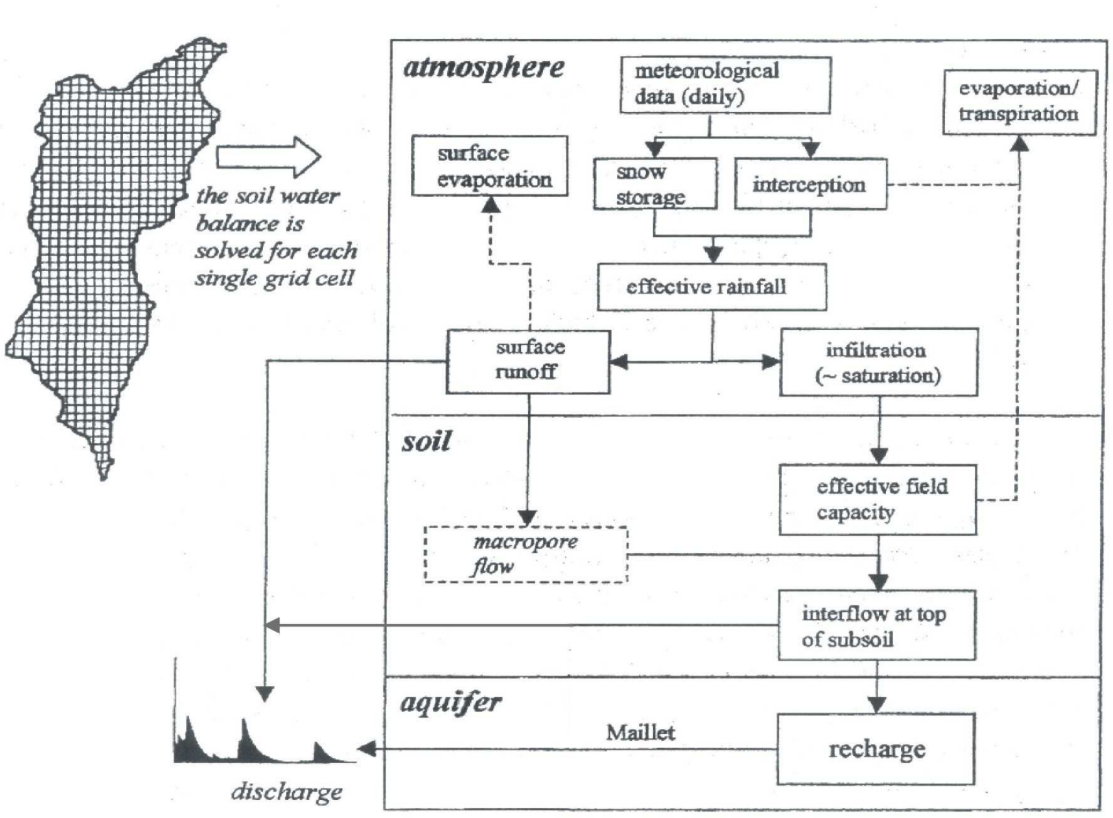

Fig. 7: Flow chart indicating the MODBIL modelling concept (UDLUFT & KÜLLS, 2000; modified).

3.1.1 Regionalisation of meteorological data, calculation of potential evaporation and effective precipitation

In selecting the calculation procedure for the regionalisation of meteorological data, a compromise between calculation speed and accuracy has to be achieved. Therefore, a relatively simple approach is chosen. First, reference altitude *(AR)*, daily precipitation *(PU)* and temperature *(TU)* – both not altitude corrected - are calculated by the inverse distance to a power method (SHEPARD, 1968) for each grid cell. In a second step, precipitation *(P)* and temperature *(T)* are corrected for altitude effects assuming a precipitation gradient of 4.4 % per 100 m and a temperature gradient of 0.6 °C per 100 m (Equ.3 and Equ.4). The calculated reference altitude is compared to the real altitude of the grid cell *(AG)* given by a digital elevation model (DEM).

$$P = PU \cdot (1 + (AG - AR) \cdot 0.00044) \qquad \text{Equ. 3}$$

$$T = TU \cdot (1 + (AG - AR) \cdot 0.0060) \qquad \text{Equ. 4}$$

The calculation of potential evaporation is based on the Penman-Monteith equation (MONTEITH, 1965) as given by ALLEN ET AL. (1998) in Equ. 5 :

$$ET0 = (0.408 \cdot \Delta \cdot (Rn - G) + \gamma \cdot (900/(T + 273)) \cdot u2 \cdot (es - ea))/(\Delta + \gamma \cdot (1 + 0.34 \cdot u2)) \qquad \text{Equ. 5}$$

With:

ET0 = reference evapotranspiration [mm/d]
Rn = net radiation at the crop surface [MJ/(m²d)]
G = soil heat flux density [MJ/(m²d)]
T = mean daily temperature at 2 m height [°C]
u2 = wind speed at 2 m height [m/s]
es = saturation vapour pressure [kPa]
ea = actual vapour pressure [kPa]
es-ea = saturation vapour pressure deficit [kPa]
Δ = slope vapour pressure curve [kPa/°C]
γ = psychrometric constant [kPa/°C]

Day length and radiation are calculated according to ALLEN ET AL. (1998).

Incoming precipitation *(P)* is separated into interception and through fall when entering the surface vegetation. For temperatures below 0 °C snowfall is added to a temporary snow storage, which decreases when temperature causes the melting process. Effective precipitation *(PE)* is calculated based on the concept of an interception store *(IT)*, where an amount of total precipitation (up to the maximum interception storage capacity) is lost depending on the actual conditions of the interception store at each time-step *(IA(t);* Equ. 6

to 9). The maximum interception storage capacity of the vegetation used in this model varies spatially and temporally for single landuse units. Intercepted precipitation is lost from the storage by evaporation (calculated with *ET0*), and the actual interception storage capacity is adjusted for the next time step. Although precipitation data represent the total precipitation over 24 hours, it is assumed that the largest part of the rain falls within a time constraint of 3 hours as observed in the field.

$IA(t) = IT$	with $P(t) > IT - IA(t-1)$	Equ. 6
$IA(t) = IA(t-1) + P(t)$	with $P(t) \leq IT - IA(t-1)$	Equ. 7
$IA(t+1) = IA(t) - ET0(t)$	with $ET0(t) \leq IA(t)$	Equ. 8
$IA(t+1) = 0$	with $ET0(t) > IA(t)$	Equ. 9

In MODBIL, effective precipitation is than calculated as

$PE(t+1) = P(t) - IA(t)$	with $P(t) > IA(t)$	Equ. 10
$PE(t+1) = 0$	with $P(t) \leq IA(t)$	Equ. 11

3.1.2 Calculation of surface runoff, infiltration, soil water content, actual evapotranspiration, interflow, and groundwater recharge

In the second model step effective daily precipitation *(PE)* is separated into direct surface runoff *(R)* and infiltration *(F)*, depending on the hydraulic conductivity of the soil surface *(KS)*, soil moisture content *(SW)* factors of landuse (land cover; *LC*), terrain slope *(TS)* and soil water content *(SW)*, as shown in Equ. 16. If effective precipitation exceeds conductivity of the soil surface, surface runoff occurs.

$F = KS$	with $PE > KS$	Equ. 12
$R = PE - KS$	with $PE > KS$	Equ. 13
$F = PE$	with $PE \leq KS$	Equ. 14
$R = 0$	with $PE \leq KS$	Equ. 15
$KS = KF \cdot LC \cdot TS \cdot SW$		Equ. 16

With:

LC(forests) = 10
LC(grassland, meadow, fields) = 2.5
LC(wetlands) = 5
LC(settled areas) = 0.5
$TS = 1/(1-\tan(\pi/[180*\beta]))$ where β = slope of the terrain [%]
$SW = 1/(0.2 + 0.008 * PS)$ where *PS* = percentage of saturation, in % of field capacity

The module version Mbd48 allows individual adjustment of the temporal dynamics of the influencing landuse parameters like interception storage, secondary evapotranspiration and irrigation, hydraulic conductivity of the soil, macropore flow, Haude factors and root depth.

Infiltration *(I)* increases soil water content *(Θ)* and influences the hydraulic conductivity of the soil surface for the next time step. Soil water content can increase up to a maximum of field capacity *(FC)*. Further water influx results in deep percolation *(DP)*. Soil water content decreases due to actual evapotranspiration *(ETa)*, which is determined by potential evapotranspiration, state of soil moisture, and the crop coefficient:

$$\Theta(t+1) = \Theta(t) + I(t) - ETa(t) \quad \text{with } FC > \Theta(t+1) \quad \text{Equ. 17}$$

$$DP(t+1) = 0 \quad \text{with } FC > \Theta(t+1) \quad \text{Equ. 18}$$

$$\Theta(t+1) = FC \quad \text{with } FC \leq \Theta(t+1) \quad \text{Equ. 19}$$

$$DP(t+1) = \Theta(t) + I(t) - ETa(t) - FC \quad \text{with } FC \leq \Theta(t+1) \quad \text{Equ. 20}$$

In this study the moisture extraction function *f(Θ)* that modifies the potential crop coefficient is used to calculate actual evapotranspiration depending on soil moisture content (cf. RENGER ET AL., 1974):

$$f(\Theta) = 0.2 + 2 \cdot ((\Theta - \Theta W)/(\Theta F - \Theta W)) - 1.2 \cdot ((\Theta - \Theta W)/(\Theta F - \Theta W)) \cdot 2 \quad \text{Equ. 21}$$

With:

Θ = soil moisture content (variable)
ΘW = soil moisture content when soil is at wilting point
ΘF = soil moisture content when soil is at field capacity

Deep percolation *(DP)* is developed if soil water content exceeds field capacity. At the soil-subsoil boundary (zone underneath the root zone) deep percolation is divided into interflow II *(WII)* and groundwater recharge (*GWR)* by comparing hydraulic conductivity of the subsoil *(KG)* with deep percolation.

$$GWR = KG \quad \text{with } DP > KG \quad \text{Equ. 22}$$

$$WII = DP - KG \quad \text{with } DP > KG \quad \text{Equ. 23}$$

$$GWR = DP \quad \text{with } DI \leq KG \quad \text{Equ. 24}$$

$$WII = 0 \quad \text{with } DP \leq KG \quad \text{Equ. 25}$$

3.2 Groundwater flow modelling

The groundwater flow models are constructed using the finite difference groundwater modelling program MODFLOW 2000 (MCDONALD & HARBAUGH, 1983; HARBAUGH ET AL., 2000), and the particle tracking code MODPATH 4.2 (POLLOCK, 1994), implemented into the graphical interfaces Groundwater Modelling System (GMS 5.1) and PMWIN (CHIANG & KINZELBACH, 2001). The finite difference schemes MODFLOW and MODPATH are well documented, and are now considered to be the de facto standard code for aquifer simulation. They are chosen for their computational efficiency in a large modelling environment, reasonable accuracy and their compatibility to the water balancing program MODBIL.
The equivalent continuum model MODFLOW was initially designed to simulate porous aquifers. Application in fractured media is subject to limitations. According to NRC (NATIONAL RESEARCH COUNCIL, 1996), the application in fractured media is reasonable where the averaging volumes are large enough to comprise a statistically representative selection of open, connected fractures, and where no change in the fluid storage (steady – state condition) takes place. The Troodos aquifer-system is typically highly fractured with connected openings ranging from mm to cm size. Compared to the size of the (hydro-) geological units, the fracture distribution can thus be regarded as homogenous.

3.2.1 Modelling tools

3.2.1.1 MODFLOW

MODFLOW is a modular finite-difference flow model developed by the U.S. Geological Survey. It is controlled by the finite difference form of the partial differential groundwater flow equation (Equ. 26).

$$\frac{\partial}{\partial x}\left[Kxx\frac{\partial h}{\partial x}\right]+\frac{\partial}{\partial y}\left[Kyy\frac{\partial h}{\partial y}\right]+\frac{\partial}{\partial z}\left[Kzz\frac{\partial h}{\partial z}\right]+W=Ss\frac{\partial h}{\partial t} \qquad \text{Equ. 26}$$

With:

Kxx, *Kyy* and *Kzz* = hydraulic conductivities along the x, y, and z coordinate axes
h = potentiometric head
W = volumetric flux per unit volume representing sources and/or sinks of water
Ss = specific storage of the porous material
t = time

MODFLOW simulates two-dimensional areal or cross-sectional, and quasi- or fully three-dimensional flow in anisotropic, heterogeneous, layered aquifer-systems. The model uses

the block centred finite difference approach for spatial discretisation. Aquifer layers may be simulated under confined, unconfined or convertible (semi-confined) conditions. The model also handles layers which pinch out, e.g. where a multi-layered system meets a single layered aquifer. External influences such as wells, areal recharge, drains, evapotranspiration and streams can be analysed and incorporated. Solution techniques available for the finite difference equations are the Direct Solution (DE45), the Preconditioned Conjugate Gradient 2 (PCG2), the Strongly Implicit Procedure (SIP) and the Slice Successive Over Relaxation (SSOR) package. The PCG2 solution was used in this study for its suitability for problems with a high number of nodes (KINZELBACH & RAUSCH, 1995).

MODFLOW has a modular structure, which consists of a main program and a series of highly independent subroutines or modules. The modules are grouped into packages. Each package deals with a specific feature of the hydro(geo-)logical system, such as interactions with river or drain cells, or with a specific method of solving the linear equations describing the flow system. The modular structure permits the analysis of specific hydrological features of the model independently. It also facilitates the development of additional capabilities, since new packages can be added without modifying the existing packages. Implicit methods approximate the flows between cells by gradients at the end of the time interval.

When the groundwater flow equation is solved with finite differences, the discretisation of the model follows a rectangular net, which is a block-centred or mesh-centred grid. MODFLOW supports the block centred grid (ANDERSON & WOESSNER, 1991). Corresponding to the grid, a rectangle of Nx cells in the x-direction and Ny cells in the y-direction forms the modelled area. All nodes in this rectangle outside the modelled area are set inactive and receive a transmissivity value of zero. For each individual element the Darcy-equation is calculated. Therefore, the partial derivatives are replaced by an algebraic equivalent, with a quotient of two finite differences of the dependent and the independent variable replacing the differential quotient (BEAR & VERRUIJT, 1987). The basic idea is that the derivative $\partial f/\partial t$ of a function $f(t)$ is defined as

$$\frac{\partial f}{\partial t} = \lim_{\Delta t \to 0} \frac{f(t+\Delta t) - f(t)}{\Delta t} \qquad \text{Equ. 27}$$

and that an obvious approximation of the derivative can be obtained by simply omitting the limiting process, $\Delta t \to 0$.

It may be noted that in the definition it was tacitly assumed that the limit does exist, and that the same limit is obtained for positive and negative values of the step Δt. When using

finite differences, the limit is replaced by some value for a finite value of Δt and the actual value may depend upon the magnitude of Δt and also upon its sign.
MODFLOW uses a hydraulic conductivity based parameter called “conductance” to determine the amount of water that flows in or out of the model due to general head, river, stream, and drain type stresses. The conductance calculation depends on the hydraulic conductivity k and the geometrical feature it is applied to. The conductance for arcs (C_{arc}) and for polygons (C_{poly}) is calculated according to Equ. 28 and Equ. 29.

$$C_{arc} = \frac{k}{t} \cdot w \qquad \text{Equ. 28}$$

$$C_{poly} = \frac{k}{t} \qquad \text{Equ. 29}$$

The thickness of the material is t and w is the width of the material along the length of the arc. When a general head, river, stream or drain attribute is assigned to an individual point, the conductance should be entered as a normal hydraulic conductivity value. The conductance is directly assigned to the cell containing the point.

MODFLOW is subject to the following limitations:

- Density, dynamic viscosity and temperature of the water must be constant throughout the modelling domain.
- The principle components of anisotropy of the hydraulic conductivity are restricted to orthogonal anisotropies. Non-orthogonal anisotropies, as they may be caused by fractures, can not be processed.

3.2.1.2 MODPATH

MODPATH is a particle tracking code that is designed as an extension for MODFLOW. After running a MODFLOW simulation, a set of particles can be tracked assuming advective transport in the flow field computed by MODFLOW. Particle tracking can be used to delineate capture and recharge areas or draw flow nets e.g. of contaminants. In addition to computing particle paths, MODPATH keeps track of the time of travel for particles moving through the system and allows thus an estimation of the residence time. By carefully defining the starting locations, it is possible to perform a wide range of analyses. In this study, MODPATH is used to visualize the flow field of the cross-section models (Chapter 4.2.1) and to estimate groundwater residence times.

In order to compute pathlines, a method must be established to compute values of the principal components of the velocity vector at every point in the flow field, based on the cell-to-cell flow rates of the finite difference model. Several methods can be used as a particle tracking method (e.g. linear, bicubic interpolation schemes, semi-analytical, Euler, Range-Kutta and Taylor series expansion). MODPATH uses a linear interpolation scheme (POLLOCK, 1994) producing a continuous velocity vector field within each cell. This interpolation is based on a partial differential equation describing conservation of mass in a steady state, three-dimensional groundwater flow system (Equ. 30).

$$\frac{\partial}{\partial x}(nv_x) + \frac{\partial}{\partial y}(nv_y) + \frac{\partial}{\partial z}(nv_z) = W \qquad \text{Equ. 30}$$

v_x, v_y and v_z are the principal components of the average linear groundwater velocity vector, n is effective porosity, and W is the volume rate of water created or consumed by internal sources and sinks.

POLLOCK (1994) describes the program essentials, capabilities and limitations in more detail in the MODPATH documentation.

3.3 Base data and data processing

The terrain elevations for the models are derived from the Digital Elevation Model, the landuse characteristics from the landuse map, both basically developed within the GRC-project by the Planning Bureau Schaller (UDLUFT ET AL., 2002) and modified by the author (Fig. 9 and Fig. 10). The areal distribution of soil and subsoil units is based on the Geological Map of Cyprus, published by the Geological Survey Department in 1995.
Subsoil permeabilites and porosities have been investigated intensely within the GRC-project (UDLUFT ET AL., 2003; UDLUFT ET AL, 2004B). Due to their importance for the presented study the hydraulic properties, derived from pumping test analysis (Table 24; Appendix B) are shown in Table 2. Well-, pumping test- and aquifer-details were extracted from the ENVIS-database. The pumping test analysis has been carried out with the program AQUIFER TEST (Version 3.02) by Waterloo Hydrogeologic Inc (WHI). Pumping tests in the fractured aquifers were analysed using the “Moench fracture flow” method. The “Neuman” and “Theis” method is applied to gravel aquifers.
The pumping tests results in the Troodos are probably biased, as the boreholes are usually drilled in zones with potentially high transmissivities. For the present study, the results can thus be treated as maximum values for specific aquifers only and are re-interpreted regarding the hydrogeological background.
The effective porosities for the single lithologies, important for the particle tracking in the cross-section models (Chapter 4.2.1), are shown in Table 1. They have been determined according to UDLUFT (1972) by analysing the water storage volume of fractured

unconfined aquifers, using the Maillet dissecation constant and the so-called “dewaterable rock-volume”.

The meteorological data used in the MODBIL models are exported from the ENVIS database, restructured and saved in ASCII format, readable by the MODBIL interface. The GIS-programmes IDRISI (Version: I32.2), and CARTALINX (Version: 1.2), both developed by Clark Labs, are used for value assignment for landuse, soil and subsoil classes and for map export in ARCINFO ASCII grid format, suitable for import to MODBIL. The modelling results are post processed in ARCVIEW GIS (Version 3.2) and ARCGIS (Version: 9.0) by ESRI Inc., mainly for statistical analysis and visualisation.

Via the ArcObjects platform, the groundwater modelling system GMS has the ability to use functions of ARCVIEW/ARCGIS. Thus, all input data for the groundwater models are pre-processed in ARCGIS and incorporated into the GMS modelling environment. The flow modelling results are post-processed both in the internal GIS-environment of GMS, and via export to ARCVIEW/ARCGIS.

The PMWIN interface, which is the modelling environment for the cross-section flow models, does not support ArcObjects. All data are thus pre-processed in ARCVIEW and IDRISI and post-processed using the PMWIN mapping functions.

Table 1: Effective porosities of geological formations in the study area.

Formation	Effective porosity [%]
Alluvium	12
Fanglomerates	10
Athalassa	2
Nicosia	1
Pakhna	0.06
Lefkara	0.06
Upper Pillow Lavas	0.01
Lower Pillow Lavas	0.01
Basal Group	0.08
Sheeted Dykes	0.05
Plagiogranite	0.05
Gabbro	0.08
Ultramafic Sequence	0.35
Ayios Photios	0.01

Table 2: Hydraulic properties of single formations in different regions of the study area, derived from pumping tests (Table 24, Appendix B).

Formation (no. of tests)	Region	Aquifer-thickness [m]		Hyd. conductivity [m/s]		Transmissivity [m²/s]		Mean conductivity [m/s]
		min	max	min	max	min	max	
Ultramafic Rocks (4)	Upper Troodos	20	50	5.89E-06	7.65E-05	2.06E-04	2.45E-03	4.40E-05
Gabbro (6)	Pitsilia, TroodosE	10	100	9.00E-07	1.20E-05	7.20E-05	1.20E-04	5.27E-07
Sheeted Dykes (3)	Troodos N	45	110	1.55E-07	3.00E-06	5.40E-05	3.00E-04	7.94E-07
Sheeted Dykes (15)	Troodos E, Pitsilia	20	175	1.14E-07	3.64E-06	1.14E-05	4.00E-04	6.90E-07
Sheeted Dykes (4)	Troodos W	10	90	2.25E-07	2.00E-05	2.25E-05	8.00E-04	8.68E-07
Basal Group (4)	Troodos N	10	70	2.14E-07	1.25E-05	1.50E-05	1.25E-04	6.35E-06
Basal Group (5)	Troodos N, NE	30	120	1.77E-07	6.67E-06	2.13E-05	2.00E-04	3.42E-06
Basal Group (11)	Troodos E	10	90	2.25E-06	9.00E-05	1.80E-04	5.50E-03	2.03E-05
Pillow Lavas (2)	Troodos E	30	50	1.20E-06	1.50E-05	6.00E-05	3.00E-04	6.60E-06
Transform Lavas and Breccias (2)	Arakapas Fault Zone	20	50	1.80E-06	1.20E-05	9.00E-05	3.00E-04	6.65E-06
Lefkara-chalks (2)	Commandaria	35	150	3.00E-07	4.00E-05	3.00E-05	1.40E-03	9.15E-07
Pakhna-chalks (6)	Commandaria	20	165	2.00E-07	9.50E-06	1.20E-05	4.75E-04	1.76E-06
Gravel (5)	Kouris River	25	80	8.10E-07	1.32E-04	6.48E-05	5.28E-03	5.72E-05
Gravel (5)	Troodos N, Solea	25	30	3.74E-05	1.01E-04	9.35E-04	2.53E-03	8.90E-05

4 Balanced groundwater models of the Troodos

The first part of this chapter deals with the water balance of the study area. Important parameters are described and discussed, especially groundwater recharge and evapotranspiration. In the second part, the balanced groundwater models are presented. Conceptual cross-section models illustrate the principle flow dynamics of the fractured Troodos aquifer-system and its interaction with the surrounding sedimentary successions. Based on this knowledge, a regional horizontal groundwater model - covering the whole aquifer-system of the Troodos - is constructed simulating aquifer resilience, changing abstraction rates, and inter-catchment flow. A sensitivity analysis concludes this chapter.

4.1 Water balance

Water balance studies are crucial for the understanding of hydrogeological processes and for a sustainable groundwater resources management. This applies especially to the study area due to its importance for the water supply of Cyprus (Chapter 1.1). For the scope of the presented study, the water balance models determine in- and outflow volumes for the groundwater models. Also, they serve as an additional calibration tool for hydraulic conductivities of single lithologies (Chapter 4.1.2), complementing the point data created by the pumping tests (Chapter 3.3).
The water balance modelling is a progression of the water balance investigations within the GRC-project (UDLUFT ET AL., 2003), using an improved version of the modelling program MODBIL (Version: 48). This version allows the separate processing of single meteorological parameters. As a consequence, all precipitation stations with valid data can be incorporated into the models (Fig. 9). This is very important, as the GRC investigations assumed a high sensitivity of the water balance to precipitation distribution - especially in the mountainous Troodos region. In the frame of the GRC project, important work within the study area - including data collection, parameterisation of hydrological units and water balance modelling – have been conducted in the Limnatis and Upper Diarizos catchment area by MEDERER (2005) and DÜNKELOH (2005A). The results of these studies provide the "starting values" for the modelling process, especially concerning hydraulic soil properties (Table 2).
For a more detailed description of water balance parameters and dynamics of the Troodos Mountains it is referred to DÜNKELOH (2009).

The modelling period comprises the hydrogeological years 1988 to 1997 (1.10.1987 to 30.09.1997), coinciding with the modelling period of the GRC-project to enable comparison of the results.
In the first part of this chapter, important meteorological, topographical and hydrophysical input parameters are described. The second part deals with the water balance components,

emphasizing groundwater recharge and evapotranspiration and the determination of abstraction rates. Calibration of the hydrophysical parameters is described in the last part of this chapter.

4.1.1 Input parameters

4.1.1.1 Meteorological data

The density of the meteorological stations network as well as the data availability and quality in Cyprus is generally good. Missing values might be a problem analysing multi-decadal time series, but for the modelling time period they amount less than 1 % per station. Due to the high base data quality, missing values are simply replaced by linearly interpolating data of neighbouring stations of similar altitude. 89 stations could be used for daily mean precipitation data, 22 stations for daily mean and maximum (14 h) temperature data, and 11 stations for daily relative humidity data (14 h; Fig. 9, Table 21 to Table 23 in Appendix A).

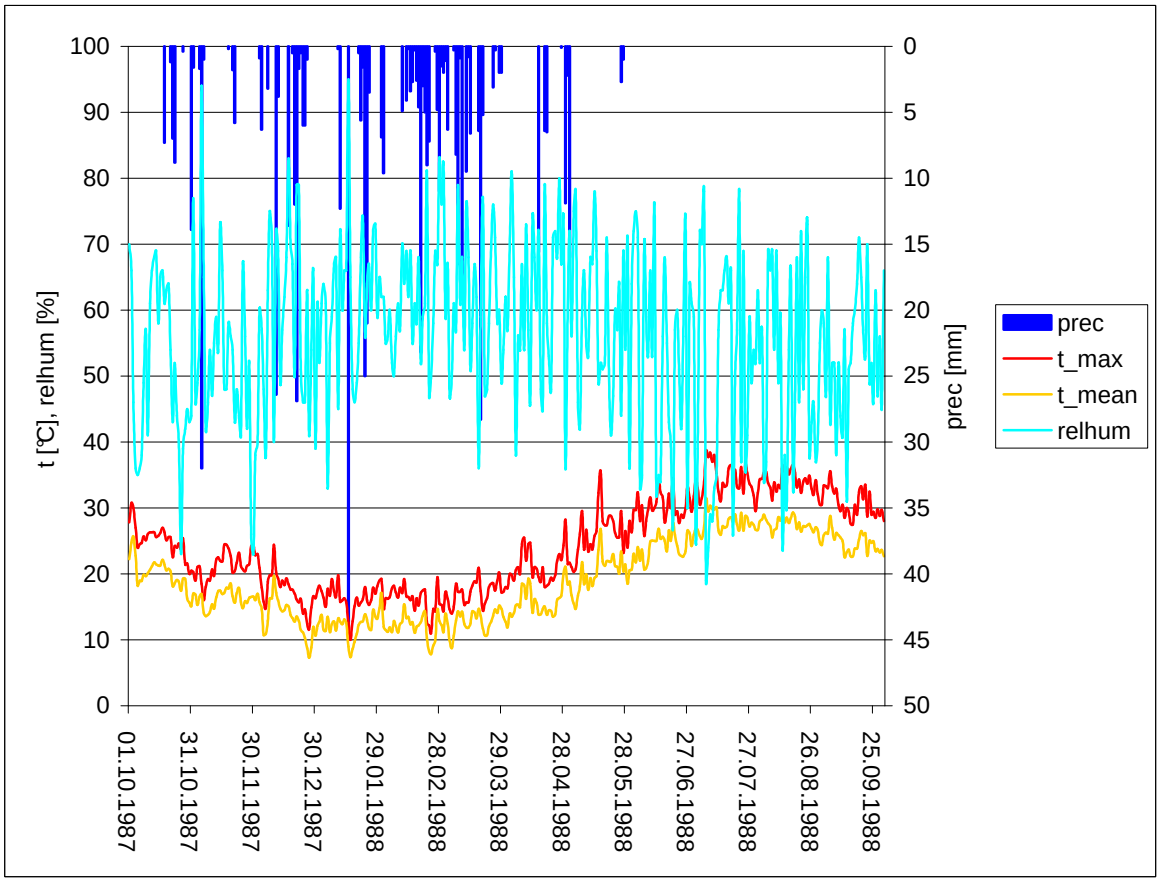

Fig. 8: Exemplary time series of station no. 164-2030 for the hydrological year 1988, including daily mean and maximum temperature (t_max, t_mean), daily 14 h relative humidity (relhum), and daily mean precipitation (prec).

4.1.1.2 Topography

The digital elevation model (DEM, Fig. 9; Chapter 3.3) forms the base for the topographic input features. In addition to the elevation matrix, DEM derived slope and aspect matrices are required for the MODBIL model. The slope and aspect maps are shown in Fig. 11 and Fig. 12.

Table 3: Statistics of the topographical input matrices.

	Elevation [m.a.m.s.l.]	Slope [°]	Aspect [°]
Minimum	0	0	0
Maximum	1915	42	345
Mean	569	15	168
Median	438	17	138

4.1.1.3 Landuse

Different landuse zones, depending on climate, relief and bedrock characteristics, have developed in the study area. Crop fields, vineyards and scrubland dominate the calcareous and Pillow Lava foothills surrounding the Troodos Mountains. This region shows the highest settlement density of the study area. In the Troodos Mountains, broad valleys and smooth landforms in the Gabbro regions favour intensive agriculture with irrigation, mainly in the vicinity of the Troodos villages (Fig. 4). Scrublands and forest prevail in the adjacent uncultivated mountainsides, in the Mount Olympos region additionally bare land. The landuse distribution of the whole study area is dominated by scrubland and pine forest, while agricultural areas cover smaller portions, mainly in low to medium elevated regions. In the western Troodos, pine forest prevails while in the eastern part large areas are covered by scrubland.
Moist landuse types – representing regions where groundwater evaporates like floodplains and springs - reach at least 5 % and thus twice the portion of the irrigated areas. Moist and irrigated landuse classes play an important role in the study as they are used for the estimation of abstraction and evaporation rates of the groundwater models (Chapter 4.1.3.2). The areal distribution in the study area is shown in Fig. 10 and Table 4.

The landuse matrix represents an improved version of the landuse raster map created within the GRC-project (UDLUFT ET AL., 2002). In addition to the landuse data processing, parameters are adjusted during the calibration process like irrigation time and the portion of potential evapotranspiration used for the secondary evapotranspiration of irrigated areas (Chapter 4.1.2).

Table 4: Areal distribution of the landuse (MODBIL classes) in the study area.

Landuse	Area [km²]	Area [%]
Scrubland (class 2)	1206.88	41.29
Pine forest (class 3)	850.20	29.09
Field (class 5)	327.06	11.19
Moist area (class 7)	170.81	5.84
Deciduous trees (class 1)	160.94	5.51
Bare land (class 10)	80.69	2.76
Irrigated area (class 6)	71.06	2.43
Settlement (class 4)	49.00	1.68
Waters (class 8)	4.19	0.14
Sealed area (class 9)	1.81	0.06
Sum	2922.64	100.00

4.1.1.4 Soil and subsoil properties

For the MODBIL water balance model, soil and subsoil hydraulic conductivities, as well as usable field capacity (pF 1.8 to 4.2) of the effective root depth (AG BODEN, 1994) are used as input parameters.

The analysis of soil samples and pumping tests in the frame of the GRC–project indicated that hydraulic conductivities in the study area are mainly influenced by geology, and usable field capacity additionally by landuse (UDLUFT ET AL., 2003). Thus, conductivity-parameterisation is based on the areal distribution of the different lithologies (Fig. 5). The usable field capacity matrix is formed by the usable field capacity per soil unit (mm/dm), defined for the single lithologies, multiplied by the effective root depth, determined for the different landuse classes according to SAXTON ET AL. (1986), and AG BODEN (1994). Starting values for all parameters are derived from proceeding investigations within the GRC-project and special investigations (MEDERER, 2005; DÜNKELOH, 2005A). These values are subject to calibration during the modelling process (Chapter 4.1.2, Table 5 and Table 6). Calibrated values are shown in Fig. 13 for usable field capacity, in Fig. 14 for subsoil permeability respectively, and for all three parameters in Table 5. Highest soil and subsoil hydraulic conductivities are estimated for the Quaternary terrace and alluvial deposits in the surrounding plains and Troodos valleys. The ultramafic rocks of the Troodos and Arakapas Sequence, the metavolcanics, as well as the silt- and mudstones of the Mamonia Terrane show relatively low conductivities. The upper Troodos exhibits a broad range of effective field capacity values. While loamy forest soils with a high root depth, covering Gabbro and Sheeted Dyke lithologies, show highest values within the study area, low field capacities are assumed for the shallow Pillow Lava soils in the northern and eastern foothills and for the bare lands.

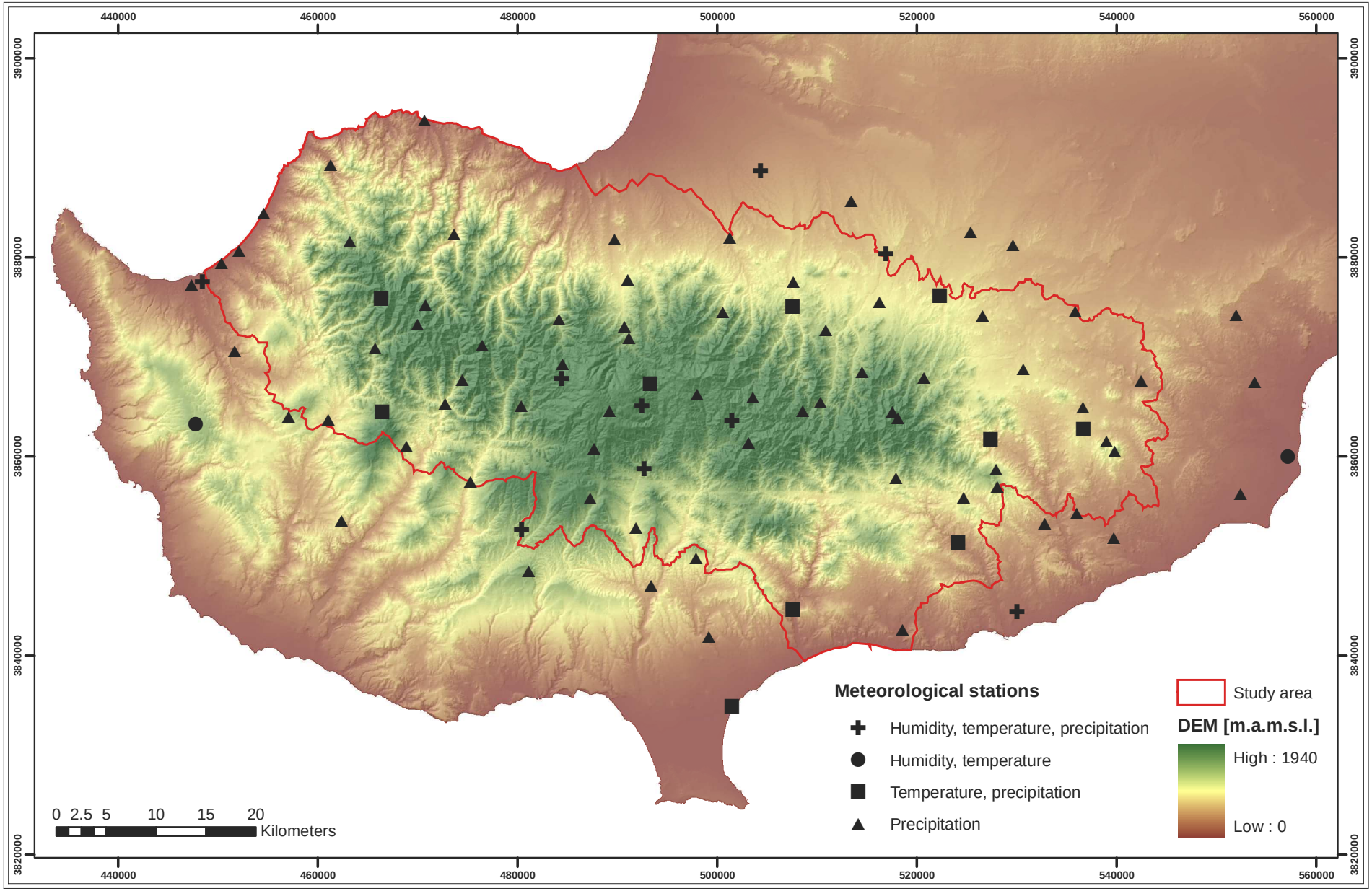

Fig. 9: Digital elevation model (DEM, raster size: 50*50 m), location of the study area and the meteorological stations used in the MODBIL model.

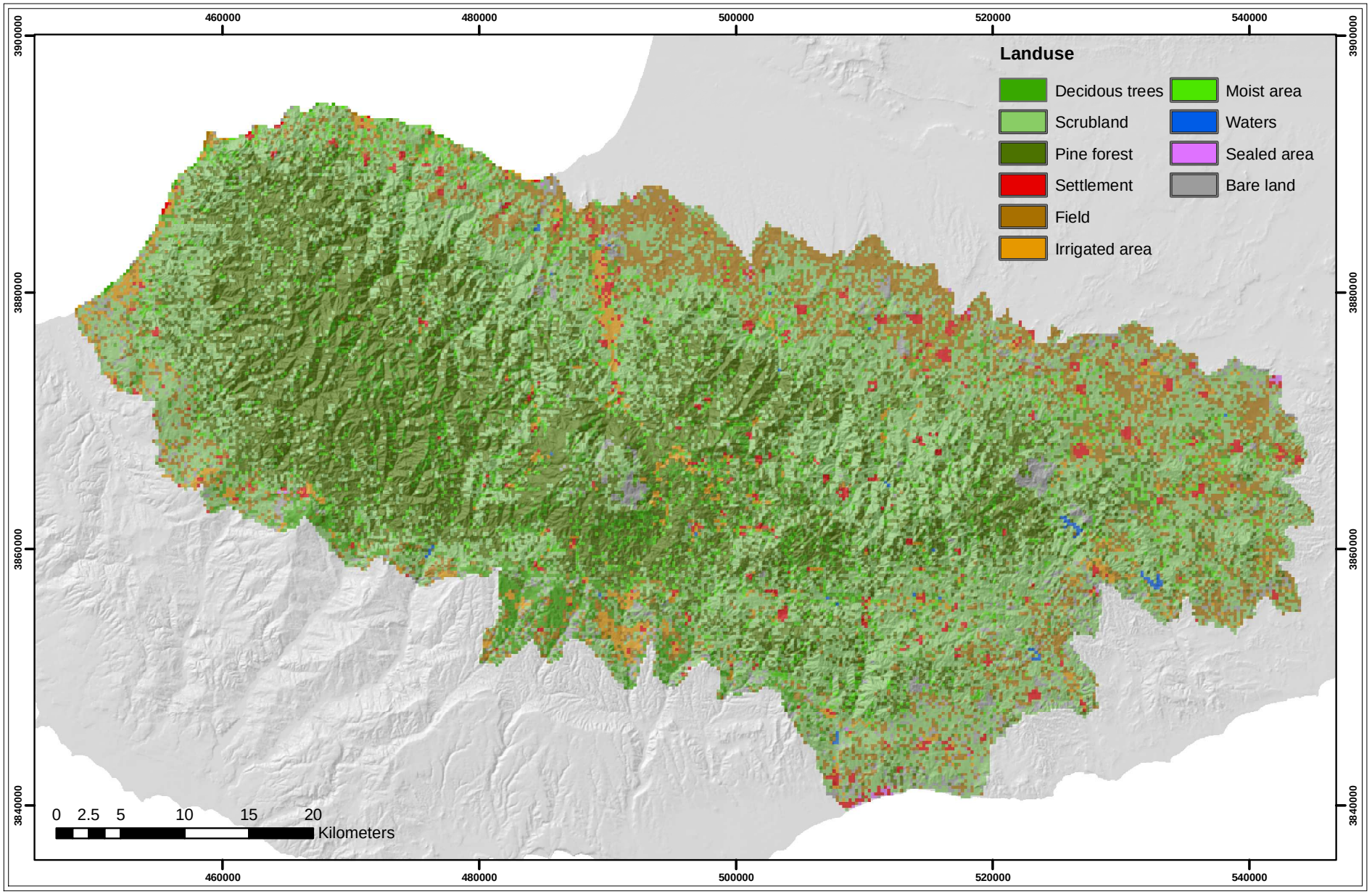

Fig. 10: Landuse of the Troodos study area.

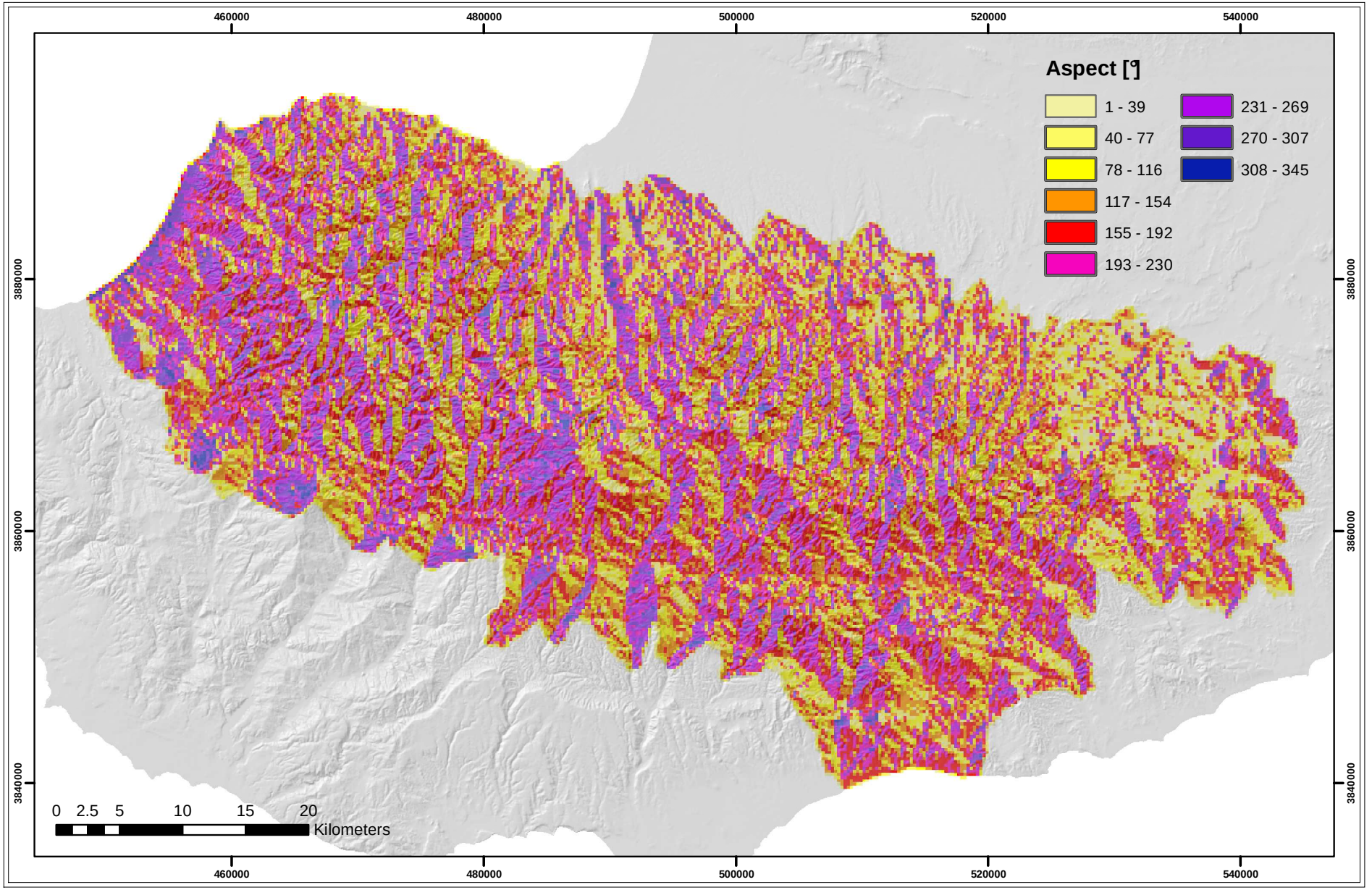

Fig. 11: Aspect map of the study area.

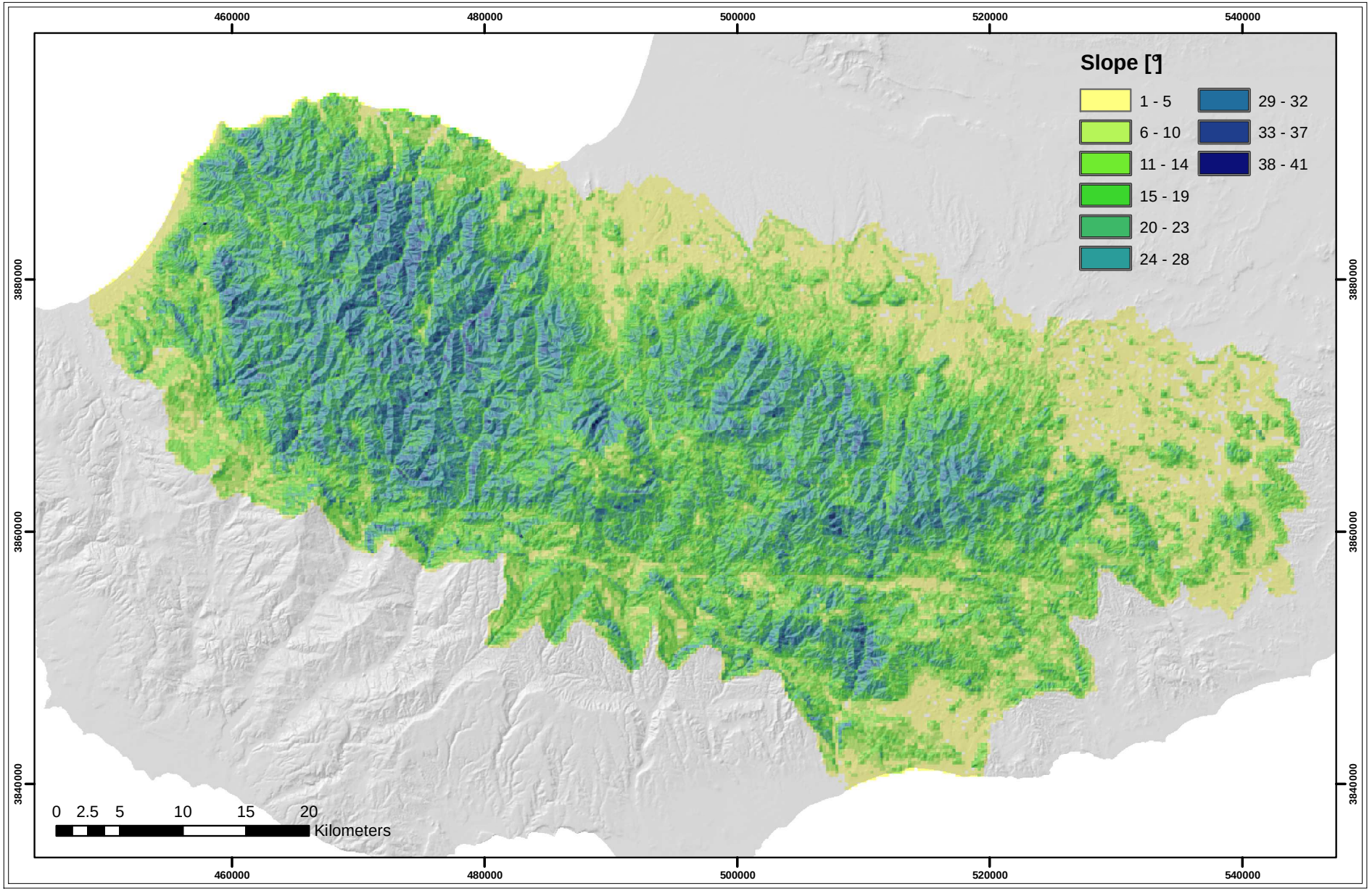

Fig. 12: Slope map of the study area.

4.1.2 Model calibration

Calibration is carried out manually by adjusting parameters by trial and error until model results match field observations with an accuracy of ± 10 %. Parameters subject to calibration are hydraulic conductivity of soil and subsoil, effective field capacity of the root depth, irrigation times, and a secondary evapotranspiration factor, which specifies the portion of potential evapotranspiration used to calculate the secondary evapotranspiration of irrigated areas. Field observations include total discharge and derived baseflow content of selected catchments (pilot catchments, Chapter 2.4). Calibration of the study area as a whole was not possible as not all discharging streams contained stream flow data over the modelling time period. Total discharge is determined using daily stream flow data from the ENVIS database. Baseflow contents are calculated as the arithmetic mean of the results of two methods: the semi-graphical method according to NATERMANN (1951) and the stream flow partitioning program PART (RUTLEDGE, 1998). GRC-investigations indicate that the Natermann method mostly yield baseflow contents about 5 to 10 % lower than the PART contents (UDLUFT ET AL., 2003).

The parameters are calibrated in the four pilot catchments (Chapter 2.4). These catchments represent the complete Troodos lithology, all landuse classes and the major exposition directions of the study area. Additionally, the selected rivers show predominantly effluent flow conditions. Lateral groundwater flow (inter catchment flow) is very likely to occur but is believed to lie within the desired maximum modelling error of ±10 %. Being part of the groundwater modelling studies, inter catchment flow of the pilot catchments and it's influence on the calibration quality is presented in Chapter 4.2.2.3.4.

In a first calibration attempt, parameters influencing evapotranspiration like effective field capacity and root depth, secondary evapotranspiration factor for irrigated areas and irrigation times (Chapter 3.1 and 4.1.3.2) are adjusted to match modelled to gauged total discharge of the single catchments. Irrigation time is set from April to September, the secondary evapotranspiration factor to 0.3.
The second calibration step includes the adaptation of soil and subsoil conductivities to match the ratio of modelled to calculated baseflow content.
The starting and calibrated values for the whole study area are shown in Table 5 and Table 6, Fig. 13 and Fig. 14. The quality control parameters for the single calibration catchments are noted in Table 7.

Table 5: Starting and calibrated hydraulic conductivities and field capacity values for the single geological formations (Fig. 5).

Formation	Soil conductivity [m/s]		Subsoil conductivity [m/s]		Effective field capacity [mm/dm]	
	starting	calibrated	starting	calibrated	starting	calibrated
Alluvium to Nicosia	1.00E-05	5.00E-05	5.00E-06	4.00E-06	13	13
Kalavassos, Pakhna	2.90E-06	2.90E-06	2.50E-07	2.50E-07	15	15
Lefkara to Perapedhi	1.80E-06	1.80E-06	2.00E-07	2.00E-07	15	15
Pillow Lavas	6.40E-06	5.00E-06	1.00E-07	2.50E-07	10	11
Basal Group	8.00E-06	8.00E-06	4.00E-07	7.00E-07	10	11
Sheeted Dykes, Plagiogranite	1.20E-05	1.20E-05	3.50E-07	4.00E-07	10	10
Gabbro	6.50E-06	6.50E-06	5.00E-07	6.00E-07	13	13
Pyroxenite to Dunite	7.80E-06	7.80E-06	2.00E-07	2.00E-07	11	11
Harzburgite, Serpentinite	7.80E-06	7.80E-06	8.00E-08	8.00E-08	11	11
Arakapas Lavas to Plutonic Rocks	6.00E-06	7.90E-06	3.00E-07	2.50E-07	12	12
Sheared Serpentinite	7.80E-06	7.80E-06	8.00E-08	9.00E-08	10	11
Ayia Varvara and Ayios Photios Group	2.00E-06	2.00E-06	1.00E-07	1.00E-07	11	11

Table 6: Starting and calibrated root depth values for the single landuse types.

Landuse (MODBIL class)	Root depth [dm]	
	Starting value	Calibrated value
Scrubland (class 2)	13.2	13.2
Pine forest (class 3)	16.8	16.8
Field (class 5)	9.6	8.0
Moist area (class 7)	18.0	19.5
Deciduous trees (class 1)	14.4	14.4
Bare land (class 10)	3.6	3.6
Irrigated area (class 6)	10.8	10.8
Settlement (class 4)	8.4	8.4
Waters (class 8)	-	-
Sealed area (class 9)	-	-

Table 7: Quality control parameters for the single calibration catchments (modelling period: 10/1987 to 09/1997).

Catchment	Total runoff [mm/a]		Baseflow content [%]	
	modelled	gauged	modelled	calculated
Upper Diarizos	160	166	68	72
Limnatis	111	115 *	60	58
Pyrgos	127	130	79	70
Kargotis	90	80	35	68

*) Transmission losses are not included

BORONINA ET AL. (2003) yielded baseflow contents of 70 % of total streamflow in the catchment of the River Kouris, reaching the order of magnitude of the present study's results (Table 7).

The quality control parameters indicate that the calibration target (maximum modelling error of ±10 %) is reached for total runoff in all catchments and for baseflow content in all but one catchment (Kargotis). In the Limnatis catchment the modelled total runoff reaches the lower acceptable limit when transmission losses are included into the calculation. In the GRC-project 10 to 15 mm/a transmission losses up to the gauging station in the Circum Troodos Sedimentary Succession were estimated (UDLUFT ET AL., 2003). Nevertheless, adaptations would have worsened the overall calibration result and have thus been neglected.

The Kargotis valley is the most intensely agriculturally used valley in the Troodos with a high percentage of irrigated lands (Kargotis: 9 %, Limnatis: 5%, Diarizos: 1 %). It is assumed that predominantly groundwater is used for irrigation and thus the baseflow content should be lower in the Kargotis catchment than the calculated average within the calibration areas. It cannot be excluded that the calculated baseflow content in this case overestimates the actual baseflow content.

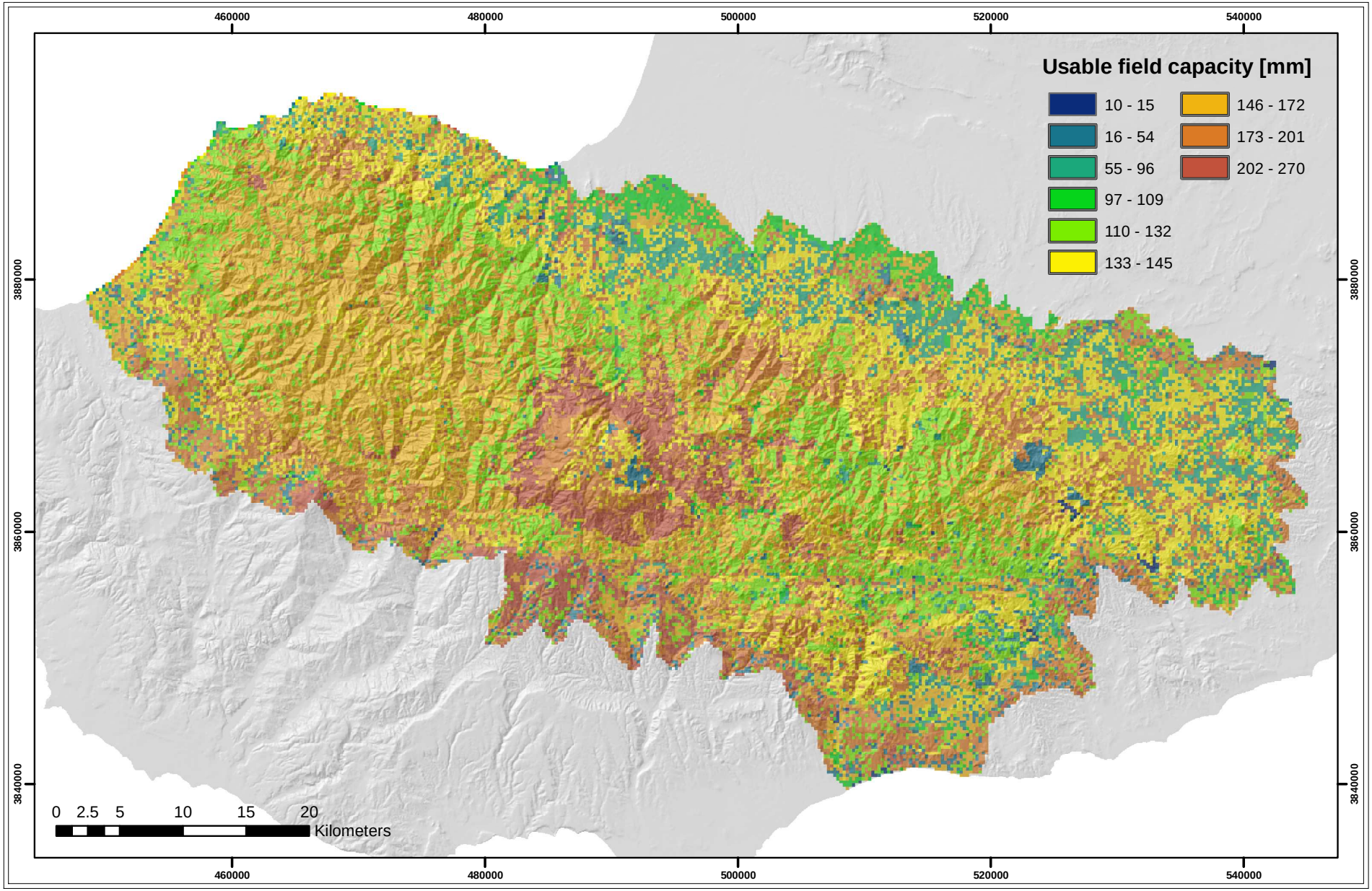

Fig. 13: Calibrated usable field capacity of the root zone in the study area.

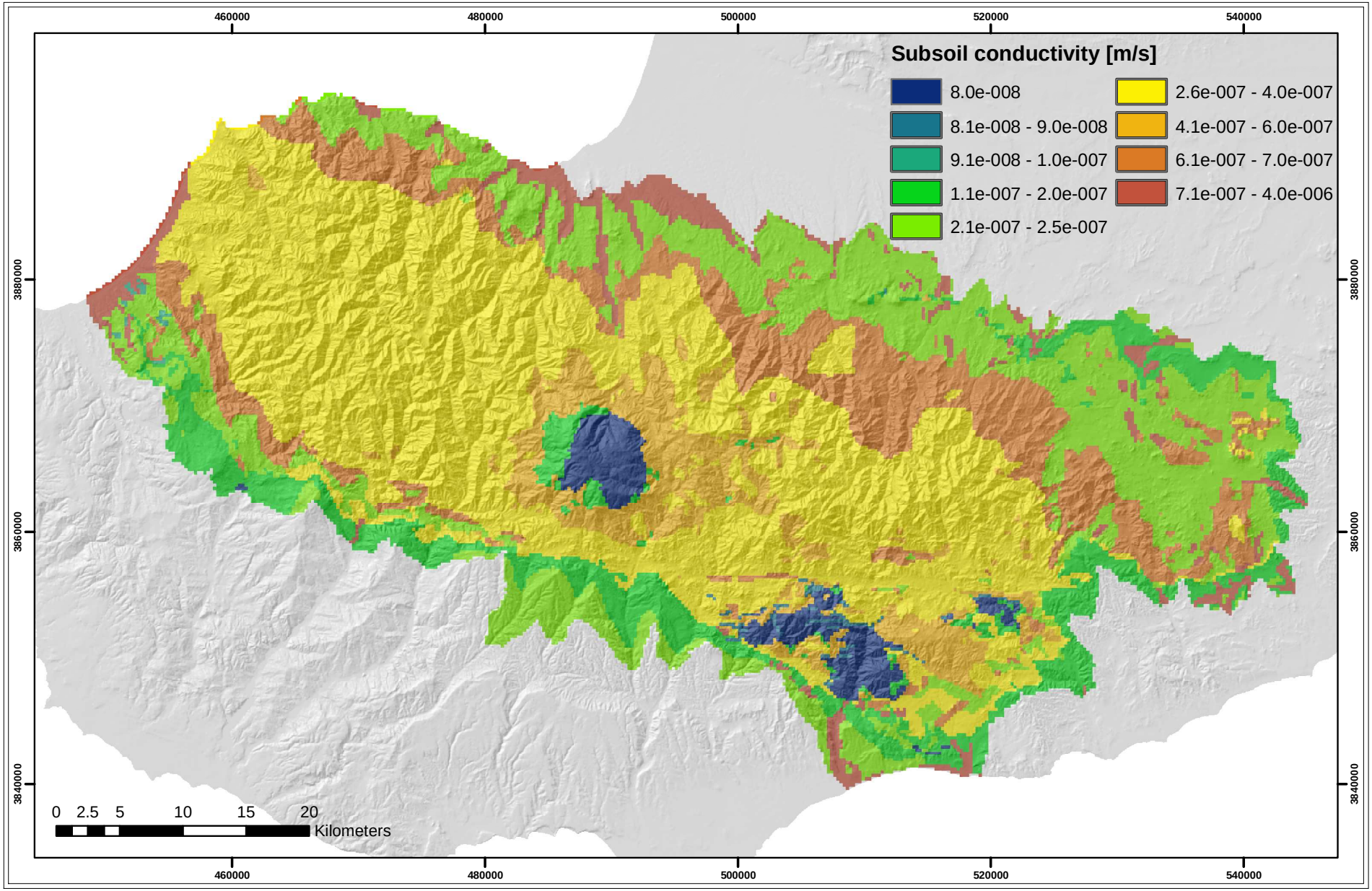

Fig. 14: Calibrated subsoil hydraulic conductivity of the different lithologies in the study area.

4.1.3 Results and discussion

The results of the MODBIL water balance modelling are presented in Table 8, results of the calibration models in the pilot catchments in Appendix C (Table 27, Table 29, Table 31 and Table 33). The single components comprise precipitation, actual and secondary evapotranspiration, surface runoff (incl. interflow), and groundwater recharge. Groundwater recharge and secondary evapotranspiration are presented in a more detail due to their importance for the balanced groundwater models. The concept of split secondary evapotranspiration into man-made and natural evapotranspiration is described in Chapter 4.1.3.2.

Table 8: Water-balance components* [mm/a] of the study area (10/1987-09/1997).

Precipitation	537
Actual evapotranspiration (incl. secondary)	461
Secondary evapotranspiration (Sec. ET)	69
Sec. ET of irrigated areas/settlements	18
Sec. ET of moist areas/waters	51
Interflow / surface runoff	28
Groundwater recharge	117

*)As the source for the secondary evapotranspiration is predominantly groundwater, the secondary evapotranspiration has to be subtracted from the groundwater recharge to yield total runoff (76 mm/a).

4.1.3.1 Groundwater recharge

For the scope of the coupled water balance and groundwater modelling approach, groundwater recharge plays the most important role of all water balance components. Besides indirect recharge, produced by transmission losses, inter basin flow or seawater intrusion, groundwater recharge forms the dominant direct input feature for the groundwater flow models. Analogue to interflow and surface runoff, groundwater recharge is influenced by all input parameters of the modelling process, above all precipitation sub-soil hydraulic conductivity. Highest groundwater recharge occurs in areas of high precipitation rates, high infiltration capacities and conductivities, and less steep slopes. This is the case in the Gabbros of the upper Troodos (max.: 390 mm/a) and to some extent in the Sheeted Dyke complex in the western Troodos (Fig. 16). Lowest recharge is produced in the impervious Serpentinites of the Arakapas Sequence and the Pillow Lava formations in the Troodos foothills (approx. 16 mm/a).

4.1.3.2 Evapotranspiration

Potential evapotranspiration in the study area ranges from 850 mm/a in the upper Troodos to 1821 mm/a in the northern and eastern lowlands (mean: 1386 mm/a). It shows a similar but reciprocal distribution compared to precipitation (Chapter 4.1.3.3). The distribution of actual evapotranspiration (Fig. 17) is similar although on a lower level. Landuse and soil water content influences are visible. Raster with secondary evapotranspiration emerge, due to high values bound to potential evapotranspiration (Chapter 3.1). They are located along river courses, settlements and agricultural areas with irrigation. The numerical distribution of the actual evapotranspiration is bimodal. A high number of values is grouped between 200 to 600 mm/a while another peak emerges from 1000 to 1400 mm/a, reflecting raster cells with secondary evapotranspiration.

4.1.3.2.1 Estimation of abstractions for irrigation

The MODBIL water balancing approach allows the estimation of man-made water abstractions for irrigation using the water consumption of secondary evapotranspiration of irrigated and settlement landuse raster cells. The secondary evapotranspiration of these landuse classes is shown in Fig. 18. The secondary evapotranspiration or water consumption for irrigation ranges from 101 to 869 mm/a. As the secondary evapotranspiration affects only selected raster cells the calculated mean for the whole study area is lower and yields here 18 mm/a.

4.1.3.2.2 Evapotranspiration of moist areas

Moist areas are usually situated close to springs, at river banks or flood plains of the effluently flowing upper and middle reaches of the Troodos rivers. Perennial shallow or outflowing groundwater causes increased evapotranspiration. This evapotranspiration is independent from precipitation dynamics and coupled to potential evapotranspiration. It is incorporated into the water balance as secondary evapotranspiration (Chapter 3.1). The secondary evapotranspiration is not included in the groundwater recharge calculation and has to be subtracted to yield total runoff (Table 8). In the groundwater flow models this is achieved by adding the MODBIL groundwater recharge as model inflow and secondary evapotranspiration as outflow (Chapter 4.2.2.1). As the flow models contain additional outflow in the form of abstraction through wells, secondary evapotranspiration has to be separated into a man-made portion (well abstraction) and a natural part (evapotranspiration through moist areas and open waters). Fig. 19 shows the distribution of moist areas and waters along the Troodos river valleys, ponds and lakes. In contrary to the actual evapotranspiration, the “natural” part of the secondary evapotranspiration is – due to the year-round water availability – controlled by potential evapotranspiration and ranges from

339 mm/a in the upper Troodos to 1367 mm/a in the lowlands and open water surfaces of the lakes. As the secondary evapotranspiration affects only selected raster cells the calculated mean for the whole study area is lower and yields here 51 mm/a.

4.1.3.3 Precipitation

Precipitation ranges from 200 to 300 mm/a in the lowlands to more than 1000 mm/a in the upper Troodos (Fig. 20). Elevation and exposition are important influencing parameters. The highest value is reached in the uppermost Troodos (1054 mm/a), the lowest (242 mm/a) in the northern lowlands at the inset of the Mesaoria Plain. It is interesting to note that the minimum is reached in the northern lowlands and not along the coastline. Additionally, north-exposed slopes receive relatively lower precipitation rates. This exposition dependency characterises the south to south west exposed slopes as the weather side of the Troodos mountains.

4.1.3.4 Interflow and surface runoff

Interflow and surface runoff depend basically on all input parameters. However geology, influencing soil and subsoil properties, plays in important role. Highest values (503 mm/a) are reached within the Serpentinite formation of the upper Troodos, where soil and subsoil permeabilities are low, precipitation and slope angles are high (Fig. 21). Medium values prevail in the Gabbro and Sheeted Dyke formations with medium to high permeabilites and medium precipitation. The Basal Group, characterised by higher subsoil conductivities and located close to the drier foothills, exhibits partly cells without surface runoff and interflow, while the overlaying low permeable Pillow Lavas produce several tens of mm per year. The mean interflow and surface runoff in the study area results 30 mm/a.

4.1.3.5 Comparison to GRC-project results

Within the GRC-project, the water balance of the Troodos was assessed for the area covering the ophiolitic lithologies of the Troodos and Anti-Troodos sub-terranes (Chapter 2.3). Compared to the present study, the Troodos region, investigated in the GRC-project includes the igneous lithologies without the Circum Troodos Succession belt. It covers thus a smaller area with a higher mean elevation and resulting higher precipitation rates. To compare the results, the output grids of the present study are downsized accordingly. The comparison of the two studies is shown in
Fig. 15 and Table 8.

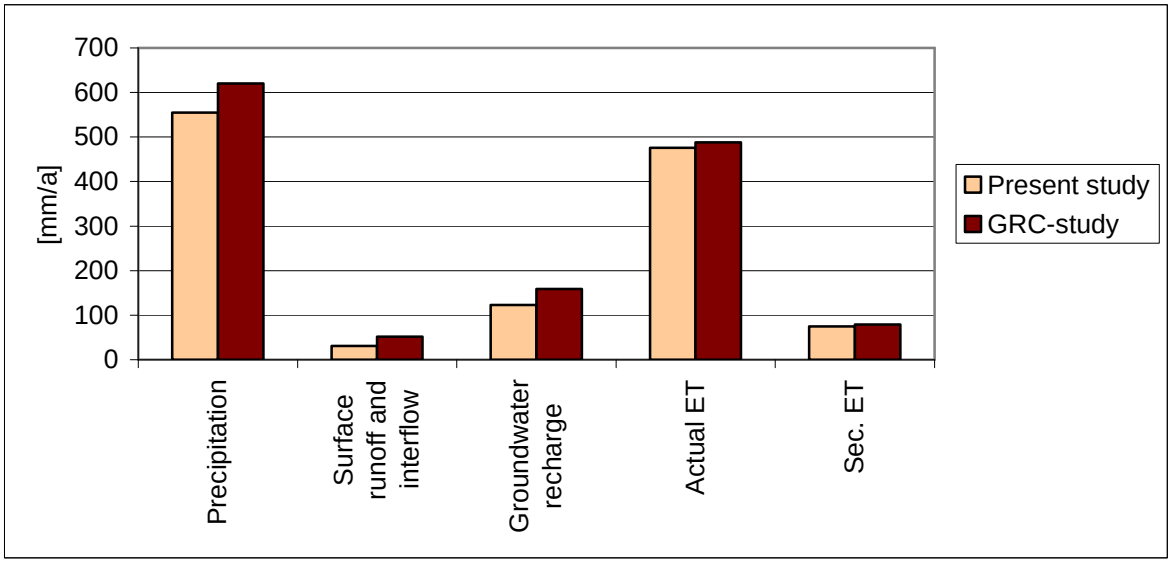

Fig. 15: Troodos water balance (10/1987 to 09/1997) of the present study (downsized to the Troodos area of the GRC-study) and the GRC-study.

Table 9: Single water balance components [mm/a] of the present study (downsized) and the GRC-study (10/1987 to 09/1997).

	Present study	GRC-study
Precipitation	555	620
Surface runoff and interflow	31	52
Groundwater recharge	123	159
Actual ET	476	488
Sec. ET	75	79

The precipitation rates of the two studies deviate largely (Fig. 15, Table 9). This might be due to the new interpolation scheme of meteorological data in the MODBIL version 48 used in the present study (Chapter 3.1). All stations with valid precipitation data can be incorporated. This should increase the accuracy of the MODBIL precipitation input raster in the high mountainous region of the Troodos, where local precipitation phenomena are difficult to model. The impact on the actual evapotranspiration is comparably small. While the precipitation is diminished by 10 % in the present study, the actual evapotranspiration decreases only by 2 %. Effective field capacities of the root depth influence the actual evapotranspiration and differences in parameterisation within the two studies have thus to be considered. There are differences concerning single root depths and field capacities but the study areas' mean effective field capacity of the root depth values are nearly identical (present study mean: 127 mm; GRC-study mean: 128 mm) and can thus be neglected.
Total runoff is affected strongest by the differences in precipitation. Groundwater recharge decreases by approx. 30 % and surface runoff and interflow by 66 %. These differences in decrease are mainly caused by model calibration, as the baseflow content of the gauged

total runoff determines the groundwater recharge content. As the groundwater recharge is “diminished” by the secondary evapotranspiration, which is merely constant in the two studies, the relative decrease has to be smaller compared to the decrease of surface runoff. This assures that the observed and calculated surface and baseflow content are on a similar level.

All in all, the comparison of the two studies might serve as an indicator, how decreasing precipitation rates affect the water balance in the Troodos. The relative decrease in total runoff and thus groundwater recharge is many times higher than the relative decrease in precipitation. This could indicate that the impact on water supply is greater than the decrease in precipitation implies.

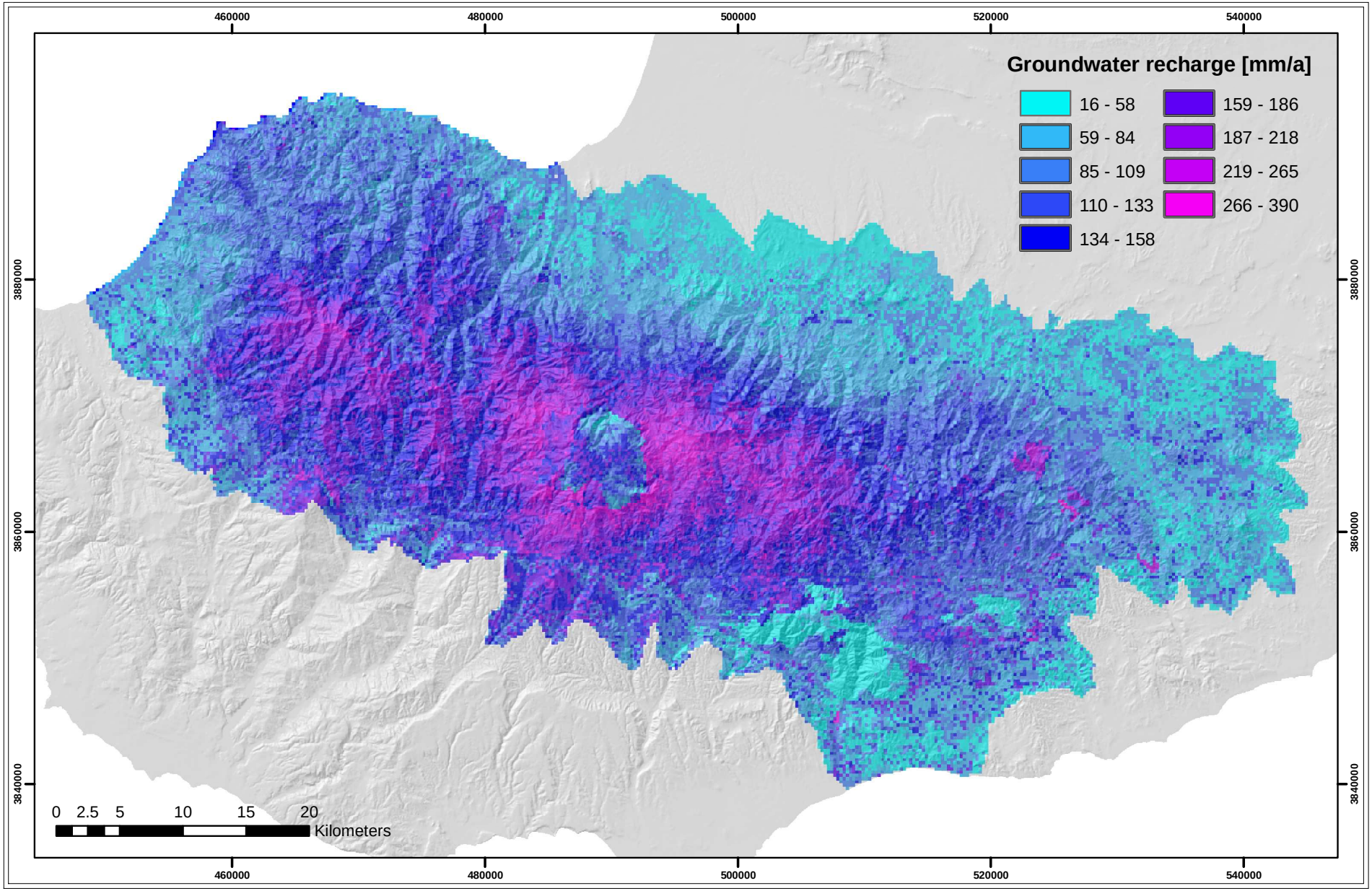

Fig. 16: Mean annual groundwater recharge in the study area.

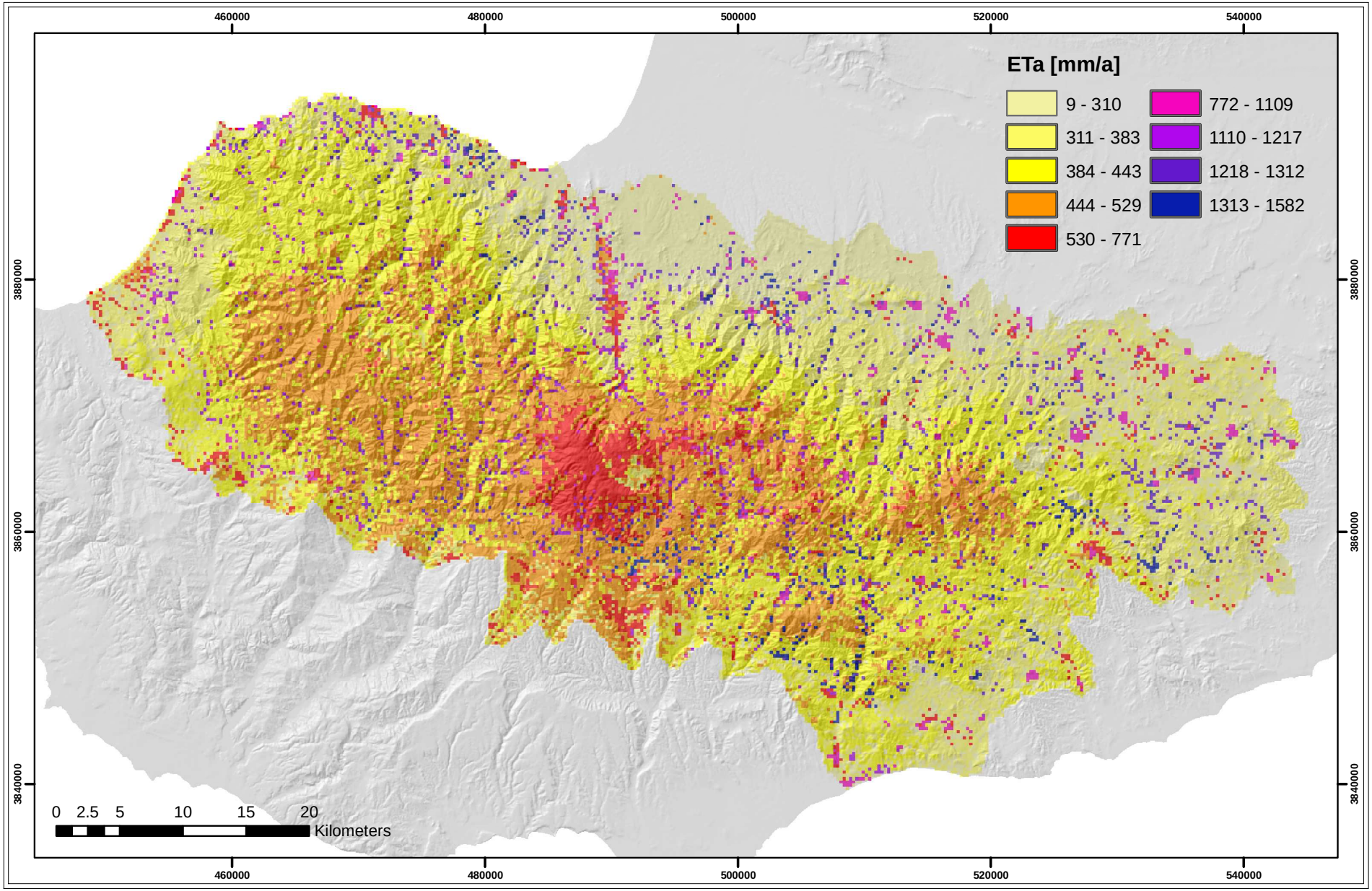

Fig. 17: Mean annual actual evapotranspiration (including secondary evapotranspiration) in the study area.

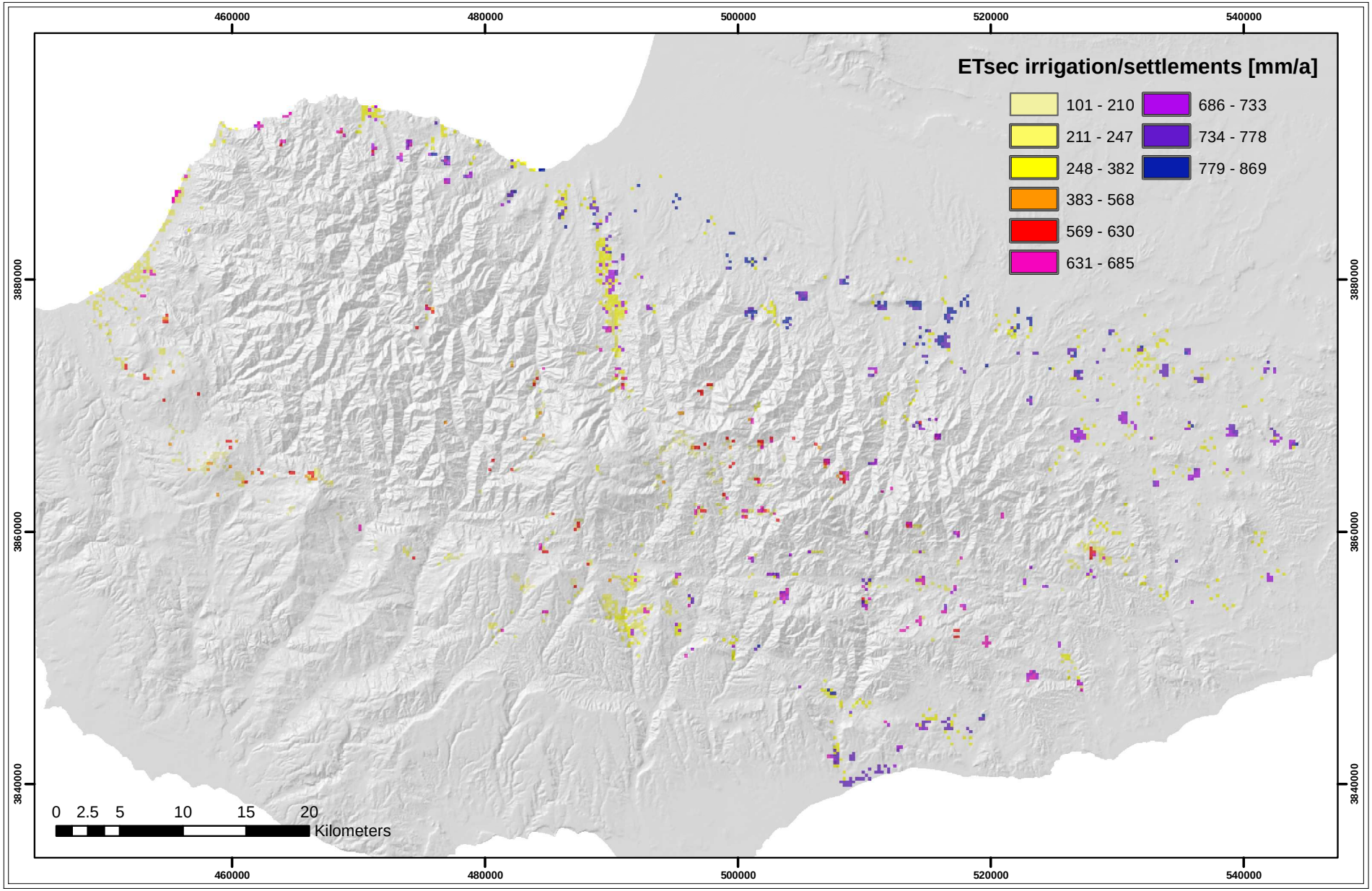

Fig. 18: Mean annual secondary evapotranspiration of irrigated area and settlement raster cells in the study area.

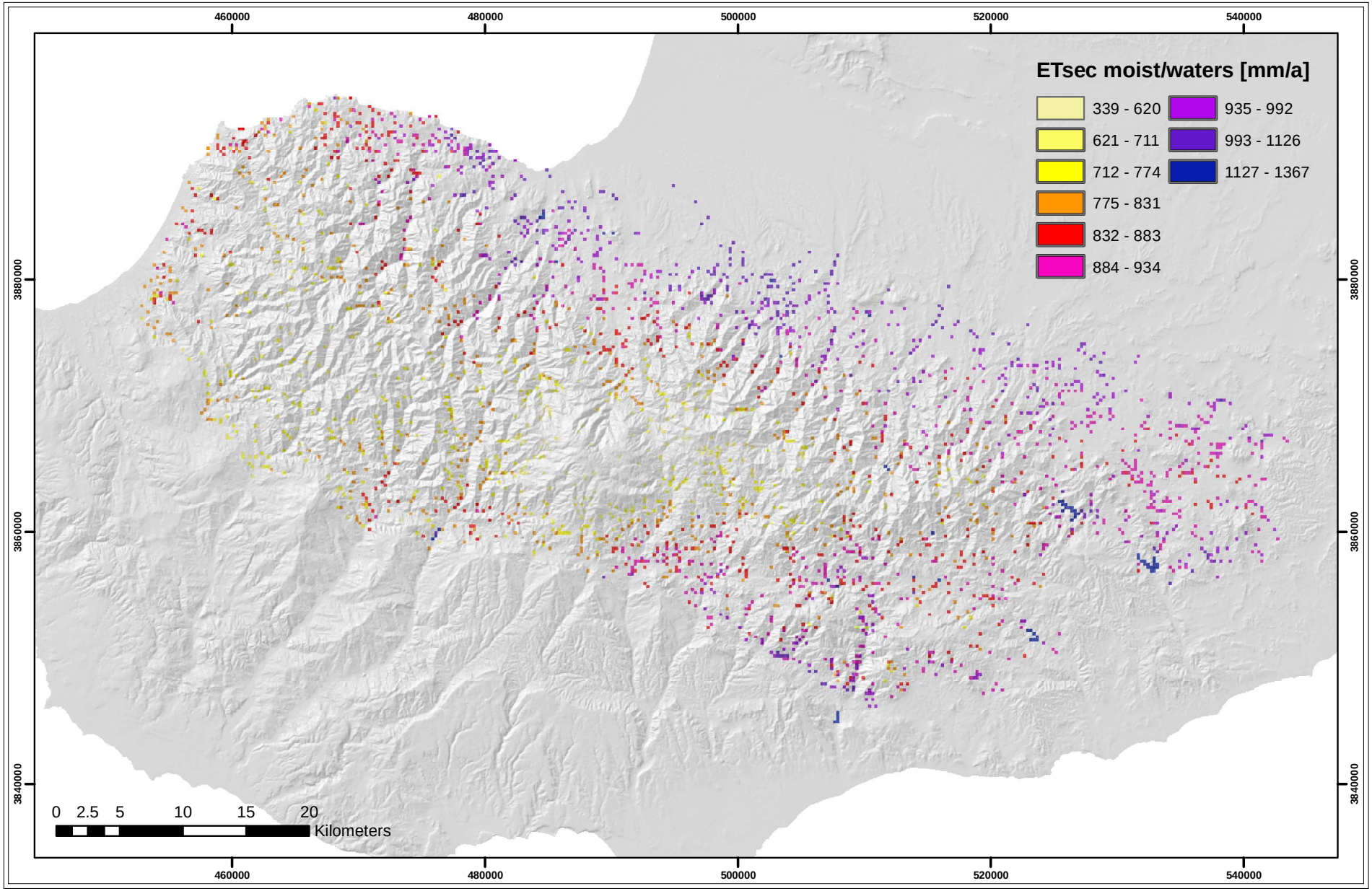

Fig. 19: Mean annual secondary evapotranspiration of moist area and waters raster cells in the study area.

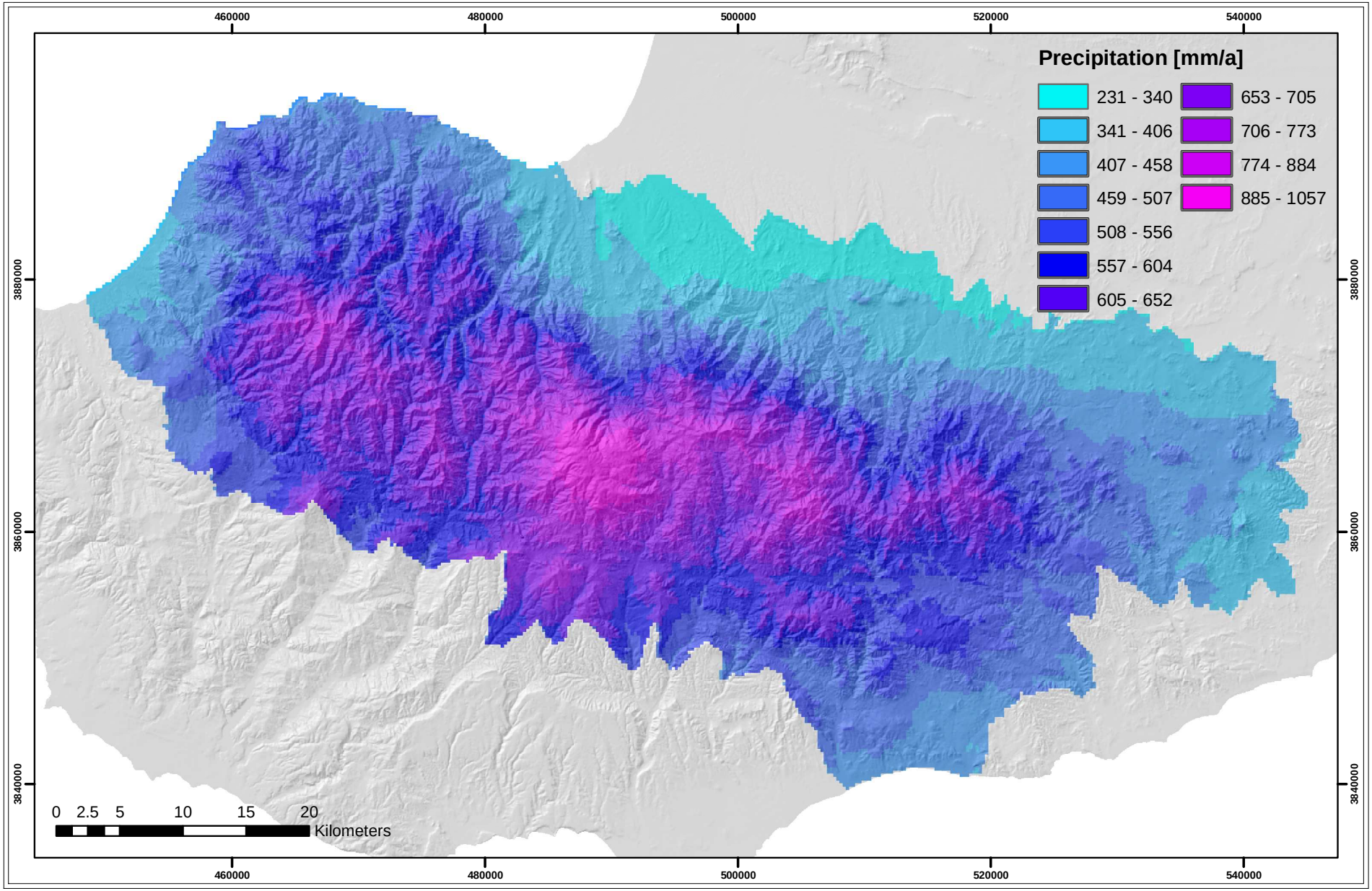

Fig. 20: Mean annual precipitation in the study area.

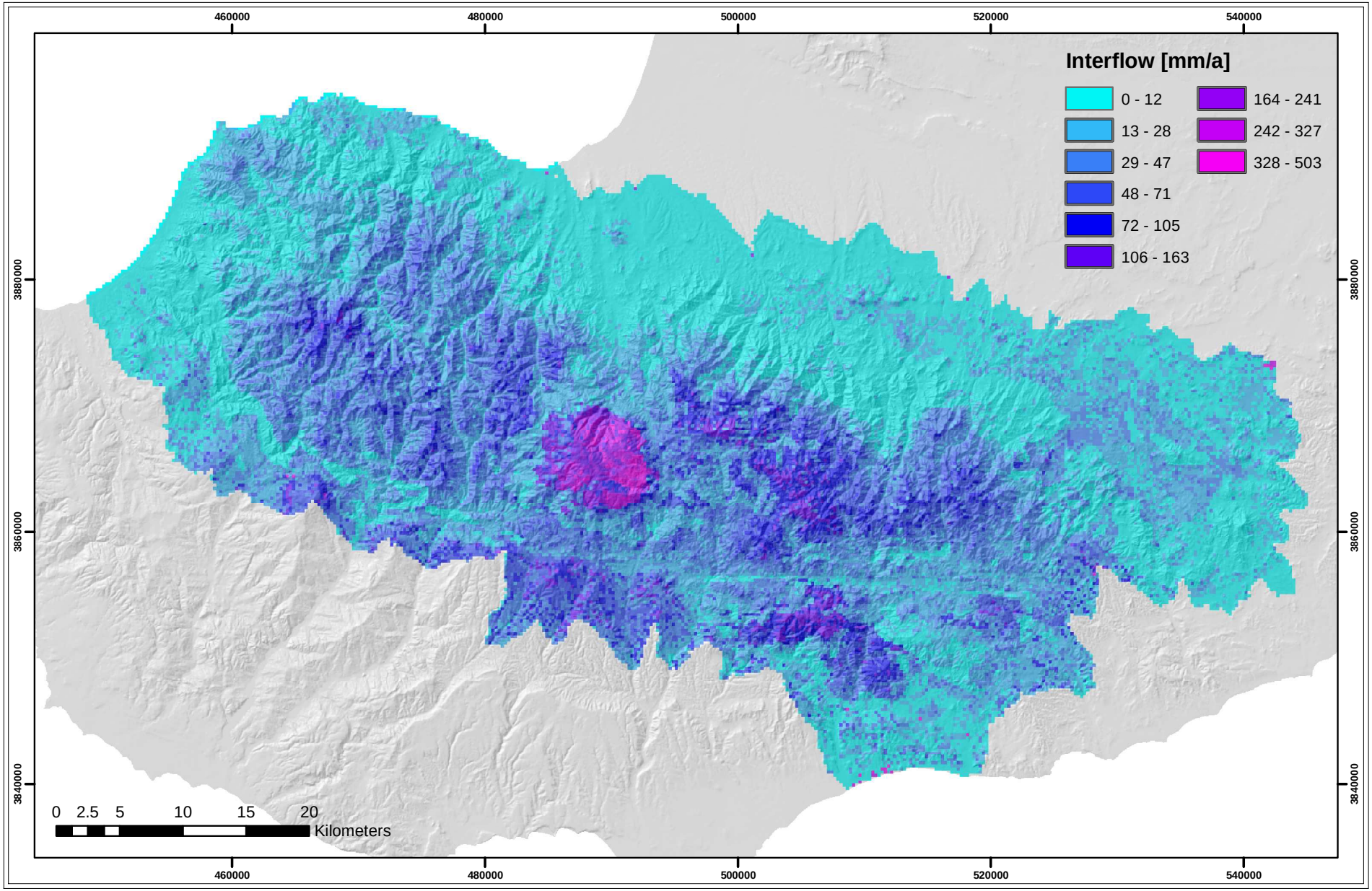

Fig. 21: Mean annual interflow and surface runoff in the study area.

4.2 Groundwater flow models

Groundwater models simulate and predict aquifer conditions with regard to groundwater quality and quantity and are thus tools for water management and decision support (KINZELBACH & RAUSCH, 1995). Additionally, they allow the determination of hydraulic aquifer parameters like transmissivity and porosity.

In the present study, the conditions of the Troodos fractured aquifer-system are modelled in two steps: First, the general flow dynamics are investigated using vertical, two-dimensional cross-section models, extending along the long and short axis of the study area. These models, developed by the author within the GRC-project (UDLUFT ET AL., 2004B, MEDERER & UDLUFT, 2004A, 2004B), are reworked and balanced with the water balance parameters of the present study (Chapter 4.1.3).
In a second step and based on the knowledge of the cross section models, a horizontal, regional groundwater model of the entire Troodos fractured aquifer-system is constructed, and different management scenarios are applied: A calibration scenario simulates actual conditions. A natural scenario eliminates all human impacts on the aquifer-system, and a strain scenario incorporates groundwater extraction rates satisfying an increasing water demand predicted for the year 2020 (SAVVIDES ET AL., 2001). Besides the management scenarios, groundwater flow studies within the pilot catchment areas show the influence of high mountainous topography on the groundwatershed and thus on inter catchment flow characteristics.

All models are balanced, including MODBIL groundwater recharge and split secondary evapotranspiration (Chapter 4.1.3.2). Therefore, the MODBIL modelling period, encompassing the hydrogeological years 1988 to 1997, is adopted.

4.2.1 Conceptual cross-section models

The models extend along N-S and W-E running cross-sections through the Troodos mountains up to the Mediterranean Sea. Three detail models are constructed: one along the N-S section and two for the W-E section (Fig. 22, Fig. 23 and Fig. 24).

The Kouris-Troodos-North model starts at the mouth of the River Kouris, passes the Arakapas Fault Zone, the upper Troodos and ends in the Kargotis valley close to the Morfou Bay. This section was chosen as it runs parallel to the main river drainage system of the upper Troodos and passes the major fault zone of Cyprus. It runs mostly along the river courses as this reflects the most stable hydraulic situation.
The Troodos West-East model ranges from the Gialia area in the West, crosses the Kouris-Troodos-North model in the upper Troodos region and ends in the Kornos area close to the

monastery Stavrovouni. For clearness reasons, the West-East model is cut into two separately processed models, the Troodos-West and Troodos-East model. These models run perpendicular to the main drainage system and will be used to study the lateral groundwater drainage characteristics in the Troodos Mountains.

4.2.1.1 Configuration

The groundwater flow models are conceptual, vertical one layer models and reflect conditions without artificial water extractions. Balanced MODBIL groundwater recharge (Chapter 4.1.3.1) is added as water input on the raster cells of the vertical layer that represent the earth's surface. Rivers are simulated with the river-package of PMWIN, allowing recharge and discharge from or to a constant storage capacity of the river-cells. Finally, the whole system is discharged by drain-cells simulating the open sea (Fig. 25, Fig. 26, Fig. 27).
For the special demand of modelling 2D-groundwater flow along vertical cross-sections, several layer characteristics have to be tested. To prevent the active grid cells from falling dry, the layer type is set to confined. The constant thickness in this vertical layer is 100 m. The grid size is set to 50 m length and 20 m depth to obtain an acceptable depth resolution .

Hydraulic conductivities and transmissivities were determined within Task 8 of the GRC-project through pumping test analysis (UDLUFT ET AL., 2004B; Table 24, Appendix B). The results are used as starting values, subject to calibration during the modelling process (Chapter 4.2.1.2).
Groundwater flow analysis with MODPATH requires effective porosity values for the single lithologies. For the specification of MODPATH as a one porosity model, the analysis and description of effective porosities is limited to the porosity with higher importance for groundwater flow (specific yield for porous aquifers and secondary permeability for fractured aquifers like the Troodos Ophiolite). Effective porosities of important Troodos lithologies were determined within the GRC-project (UDLUFT ET AL., 2004B) with a volume balancing method according to UDLUFT (1972), using a dissecation constant (MAILLET, 1905) and the "dewaterable" rock-volume of a specified aquifer. Table 1 shows the resulting porosities.

A depth factor corrects hydraulic conductivity and effective porosity (for details see UDLUFT ET AL., 2004B). Personal investigations and discussions with hydrogeologists of the Geological Survey Dept. of Cyprus led to the assumption that most of the groundwater percolates within the upper 150 m below surface. For this part, the depth factor is 1 meaning that the initial values are not corrected. Below 150 m up to 2500 m the depth factor is diminished exponentially by half a log cycle per 1000 m depth-increase (in 200 m steps). Below 2500 m the depth factor remains constant, implying that porosity and

conductivity increasing pressure solution processes in the rocks are in balance with porosity decreasing compaction.

4.2.1.2 Calibration

Hydraulic conductivity and parameters of the PMWIN river package are calibrated using a trial and error method. Due to the model configuration as a confined, one layer vertical model without artificial extractions, an adjustment of hydraulic heads to measured piezometry through observation wells was not practicable. Instead, heads are adjusted by avoiding internal sinks and overflow of single model cells. Additionally, hydrogeological information based on previous hydro-isotope and landuse investigations (UDLUFT ET AL., 2003; UDLUFT & KÜLLS, 2003) and discussions with Cypriot hydrogeologists are used. The results are shown in Table 10.

The parameters of the river package are calibrated in the Kouris-Troodos-North model as it runs parallel to the major drainage system. River leakage flowing into the model as indirect recharge and the amount of direct groundwater recharge are compared to reach a reasonable ratio. As the model is treated as a closed physical system, indirect recharge cannot exceed the amount of direct recharge. UDLUFT ET AL. (2003) postulate that indirect recharge in a semi-arid region might reach the order of magnitude of direct recharge. A ratio of indirect to direct recharge of 1 to 2 yields best results in the final calibration run.

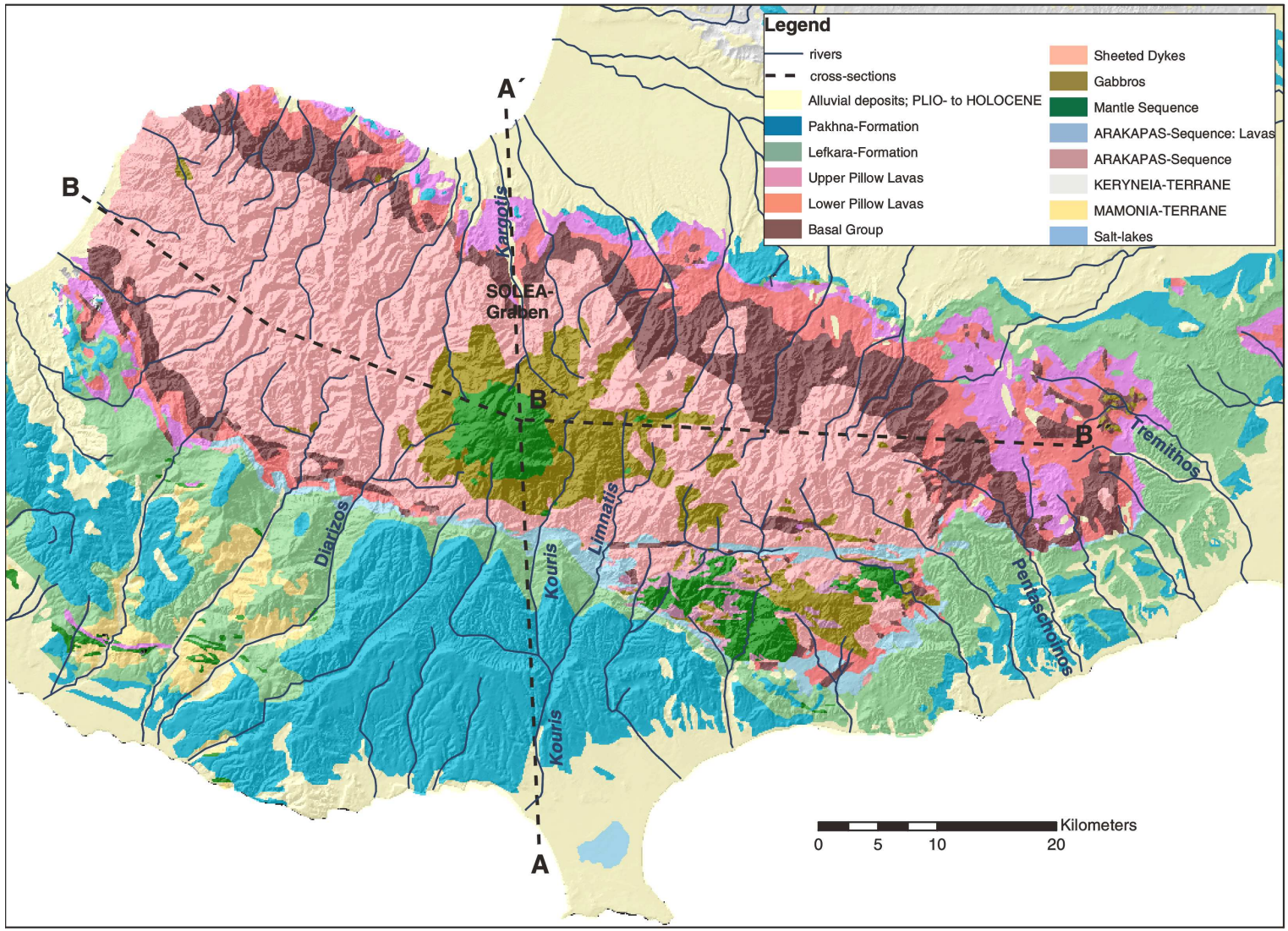

Fig. 22: Simplified geological map with the course of the cross-sections.

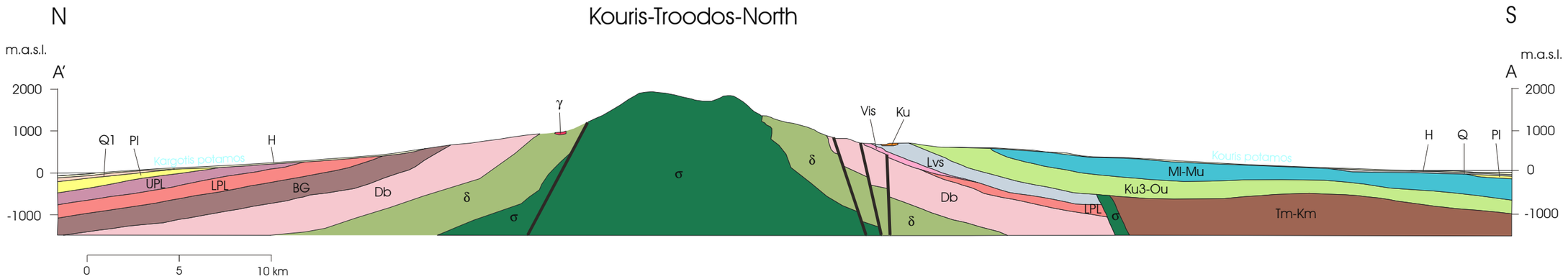

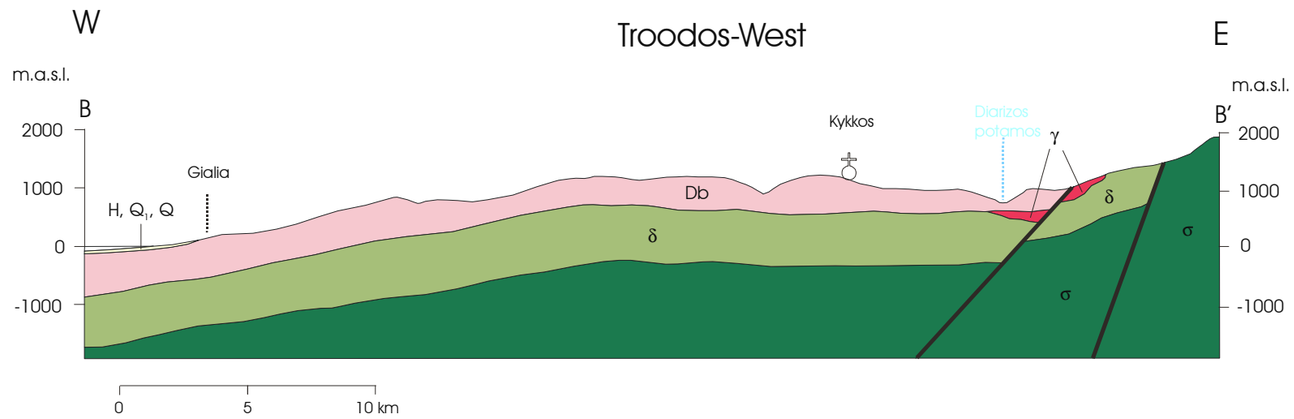

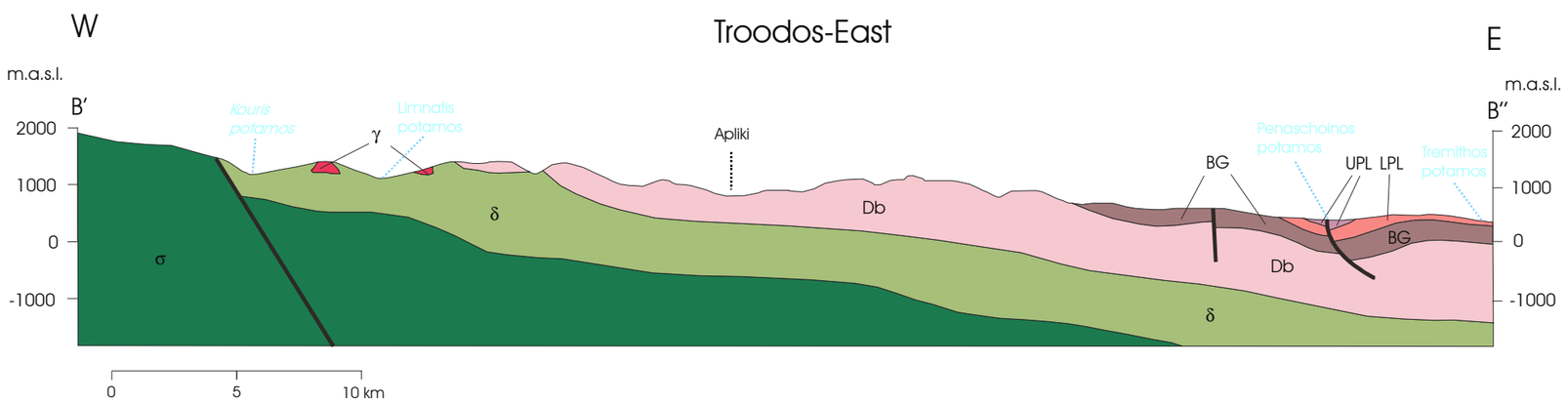

Fig. 23: Geological cross-sections of the study area, forming the base of the cross-section models.

Fig. 24: Legend of the geological cross-sections (Fig. 22 and Fig. 23).

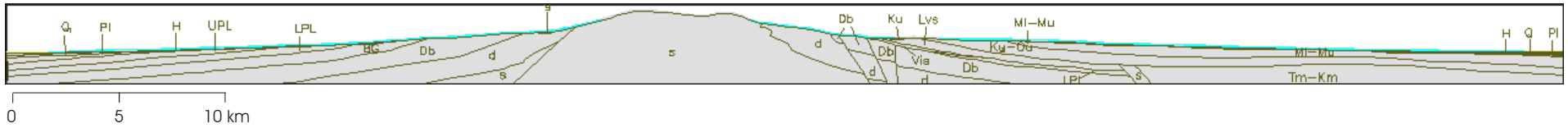

Fig. 25: Configuration of the Kouris-Troodos-North model (grey: active cells; blue: river cells; yellow: drain cells; no vertical exaggeration).

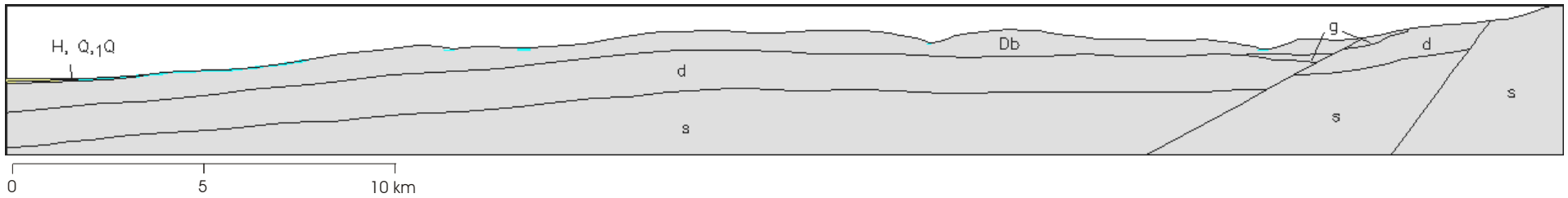

Fig. 26: Configuration of the Troodos-West model (grey: active cells; blue: river cells; yellow: drain cells; no vertical exaggeration).

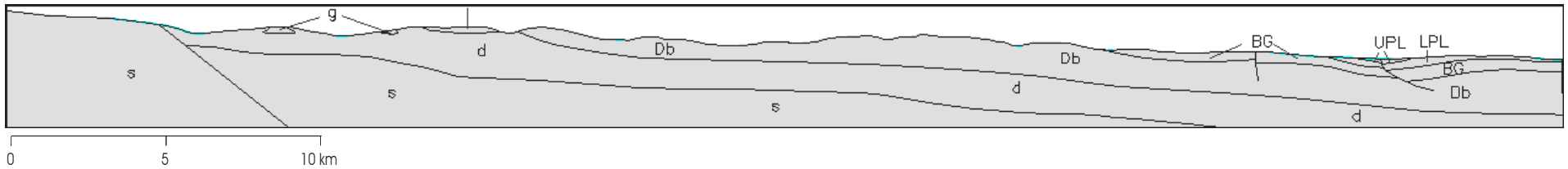

Fig. 27: Configuration of the Troodos-East model (grey: active cells; blue: river cells; yellow: drain cells; no vertical exaggeration).

Table 10: Measured and modelled aquifer properties of formations, regions and models based on pumping test results (Table 24, Appendix B).

Formation	Region	Models	Aquifer-thickness [m]		Hyd. conductivity [m/s]		Transmissivity [m²/s]		Hyd. conductivity [m/s]	Hyd. conductivity [m/s]
			min	max	min	max	min	max	mean	modelled
Ultramafics	Upper Troodos	All	20	50	5.89E-06	7.65E-05	2.06E-04	2.45E-03	4.40E-05	5.00E-08
Gabbro	Pitsilia, TroodosE	All	10	100	9.00E-07	1.20E-05	7.20E-05	1.20E-04	5.27E-07	1.20E-07
Sheeted Dykes	Troodos N	Kouris-Troodos N	45	110	1.55E-07	3.00E-06	5.40E-05	3.00E-04	7.94E-07	5.00E-07
Sheeted Dykes	Troodos E	Troodos E	20	175	1.14E-07	3.64E-06	1.14E-05	4.00E-04	6.90E-07	2.00E-07
Sheeted Dykes	Troodos W	Troodos W	10	90	2.25E-07	2.00E-05	2.25E-05	8.00E-04	8.68E-07	2.00E-07
Basal Group	Troodos N	Kouris-Troodos N Troodos E	10	70	2.14E-07	1.25E-05	1.50E-05	1.25E-04	6.35E-06	8.00E-07
Basal Group	Troodos N, NE	Troodos E	30	120	1.77E-07	6.67E-06	2.13E-05	2.00E-04	3.42E-06	8.00E-06
Basal Group	Troodos E	Troodos W	10	90	2.25E-06	9.00E-05	1.80E-04	5.50E-03	2.03E-05	6.00E-06
Pillow Lavas		All	30	50	1.20E-06	1.50E-05	6.00E-05	3.00E-04	6.60E-06	7.00E-08
Transform Lavas and Breccias	Troodos S	Kouris-Troodos N	20	50	1.80E-06	1.20E-05	9.00E-05	3.00E-04	6.65E-06	6.50E-07
Lefkara-chalks	Troodos S	Kouris-Troodos N	35	150	3.00E-07	4.00E-05	3.00E-05	1.40E-03	9.15E-07	2.50E-07
Pakhna-chalks	NW Lemesos	Kouris-Troodos N	20	165	2.00E-07	9.50E-06	1.20E-05	4.75E-04	1.76E-06	3.50E-07
Gravel	Kouris	All	25	80	8.10E-07	1.32E-04	6.48E-05	5.28E-03	5.72E-05	7.00E-05
Gravel	Troodos N	All	25	30	3.74E-05	1.01E-04	9.35E-04	2.53E-03	8.90E-05	7.00E-05

4.2.1.3 Results and discussion

4.2.1.3.1 Kouris-Troodos-North model

Vertical groundwater movement prevails in the upper Troodos, while sub-horizontal, undulating flow dominates the Troodos foothills and coastal plains (Fig. 31, Fig. 32 and Fig. 33). The transition of steeply inclined slopes of the ultramafic core to the smoother Gabbros' topography favours groundwater outflow along the lithological borders. A second region of preferred outflow is observed in the low permeable Pillow Lavas and Basal Group formations of the Kargotis valley (Fig. 32). The Pillow Lavas form a barrier, endorsing a relative groundwater rise. Remarkable is the quasi stratiform groundwater flow in the Gabbro and Sheeted Dyke lithologies (Fig. 32), especially in the Upper Kargotis valley where the dip of the layers is sub-parallel to topography. In the southern part of the model, the Arakapas Fault Zone forms a groundwater drain with deeply incised valleys and heavily fractured rocks (Fig. 33). Part of the Troodos groundwater flows through the fault zone and recharges the lithologies of the Circum Troodos Sedimentary Succession as isotope investigations of UDLUFT & KÜLLS (2003) and BORONINA ET AL. (2005) postulate. Low hydraulic conductivities and relatively high effective porosities of the Ultramafics in the upper Troodos explain the observed groundwater travel times of several hundreds of years (for deeper percolating groundwater even thousands of years), while groundwater flow in the Gabbro or Sheeted Dyke lithologies is mostly limited to a few tens of years (Fig. 31, Fig. 32 and Fig. 33). Isotope investigations of UDLUFT & KÜLLS (2003) yielded groundwater ages greater than 50 years in two wells of the Arakapas fault zone and in the Basal Group, representing the slow percolation system originating in the upper Troodos and discharging to the sea, the Arakapas fault zone or the sediments of the Circum Troodos Sedimentary Succession. The bulk of samples represented the fast draining system with inferred ages of 10 to 15 years or less (Chapter 4.2.2). BORONINA ET AL. (2005) reports residence times of ten years or less in 12 of 14 springs in the Upper Kouris catchment supporting the results of the present study. However, the small number and the regional character of the samples limits their expressiveness.

Fig. 28 and Table 11 show the water budget parameters for the Kouris-Troodos-North model. Approx. 20 % of the total model inflow end up as sea loss, while 80 % discharge in rivers and springs. The highest turnover rates are determined for the Alluvium (flow rate: 2.23E-02 m³/s), followed by the Terrace deposits, Lefkara limestones, Basal Group, Sheeted Dykes, Gabbros, and Serpentinite lithologies with approx. 5.00 E-03 m³/s. High turnover rates of the low permeable Serpentinites are reasonable as they are situated in the high precipitation area of the upper Troodos. Nicosia and Pakhna formation, as well as the Pillow Lavas yield around 3.00E-03 m³/s. Lowest flow volumes (< 5.00E-04 m³/s) are detected for low permeable lithologies with a low areal extension in the model, like the Perapedhi formation and the Ayios Photios Group.

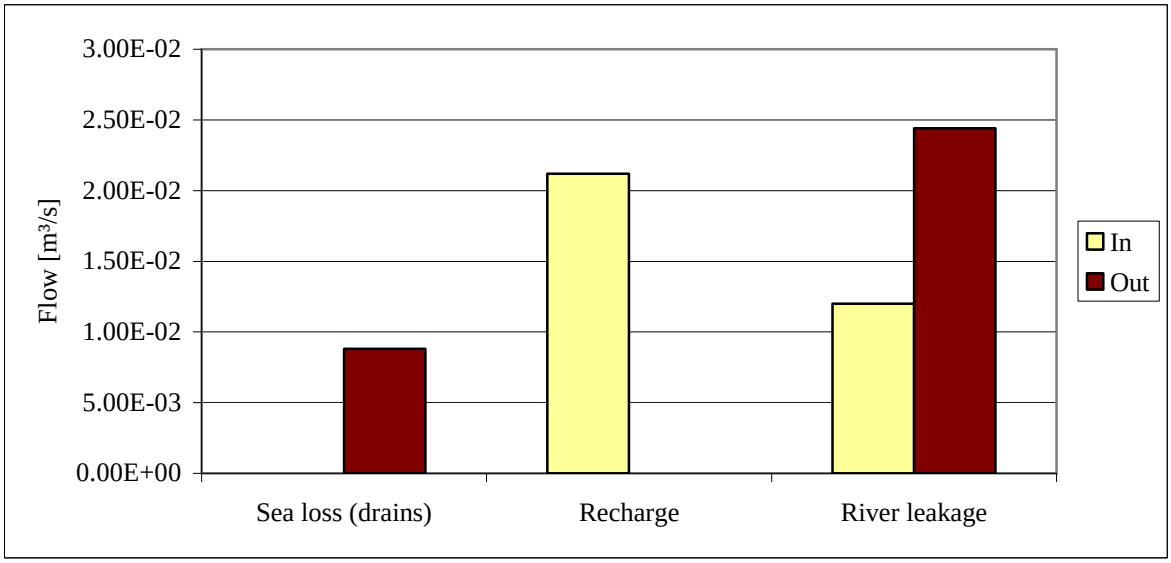

Fig. 28: Water budget of the Kouris-Troodos-North model (10/1987-09/1997).

Table 11: Water budget of the Kouris-Troodos-North model (10/1987-09/1997).

Flow term [m³/s]	In	Out	In-out
Sea loss (drains)	0.00E+00	8.80E-03	-8.80E-03
Recharge	2.12E-02	0.00E+00	2.12E-02
River leakage	1.20E-02	2.44E-02	-1.24E-02
Sum	3.32E-02	3.32E-02	2.10E-07

4.2.1.3.2 Troodos-West and Troodos-East model

Both models run perpendicular to the main drainage direction of the Troodos. The flow characteristics are shown in Fig. 34 and Fig. 35. The fast drainage system in the non-ultramafic lithologies is even more pronounced as in the Kouris-Troodos-North model. Nearly all particles discharge within a time period of ten years (Fig. 34 and Fig. 35). This is consistent with residence times calculated by BORONINA ET AL. (2005).

As in the Kouris-Troodos-North model, vertical flow dominates the upper Troodos region but the flow depth seems to be lower. The upper Troodos is discharged by the Rivers Kouris and Limnatis to the east and the River Diarizos to the west. Groundwater flow from the Upper Troodos beyond these rivers seems to be prohibited by these deeply incised drains. In the Eastern Troodos, the Pentaschoinos and Tremithos catchments receive water from the upper Pediaios tributaries. This might increase the water availability in these catchments, which are situated in a regional fracture zone and show a high density of wells (Fig. 40).

The water budget parameters for the Troodos-West and Troodos-East model are shown in Fig. 29 and Fig. 30, Table 12 and Table 13. Sea loss occurs in the Troodos-West model. In both models, inflow through riverbed infiltration is negligible as they mostly cross the rivers in the upstream reaches, where effluent conditions prevail. Nevertheless, the downstream parts of the River Gialia in the westernmost part of the Troodos-West model (Fig. 34) and the River Pentaschoinos and Tremithos in the Troodos-East model (Fig. 35) show small amounts of infiltration (Table 12 and Table 13).
Besides hydrogeological and recharge characteristics, turnover volumes of the lithologies depend largely on the areal portion they share in the study area. Thus, the Sheeted Dykes show highest rates in both models (flow rate: 2.00 – 4.00E-02 m³/s), while the Gabbros in the Eastern model reach the order of magnitude of the Sheeted Dykes. Gabbros and Plagiogranites in the Western model and the Basal Group in the Eastern model reach approx. 1.00E-02 m³/s, while the remaining lithologies show turnover rates of 5.00E-03 m³/s and smaller.

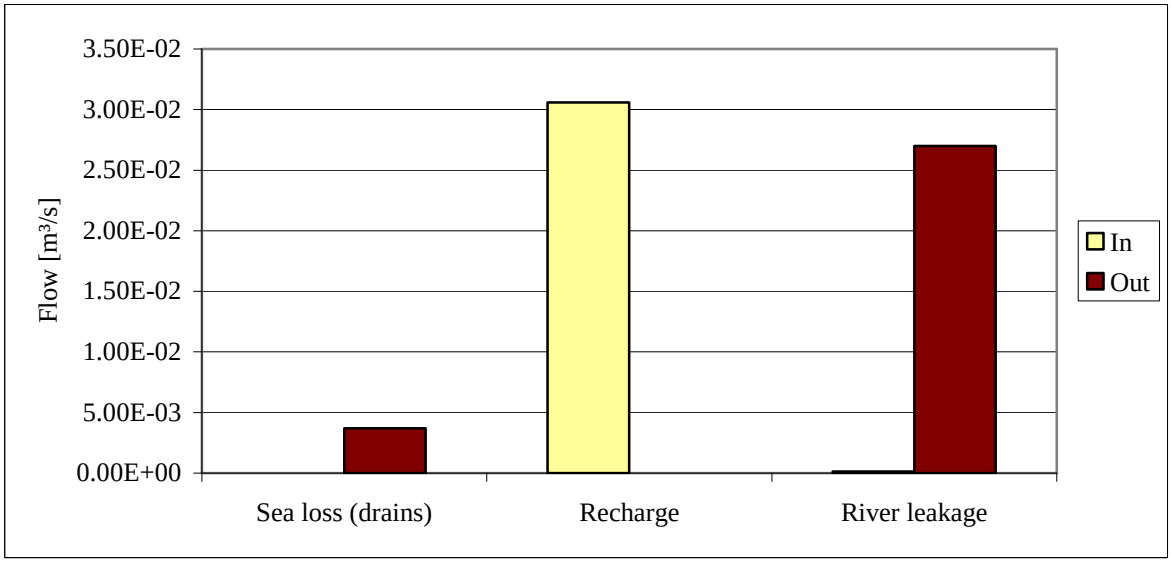

Fig. 29: Water budget of the Troodos-West model (10/1987-09/1997).

Table 12: Water budget of the Troodos-West model (10/1987-09/1997).

Flow term [m³/s]	In	Out	In-out
Sea loss (drains)	0.00E+00	3.70E-03	-3.70E-03
Recharge	3.06E-02	0.00E+00	3.06E-02
River leakage	1.30E-04	2.70E-02	-2.69E-02
Sum	3.07E-02	3.07E-02	3.00E-05

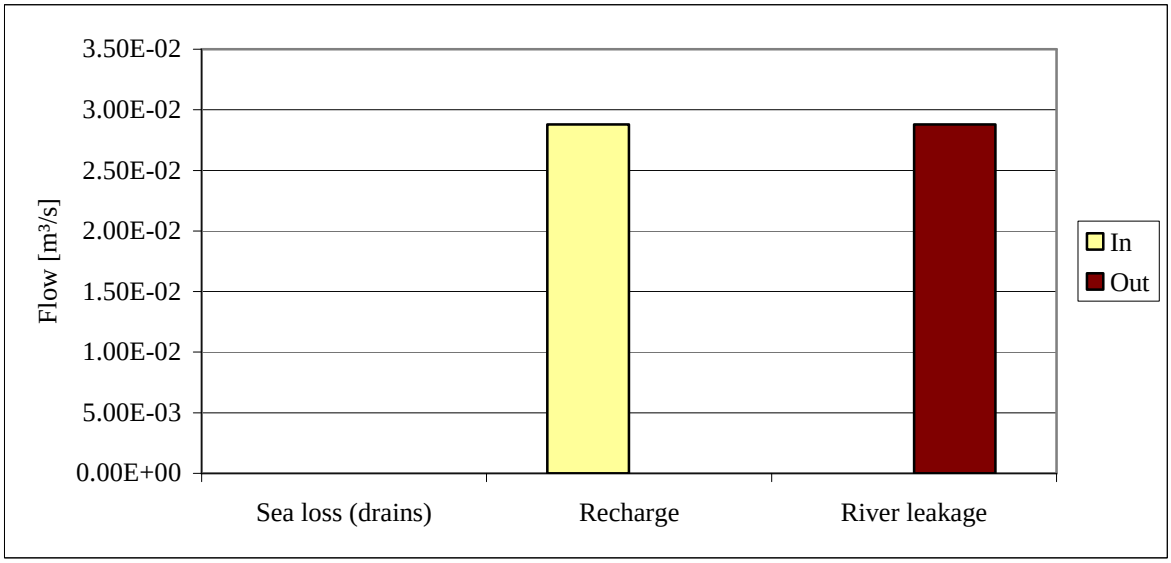

Fig. 30: Water budget of the Troodos-East model (10/1987-09/1997).

Table 13: Water budget of the Troodos-East model (10/1987-09/1997).

Flow term [m³/s]	In	Out	In-out
Sea loss (drains)	0.00E+00	0.00E+00	0.00E+00
Recharge	2.88E-02	0.00E+00	2.88E-02
River leakage	1.10E-05	2.88E-02	-2.88E-02
Sum	2.88E-02	2.88E-02	1.10E-05

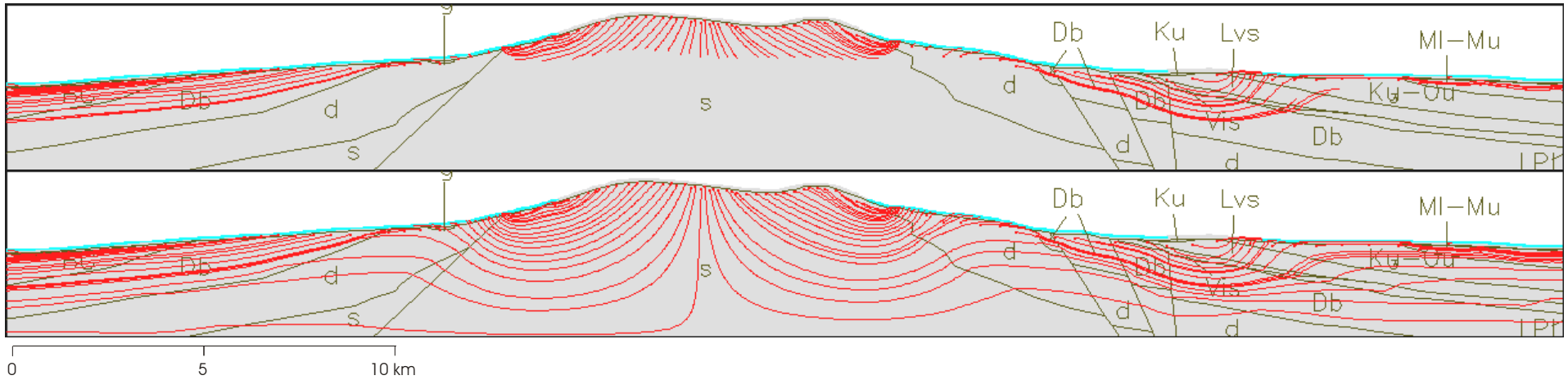

Fig. 31: Pathlines of the upper Troodos part of the Kouris-Troodos-North model for a time period of ten and 500 years (no vertical exaggeration).

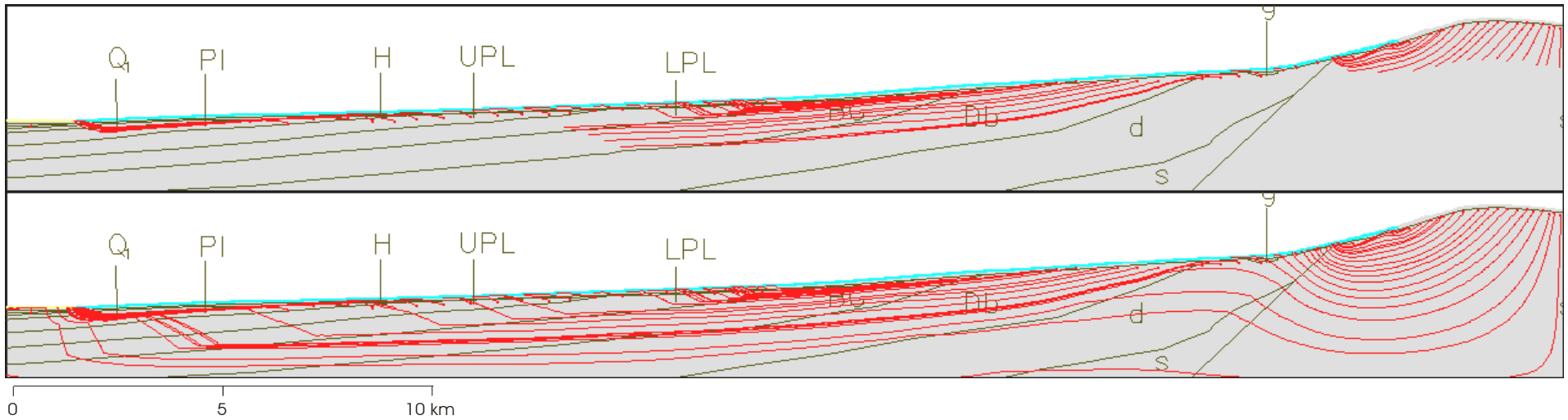

Fig. 32: Pathlines of the Troodos-North part (Kargotis valley) of the Kouris-Troodos-North model for ten and 500 years (no vert. exagg.).

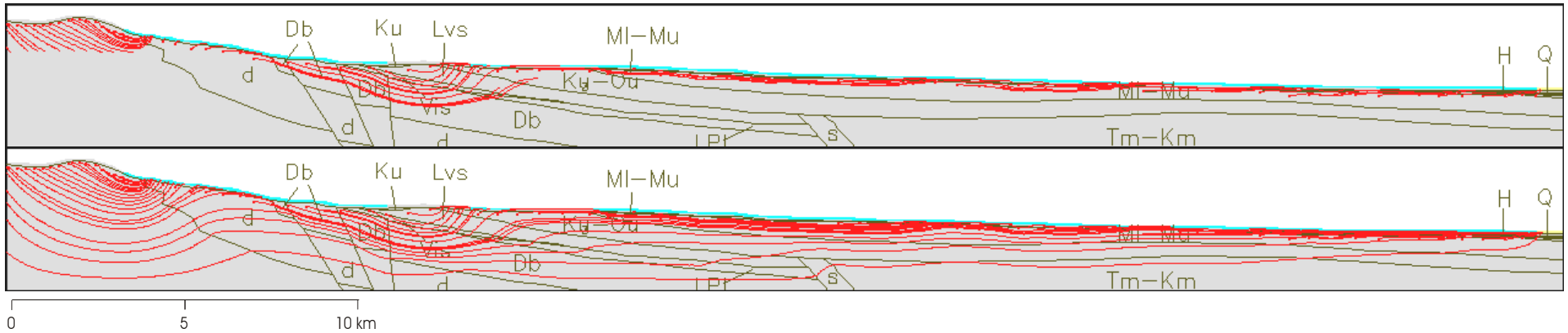

Fig. 33: Particle pathlines of the Troodos-South part (Kouris valley with Arakapas fault zone) of the Kouris-Troodos-North model for ten and 500 years respectively (no vertical exaggeration).

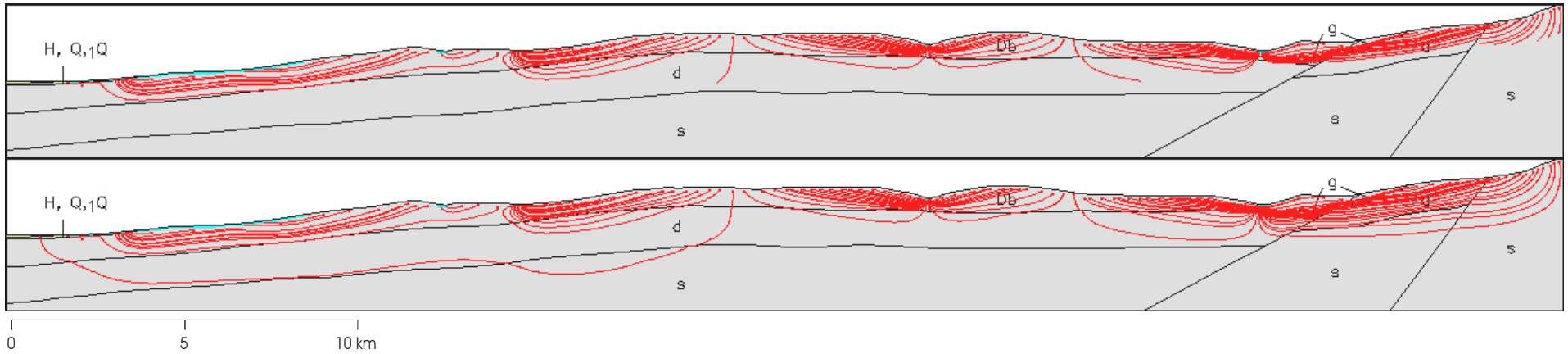

Fig. 34: Particle pathlines of the Troodos-West model for a time period of ten and 500 years (no vertical exaggeration).

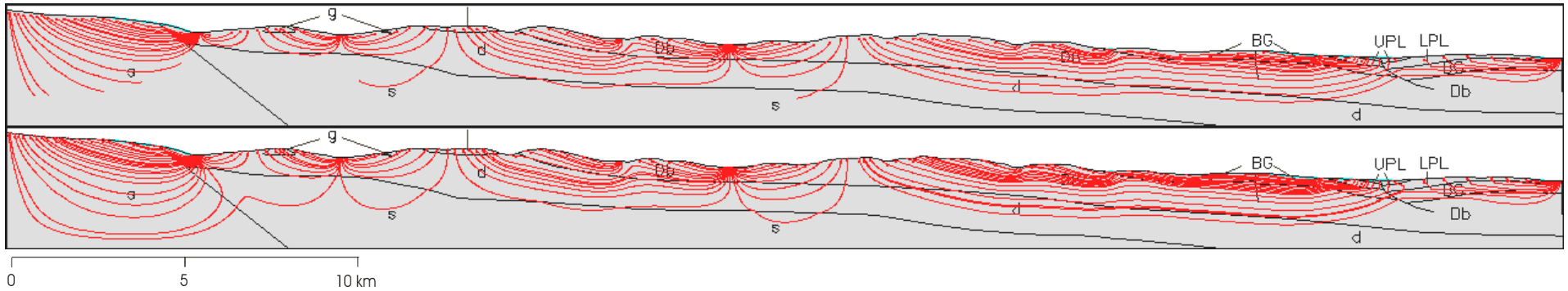

Fig. 35: Groundwater flow characteristics of the Troodos-East model for a time period of ten and 500 years (no vertical exaggeration).

4.2.2 Regional groundwater model of the Troodos

While the cross-section models focus on the general groundwater flow characteristics, the regional groundwater model emphasizes quantitative aspects. The regional model sets the base to manifold application feasibilities for water management. For the scope of this study, it is restricted to the analysis of different groundwater abstraction rates and lateral flow studies. In the calibration scenario, groundwater abstractions are simulated and quantified to reflect actual aquifer conditions. A "natural" scenario presents the restoration capabilities by simulating conditions without artificial abstractions. A third scenario reflects the aquifer response to increased abstraction rates to satisfy a predicted water demand of the year 2020.
The first step of the modelling process comprises the configuration and balancing of the groundwater model. MODBIL calculated groundwater recharge and secondary evapotranspiration (Chapter 4.1.3) are used as in- and outflow components. Well regions are defined in which the groundwater abstraction rates were adapted to meet the MODBIL calculated abstraction volumes (Chapter 4.1.3.2.1). After balancing, adjusting of hydraulic conductivities of the (hydro-) geological formations minimised the variation of modelled to observed water levels at selected wells until the calibration target was reached (Chapter 4.2.2.2). The calibrated model reflects the state of the aquifer within the modelling time period (Chapter 4.2.2.3.1) including the simulation of groundwater abstraction rates based on the MODBIL split secondary evapotranspiration concept (Chapter 4.1.3.2). Management scenarios are created by changing groundwater abstraction rates (Chapter 4.2.2.3.2 and 4.2.2.3.3).
The last part of the groundwater flow studies deals with the characterisation and quantification of inter-catchment flow in the pilot catchments of the upper Troodos (Chapter 4.2.2.3.4). A conductivity and abstraction rate sensitivity analysis concludes the regional modelling chapter.

4.2.2.1 Configuration

The model is configured as a one layer model with an average layer thickness of 300 m for the Troodos lithologies, and 150 m thickness for the overlying sedimentary formations (Fig. 5). Borehole log and pumping test investigations within the GRC-project indicate that the Troodos lithologies contain favourable aquiferous properties up to a depth of 150 to 200 m (UDLUFT ET AL., 2003). Due to model instabilities, the layer thickness had to be increased in the mountainous regions up to 300 m. The model raster comprises 48164 active raster cells with a constant raster edge length of 250 m. The active raster covers 3010.25 km² and thus nearly one third of the island's area.
The boundary conditions were set with the MODFLOW-IBOUND package of GMS. The active cells are usually bound by no-flow boundaries (Fig. 39). As modelling the fractured igneous aquifer-system of the Troodos is the main objective of this study, a buffer belt of 3

to 5 km width surrounding the fractured igneous aquifer in the range of the Circum Troodos Sedimentary Succession (Fig. 5) is established, to minimise disturbing influences on the head stage in the vicinity of the study area's boundary. The coastline is formed by specified head cells allowing water fluxes into and out of the model (Fig. 39).
Starting hydraulic conductivity values are applied to the single geological formations and are based on GRC-project studies (UDLUFT ET AL, 2003), and the present water balance and cross-section modelling procedures (Chapter 4.1.1.4 and 4.2.1.1).
Rivers are simulated using the river package (Fig. 39). Small, isolated and presumably influently flowing reaches in the lowlands or downstream of dams - as well as springs - are designed as drains. Lakes are simulated using general head cells, smaller ponds as river cells. General head conditions are specified – similar to river or drain cells - by assigning a head and a conductance to a selected set of cells. If the water table elevation rises above the specified head, water flows out of the aquifer. If the water table elevation falls below the specified head, water flows into the aquifer. In both cases, the flow rate is proportional to the head difference. Water inflow to the flow model was generated using the MODBIL calculated groundwater recharge (Chapter 4.1.3.1). The split secondary evapotranspiration concept (Chapter 4.1.3.2) is used to quantify part of he model's outflow. The secondary evapotranspiration of moist areas is incorporated with the GMS evaporation package, the evaporation of irrigated areas is simulated through abstraction wells. The model contains 1984 abstraction wells (Fig. 40), meeting the following thematic, temporal and spatial eligibility criteria: The wells have to be classified as abstraction wells in the ENVIS database, they have to be located in the study area and sunk before 1997, in accordance to the modelling time period from 10/1987 to 09/1997. 149 of these wells, containing groundwater level data, were used as observations (Chapter 4.2.2.2.1, Fig. 40).

4.2.2.2 Calibration

Calibration is performed in different steps, mostly by trial and error, and for the calibration of the hydraulic conductivities additionally with the parameter estimation module PEST (DOHERTY, 2004). First, well extraction rates and riverbed infiltration volumes are calibrated in the pilot catchments (Chapter 2.4) by baseflow balancing. Based on the results of the pilot catchments, *well regions* with uniform abstraction rates are defined for the whole study area. Well abstraction rates in the well regions are determined using the split secondary evapotranspiration calculated with MODBIL (Chapter 4.1.3). Abstraction rate adjustment is executed simultaneously in the pilot catchments and well regions. Using this approach, the calibration results of the pilot catchments can be extrapolated to the whole study area in accordance with the overall water balance. In a second step, the hydraulic conductivities of the different lithologies are customised to minimise the difference between observed and calculated groundwater levels, including local fine tuning of abstraction rates of single wells. In a final step, discharge of major springs and water levels of lakes are calibrated.

4.2.2.2.1 Observations

149 wells containing groundwater level data in the ENVIS database within the modelling time period are used as point observations (Fig. 40; Table 26, Appendix B). Groundwater level data exists for a few wells as time series but mostly as single measurement data. For the time series data, the modelling-time-average of the single wells is used. An error of less than 40 m in piezometric head difference is found to be reasonable in a high mountainous region with slopes ranging from 10 to 40 degree, and a raster cell size of 250 * 250 m.
The rivers of the four pilot catchments (Chapter 2.4) are used for flux observations (Table 14, Fig. 36).

4.2.2.2.2 Well abstraction rates, riverbed infiltration and spring discharge

Well abstraction and riverbed infiltration influence the runoff volumes, the water balance and the groundwater level and are thus calibrated first. Analogous to the MODBIL water balance procedure, calibration is carried out exemplarily in the pilot catchments (Chapter 2.4). The results are extrapolated into so called *well regions* (Fig. 40) with constant abstraction rates and consistent hydrogeological and landuse properties, to ensure the compliance of the study area's water balance with the MODBIL water balance. Starting abstraction rate values for the single well-regions are based on the pilot catchments and are counterchecked and adapted to the abstraction needs calculated with MODBIL (secondary evapotranspiration of irrigated areas and settlements). Calibration target is 10 % or less relative error, compared to the calculated baseflow content in the pilot catchments (Table 14, Fig. 36, Table 15; Chapter 4.1.2), and compared to the MODBIL derived water balance components in the well regions. The MODBIL derived water balances for the single well regions are shown in Appendix C (Table 35, Table 37, Table 39, Table 41 and Table 43). After the adjustment of hydraulic conductivities with the PEST module (Chapter 4.2.2.2.3) the abstraction rates are fine tuned in the final calibration step to minimise groundwater level errors.

Table 14: Quality control parameters (baseflow at gauging stations) and calibrated single well abstraction rates in the pilot catchments.

Pilot catchment	Single well abstraction rate [m³/s]	Observed* flow [m³/s]	Computed flow [m³/s]
Diarizos	0.00060	0.476	0.435
Limnatis	0.00092	0.275	0.264
Pyrgos	0.00055	0.111	0.120
Kargotis	0.00092	0.149	0.147

*) For details concerning the baseflow separation techniques see Chapter 4.1.2.

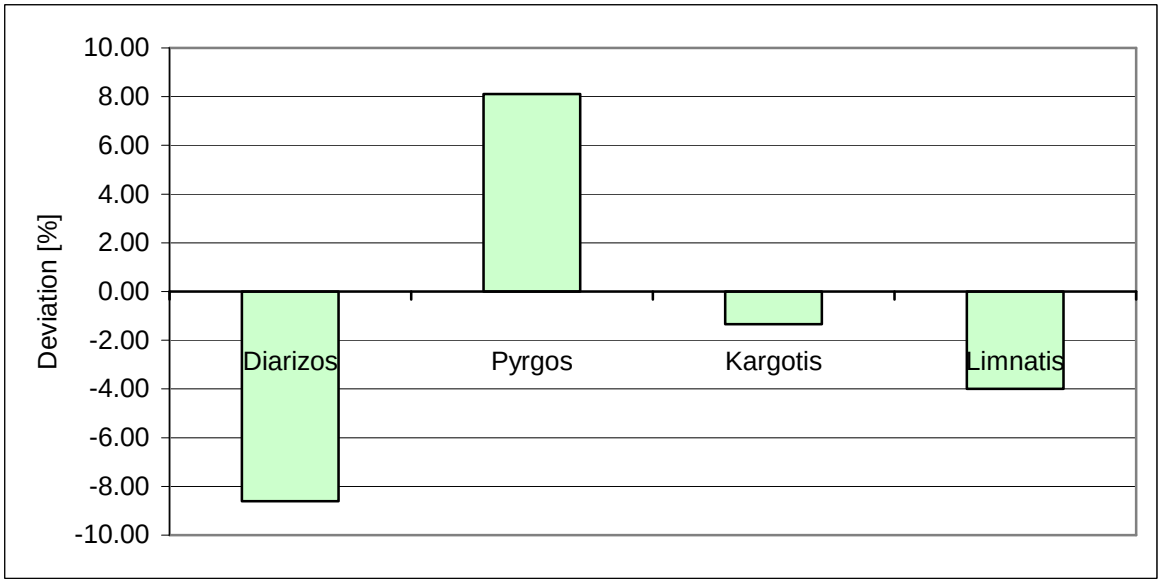

Fig. 36: Deviation (relative error) of computed to observed flow in the four pilot catchments. Calibration target is 10 % or less relative error.

Table 15: Quality control parameters and calibrated single well abstraction rates of the well regions.

Well region	Single well abstraction rate [m³/s]	MODBIL derived abstraction rate [m³/s]	Calibrated abstraction rate [m³/s]
Troodos NW	0.00055	0.198	0.179
Troodos SW	0.00060	0.083	0.076
Troodos Central	0.00092	0.717	0.709
Troodos NE	0.00050	0.304	0.193
Troodos SE	0.00090	0.305	0.279

Applying the MODBIL abstraction rate in the Troodos NE region yields drawdown values, exceeding the tolerable maximum. A reason might be the Vasilikos - Pentaschoinos Project of the Water Development Department that diverts large quantities of surface water from dams to irrigation schemes, resulting in lower groundwater portions in the irrigation waters in this area. As a consequence, the single well abstraction rates are lowered, yielding a regional abstraction rate deviating from the MODBIL calculated value (Table 15).

Hydraulic riverbed- and lake conductance (Chapter 3.2.1.1), as well as stage values are adjusted to enable effluent flow conditions in the igneous lithologies and transmission losses in the Troodos Sedimentary Succession. The transmission losses range from 1 to 4 mm/a per km infiltration length as determined within the GRC-project (UDLUFT ET AL.,

2003). Suitable values for the river stage are 0.3 m and for the conductance of the riverbed 2.00E-06 m/s. The elevation for the lakes is set constant to the stage of the river cell at the lake inflow and the conductance to 1.00E-08 m/s.
Spring discharge data in the ENVIS database is mostly discontinuous and thus not usable for model calibration. Major spring locations are incorporated into the model as drain cells with riverbed hydraulic conductivity (2.00E-06 m/s). Within the calibration process, the elevation of the spring cells is adjusted to enable outflow.

4.2.2.2.3 Hydraulic conductivities of the single lithologies

The hydraulic conductivities of the different lithologies are calibrated using groundwater head data of the 149 observation points (Chapter 4.2.2.2.1, Table 26, Appendix B). Proceeding studies within the GRC-project and special investigations (MEDERER, 2005; DÜNKELOH, 2005A) are used to derive starting values. Lithologies with an large areal distribution and a corresponding large number of observations are calibrated using the PEST module. Lithologies with a small density of observations are calibrated manually. The correspondence of computed vs. observed heads of the calibration model run is shown in
Fig. 37. 75 % of the computed heads show an absolute error smaller than the desirable maximum error of ± 40 m (Fig. 38). The starting and calibrated hydraulic conductivities of the single lithologies are shown in Table 16.

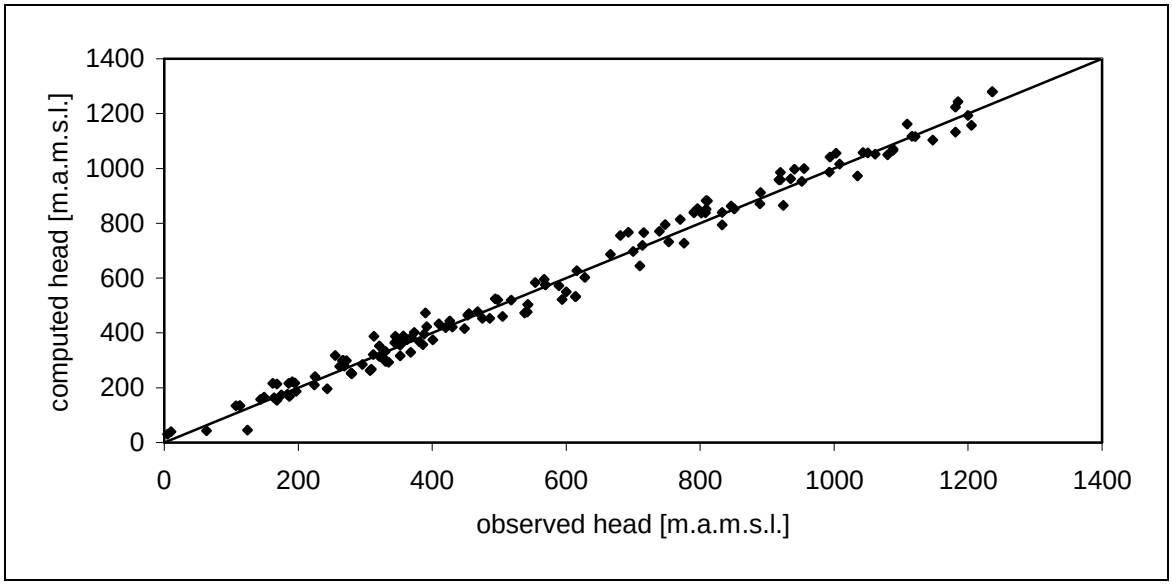

Fig. 37: Computed vs. observed heads of all observation points (n = 149). Values on the 45 degree line show perfect correspondence.

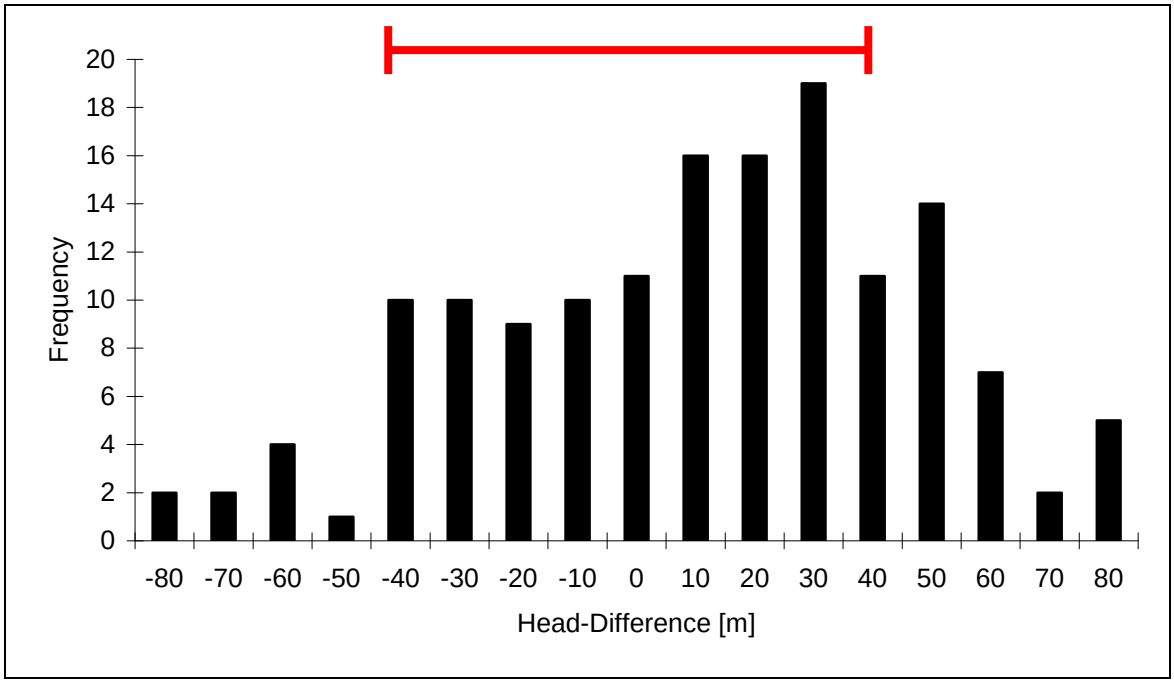

Fig. 38: Frequency distribution of the observation points' head-differences (n = 149). The horizontal bar marks values within the maximum error range (±40 m head difference).

Table 16: Starting values and calibrated hydraulic conductivities of the single lithological formations.

Formation	Hydraulic conductivity [m/s]		Formation	Hydraulic conductivity [m/s]	
	starting	calibrated		starting	calibrated
Alluvium	5.00E-06	9.30E-06	Basal Group	4.00E-07	2.20E-07
Terrace deposits, Fanglomerats	5.00E-06	4.00E-06	Sheeted Dykes	3.50E-07	1.00E-07
Nicosia	5.00E-06	3.80E-06	Plagiogranite, Gabbro	5.00E-07	1.70E-07
Kalavasos	2.50E-07	5.00E-07	Pyroxenite, Wehrlite, Dunite	2.00E-07	6.00E-08
Pakhna	2.50E-07	1.90E-07	Harzburgite	8.00E-08	9.00E-08
Lefkara	2.00E-07	1.80E-07	Serpentinite	8.00E-08	6.00E-08
Kathikas, Moni, Kannaviou	2.00E-07	7.50E-08	Arakapas Breccia, Lavas	3.00E-07	4.00E-07
Perapedhi	2.00E-07	8.00E-08	Arakapas Plutonics	3.00E-07	5.00E-07
Upper Pillow Lavas	1.00E-07	1.10E-07	Sheared Serpentinite	8.00E-08	9.00E-08
Lower Pillow Lavas	1.00E-07	9.80E-08	Ayia Varvara Ayios Photios	1.00E-07	1.00E-07

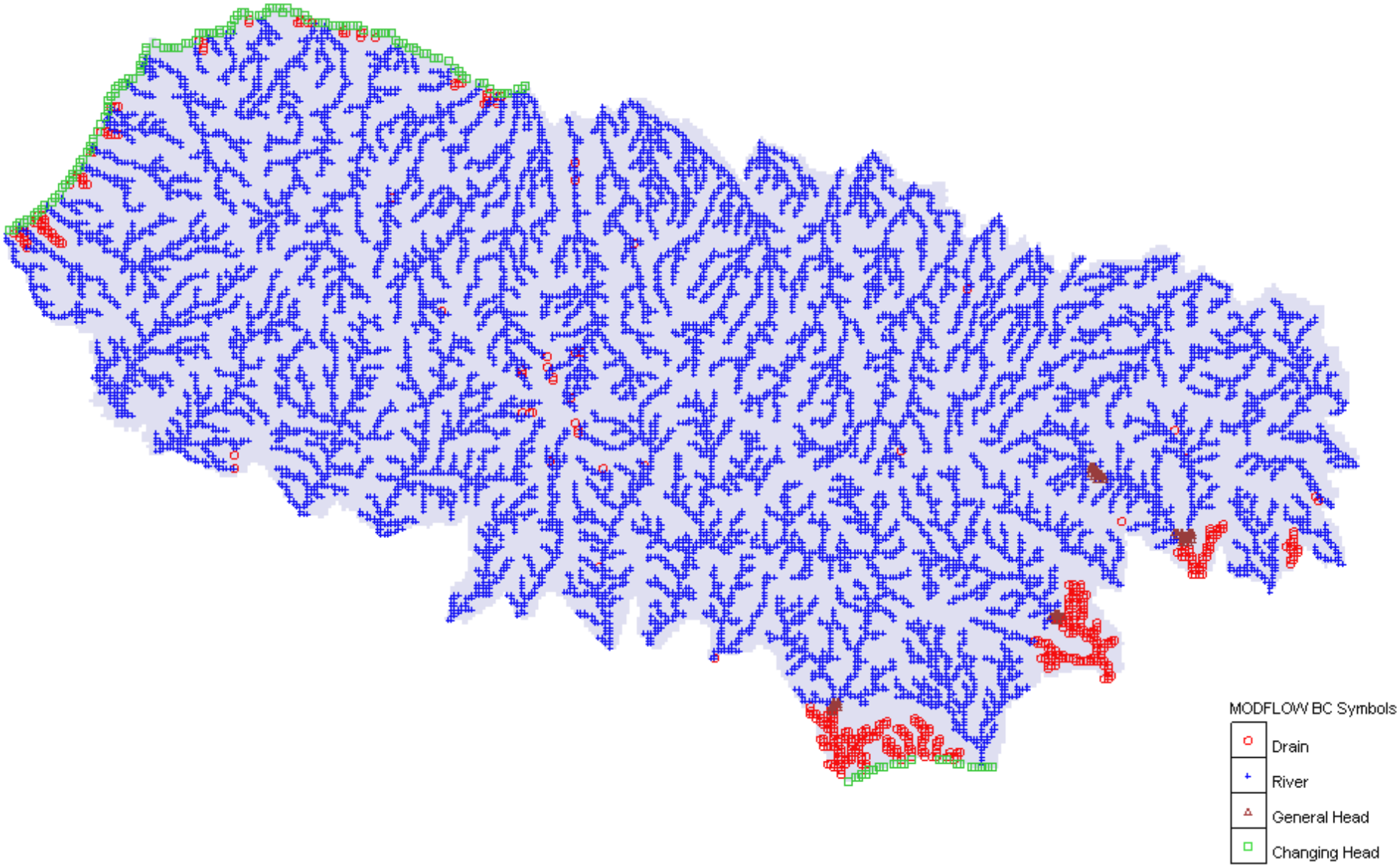

Fig. 39: Boundary conditions of the Troodos groundwater flow model. The active grid is indicated grey. Drain cells mark river segments with influent flow conditions, isolated drain cells represent springs (Table 25, Appendix B).

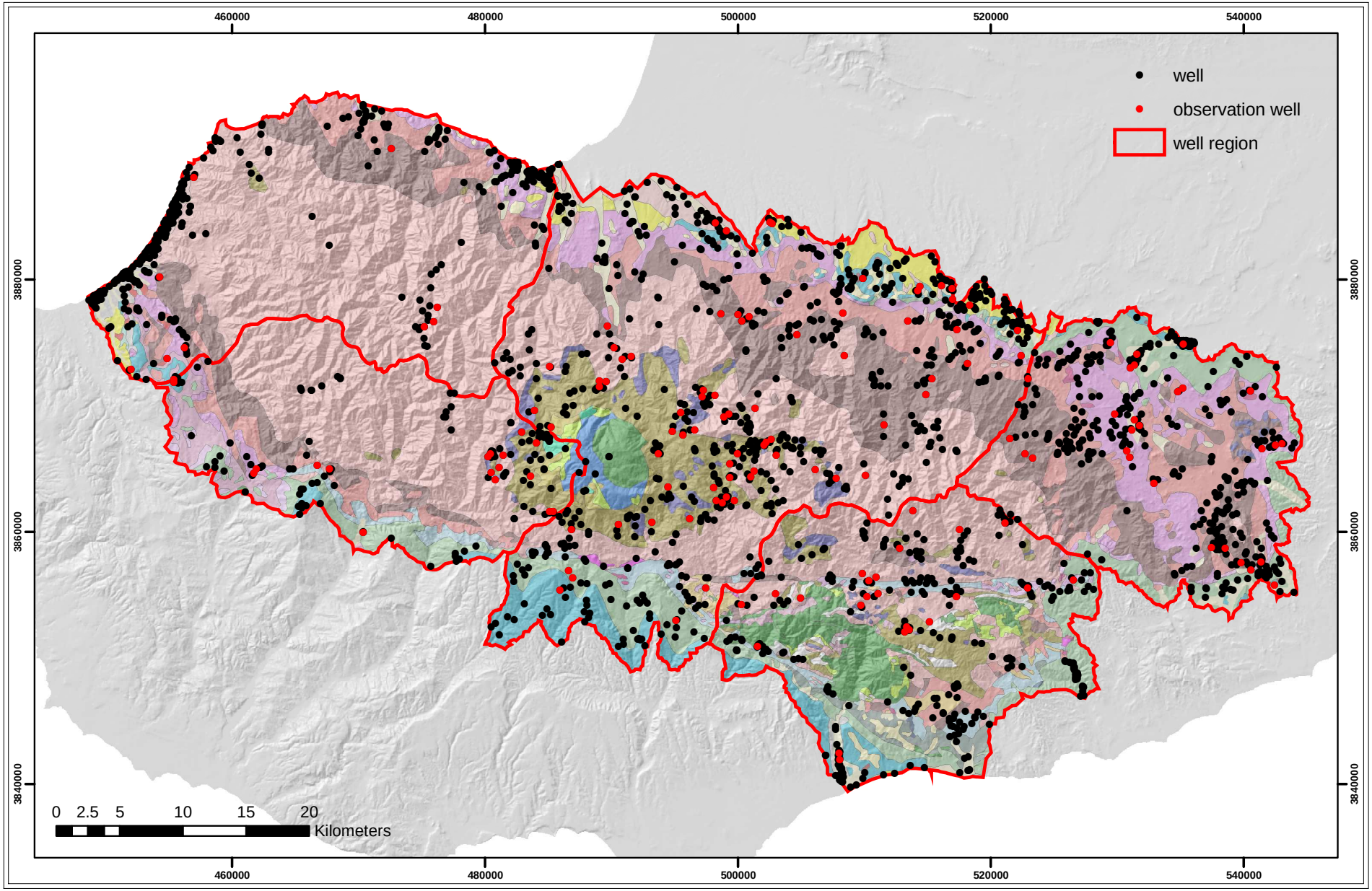

Fig. 40: Abstraction and observation wells and well regions superimposed on geology (geological legend see Fig. 5).

4.2.2.3 Results and discussion

The results of the regional groundwater flow modelling include a calibration run simulating actual aquifer conditions, as well as management and sensitivity scenarios. Lateral groundwater flow characteristics are studied exemplarily in the pilot catchments to identify inter-catchment flow.

4.2.2.3.1 Calibration run

The calibration run reflects the aquifer conditions for the modelling time period from 10/1987 to 09/1997. Groundwater heads are influenced by hydraulic conductivity, by topography and by groundwater storage change through recharge, discharge, evapotranspiration and abstraction. In the study area, topographic influences prevail. Roughly speaking, the groundwater heads follow the mountainous surface and reach a maximum of 1786 m.a.m.s.l. in the uppermost Troodos, while lying locally below sea level along the coastline with a minimum of –14 m.a.m.s.l. (mean: 511 m.a.m.s.l.; Fig. 41). Negative values might indicate local sea water intrusions. However, they lie within the maximum absolute modelling error of ± 40 m. This error is assumed for the mountainous part of the study area and is believed to be lower along the coastline. But nevertheless, the regional modelling character of this study limits the significance for the identification of local sea water intrusion events. WAGNER ET AL. (1990) and results of hydrochemical investigations within the GRC-Project (UDLUFT & KÜLLS, 2004) have not yielded evidence for major sea water intrusions in the study area.

The effect of single parameters on the water level is very graphic in the depth to water table map (Fig. 42). The depth to water table in the study area ranges from 0 to 276 metres below surface (mean: 55 m.b.s.; median : 34 m.b.s). Largest depth values are found below the upper slopes of the Sheeted Dykes and Sheared Serpentinite ridges, and in the eastern Troodos in areas with a high well density. Lowest values are generally found at the receiving waters and in areas with high recharge rates and low permeabilites; for instance in the upper Troodos and in the Pillow Lava promontories.

Inaccuracies concerning the groundwater head stage might occur along the river segments. This is mainly due to the fact that GMS interpolates river stage and river elevation on the base of finite elements, while the starting groundwater heads are derived from the digital elevation model raster. This error is believed to lie within several meters of head-difference and thus within the maximum tolerable error range of ± 40 m.

The flow budget for the entire study area is summarised in Table 17. The budgets for the single pilot catchments and well regions are shown in Appendix C.

MODBIL calculated recharge and riverbed infiltration form the main model inflow sources while constant heads (open sea) and general heads (lakes) infiltrate only small amounts. Groundwater outflow mainly occurs through rivers, evapotranspiration of moist areas, waters and well discharge. It is interesting to note that evapotranspiration controlled model outflow reaches the order of magnitude of river discharge. Discharge to the sea, to springs and lakes is of minor importance. 27 % of the study area's boundary is bordered by the open sea. Comparably low is the outflow to the sea through constant head cells (3 mm/a). Spring discharge reaches a similar order of magnitude. The modelled discharge of major springs in the study area (Fig. 39) yields 0.047 m³/s (0.5 mm/a) and is part of the drains outflow in the overall flow budget (Table 17). It has to be noted that spring discharge was not subject to calibration (Chapter 4.2.2.2.2) and has only been used as an indicator for qualitative discharge changes.

Table 17: Modflow flow budget of the calibration run in the study area (area: 2924 km²; time period: 10/1987-09/1997). Secondary Evapotranspiration (Sec. ET) is described in detail in Chapter 4.1.3.2.

	In		Out	
	mm/a	m³/s	mm/a	m³/s
Constant heads	0	0.028	3	0.317
Drains	0	0.000	3	0.267
General heads	0	0.040	0	0.019
Rivers	12	1.072	61	5.655
Wells	0	0.000	16	1.440
Recharge	118	10.968	0	0.000
Sec. ET moist areas/waters	0	0.000	48	4.412
Total Flow	131	12.108	131	12.110

4.2.2.3.2 Natural scenario

The natural scenario reflects conditions in the study area without artificial groundwater abstractions. The single well abstraction rates have thus been set to zero. This scenario is chosen to show the artificially created drawdown and the recovery potential in different parts of the Troodos fractured aquifer-system.

The range of groundwater heads in the natural scenario is similar to the calibration run (Chapter 4.2.2.3) although the heads are slightly elevated. Heads range from – 5 to 1796 m.a.m.s.l. with a mean of 519 m.a.m.s.l. The depth to water table ranges from zero metres below surface (m.b.s.) to 260 m.b.s., with a mean of 46 m.b.s. and a median of 26 m.b.s., and lie several meters above the water table depth of the calibration run (mean: 55 m.b.s., median: 34 m.b.s).

The absolute head-differences between natural and calibration run are shown in Fig. 43, the relative differences in Fig. 44. Affected are the main abstraction areas and their surroundings, especially in the upper, northern and eastern Troodos (Fig. 44). The differences are negative, implying a relative groundwater rise (mean: -8 m). This indicates that a groundwater abstraction reduction of 16 mm/a (Table 17) in the Troodos corresponds to a mean groundwater rise of 8 m.

The aquifer response depends mainly on hydraulic properties and storage change. Relative groundwater rise in the natural run is highest where well density and thus abstraction rates are high, and recharge volumes and hydraulic conductivities are low. This is the case in the main abstraction zones of the Pillow Lava promontories in the northern and eastern Troodos. In these areas, groundwater rises about 50 to 100 m and reaches a local maximum of – 133 m difference to the calibration run. In the Pitsilia area, the main abstraction zone of the upper Troodos within the Gabbro lithologies, groundwater rise is much lower and reaches a few tens of meters. High recharge rates combined with medium hydraulic conductivities diminish the aquifer's sensitivity to abstraction rate changes. In the remaining abstraction zones with a low or medium well density, the differences rather exceed a few tens of metres. Even along the coastline in the western Troodos, where agricultural use is intense and well density high, the groundwater rise is small. The cross-section model of the western Troodos indicates, that the proximal, high recharge areas of the western Troodos supply the Terrace Deposit aquifers along the coast with indirect groundwater recharge (Fig. 34). Field observations, localising beach rock within the Terrace Deposits and thus groundwater outflow to the sea, are another indicator for these lateral flows. They increase the amount of extractable groundwater along the coast and reduce the sensitivity to groundwater abstraction rate changes.

Table 18: Modflow flow budget of the natural scenario in the study area (area: 2924 km²; time period: 10/1987-09/1997). Secondary Evapotranspiration (Sec. ET) is described in detail in Chapter 4.1.3.2

	In		Out	
	mm/a	m³/s	mm/a	m³/s
Constant heads	0	0.012	5	0.441
Drains	0	0.000	4	0.362
General heads	0	0.039	0	0.019
Rivers	10	0.938	72	6.714
Wells	0	0.000	0	0.000
Recharge	118	10.972	0	0.000
Sec. ET moist areas/waters	0	0.000	48	4.423
Total flow	129	11.960	129	11.960

The flow budget of the whole study area is shown in Table 18. Compared to the calibration run, the total flow is diminished by the well abstraction rate (16 mm/a) and, as a consequence of higher groundwater levels, by a lowered riverbed infiltration rate. The groundwater surplus is proportionately discharged through river, drain and constant head cells. Spring discharge increases about 40 % compared to the calibration run and yields 0.067 m³/s (0.7 mm/a).

4.2.2.3.3 Increased abstractions scenario

In this scenario, the response of the aquifer to increased groundwater abstractions is tested. The single well abstraction rates are adjusted to satisfy increased future water demands as predicted by SAVVIDES ET AL. (2001) in the frame of the WDD-FAO project (Chapter 1.3). According to SAVVIDES ET AL. (2001), the total annual water consumption of the island increases from 265.9 million m³ (year 2000) to 313.7 million m³ in the year 2020, which corresponds to an increase of 18 %. While the consumption of agriculture is believed to stay on a constant level, the domestic demand increases by the factor 1.5. Failing with detailed data, the island wide increase of 18 % is assumed for the study area as well. The percentage of water demand supplied by wells can only be estimated for the study area. For the whole island, the well abstracted portion of the total water consumption results approx. 48 %, surface water 38 %, desalinated water 13 % and springs 1%. Villages and privately irrigated areas, characteristic for the study area, are mainly supplied by wells (SAVVIDES ET AL., 2001). Supply with surface water from ponds and small dams is common in the Troodos but the percentage is believed to be lower, as the main portion of surface water collected in the large dams of Cyprus is used for irrigation in the lowlands. As desalinated water is not used for water supply in the study area, and with an assumed lower content of surface water, the author estimates the well abstracted percentage for water supply in the study area to be around 70 to 80 percent. In this study, a conservative groundwater management scenario is created, where the predicted increase in water demand of 18 % is completely satisfied with groundwater. Consequently, all single well abstraction rates have been increased equally by 18 % in this scenario

Compared to the calibration run the spread of groundwater heads is slightly lower: Heads range from – 18 to 1786 m.a.m.s.l. (mean: 509 m.a.m.s.l.). The depth to water table range is equal to the calibration run with a minimum at 0 m.b.s. and a maximum at 276 m.b.s. With a mean of 56 m.b.s. and a median of 36 m.b.s. the water table lies one to two meters deeper compared to the calibration run, and ten meters deeper compared to the natural scenario. Head-differences between calibration and increased abstraction scenario (Fig. 45 for absolute values; Fig. 46 for relative head-differences) show the specific differences: Positive differences imply drawdown of heads. Drawdown is restricted to the groundwater abstraction areas and their surroundings (Fig. 46). Thus, large areas of the western and south-western Troodos are unaffected. Drawdown results ten metres or less in most of the

abstraction areas including the Pitsilia, the main abstraction area in the central Troodos. Sensitivity to increasing abstractions rises in the northern and eastern lowlands, especially in the low permeable Pillow Lavas, where drawdown ranges from 10 to 40 m. Drawdown reaches high values (maximum: 72 m) in the northern and southeastern Troodos, along the boundary of the study area. The head-differences between the natural and increased abstraction scenario show a similar areal distribution, but the absolute values are much higher (Fig. 47). They reach values above 100 m in the main abstraction zones of the northern and eastern Troodos with a local maximum of 191 m. In the north-eastern Troodos, close to the boundary, groundwater flow into the drawdown zone from all directions is restricted and thus local drawdown values might be exaggerated.

The flow budget is shown in Table 19. Quality and quantity of the groundwater flow are similar to the calibration run. Well abstractions are higher and thus discharge through receiving waters and springs is slightly lower. Spring discharge yields 0.0458 m³/s (0.5 mm/a). Under an 18 % increase of groundwater abstraction, spring discharge decreases only by 5 %. This might be due to the fact that most of major springs are situated in the upper Troodos, where the well density and thus the effect of increased abstraction rates is rather small.
Compared to the natural scenario (Table 18) the flow budget differences are more pronounced: Inflow through constant head cells is three times higher in the increased abstraction scenario, indicating an elevated risk for sea water intrusions in the lowlands. Riverbed infiltration increases by 20% - due to the lower groundwater heads in the increased abstraction scenario - resulting in a slightly increased total flow. General head flow, recharge and secondary evapotranspiration stay on a similar level. Well abstractions – forming approx. 14 % of the total flow – produce smaller outflow through rivers (approx. 20 % decrease), constant heads (approx. 30 % decrease) and drains (approx. 30 % decrease), compared to the natural scenario. Discharge of major springs drops by 33 %.

Table 19: Modflow flow budget of the increased abstraction scenario in the study area (area: 2924 km²; time period: 10/1987-09/1997). Secondary Evapotranspiration (Sec. ET) is described in detail in Chapter 4.1.3.2.

	In		Out	
	mm/a	m³/s	mm/a	m³/s
Constant heads	0	0.035	3	0.294
Drains	0	0.000	3	0.255
General heads	0	0.040	0	0.019
Rivers	12	1.088	59	5.496
Wells	0	0.000	18	1.662
Recharge	118	10.957	0	0.000
Sec. ET moist areas/waters	0	0.000	47	4.404
Total flow	131	12.119	131	12.129

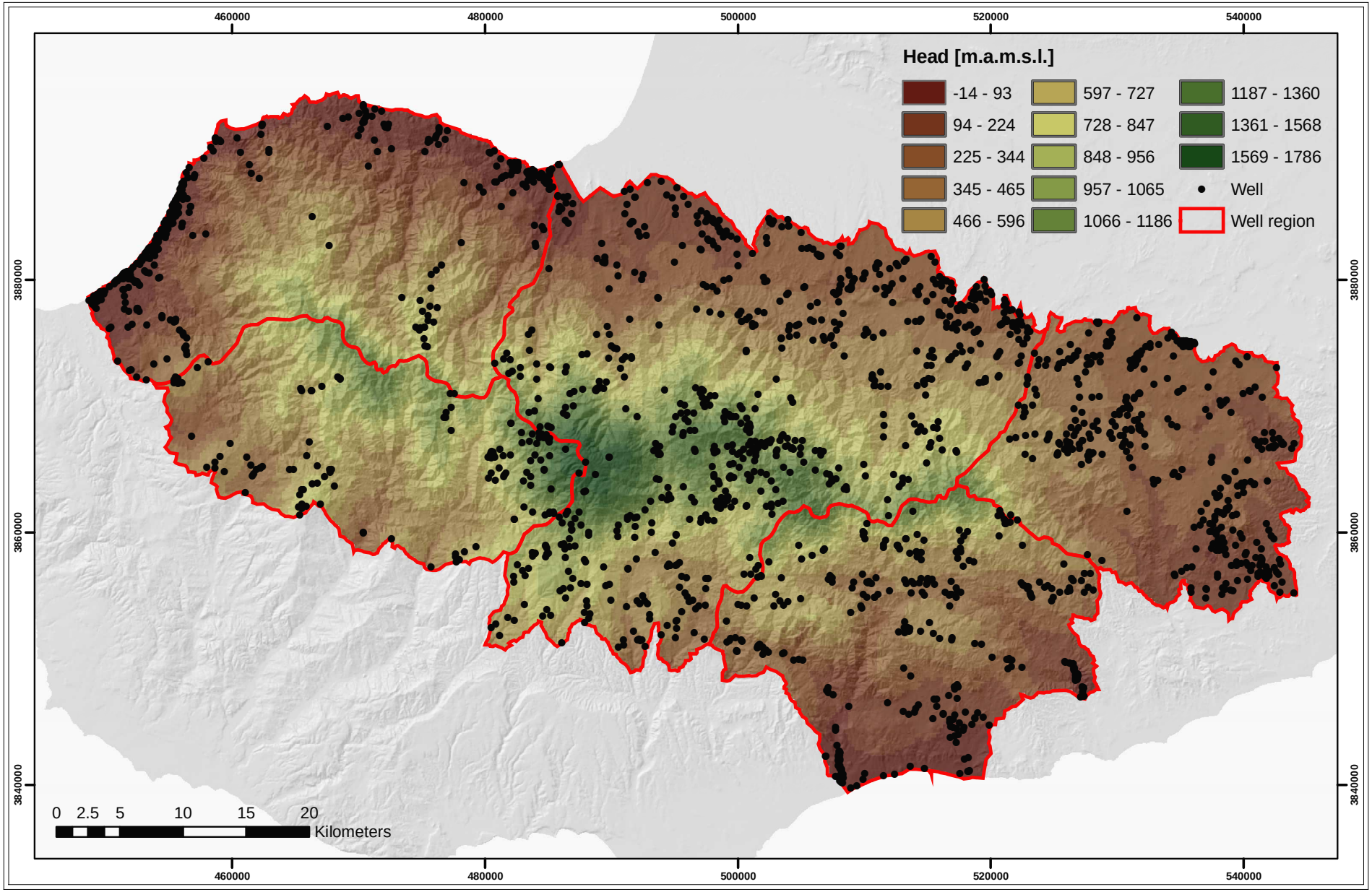

Fig. 41: Groundwater heads of the calibration run.

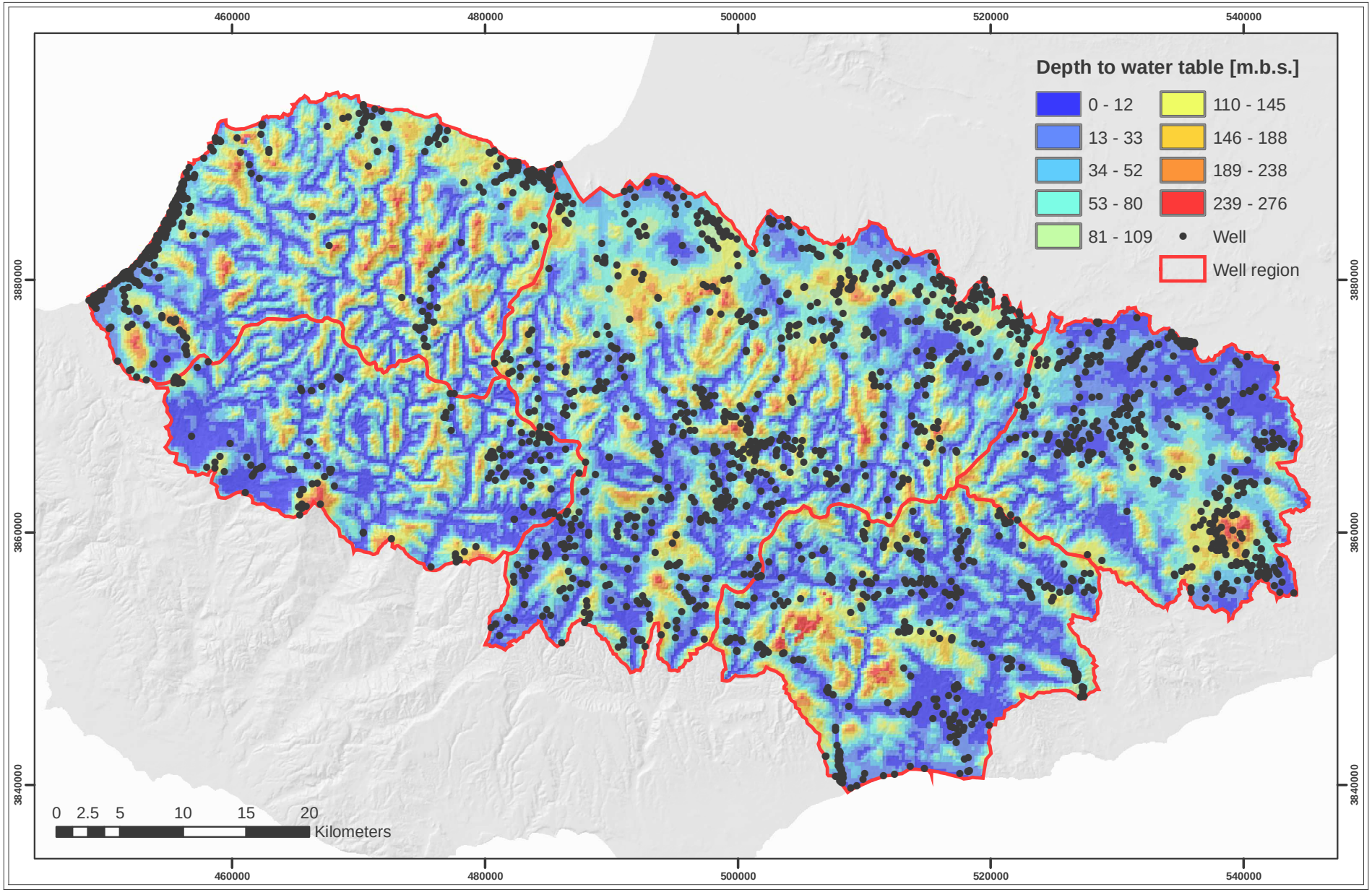

Fig. 42: Depth to water table of the calibration run.

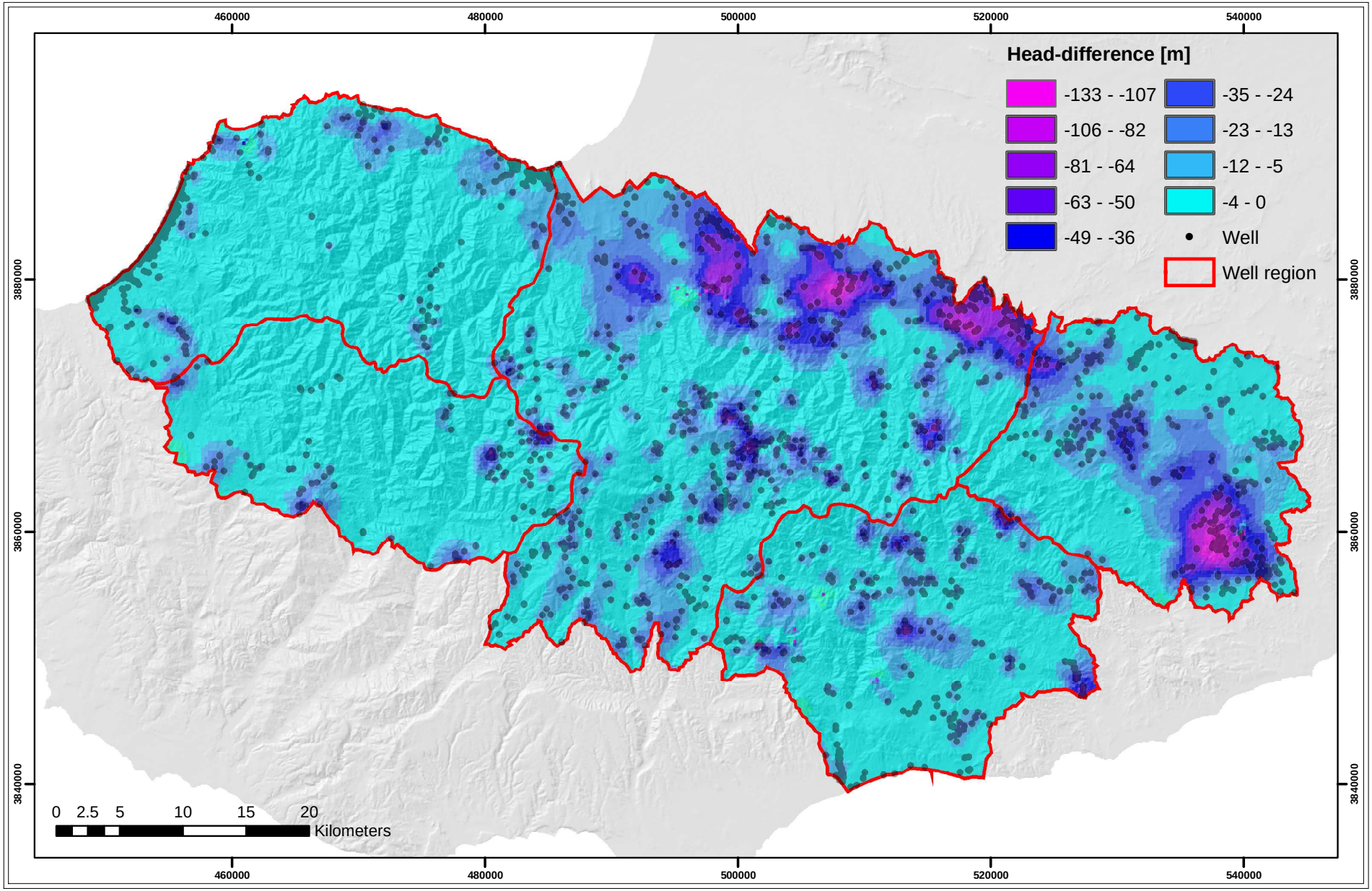

Fig. 43: Absolute head-difference between calibration run and natural scenario.

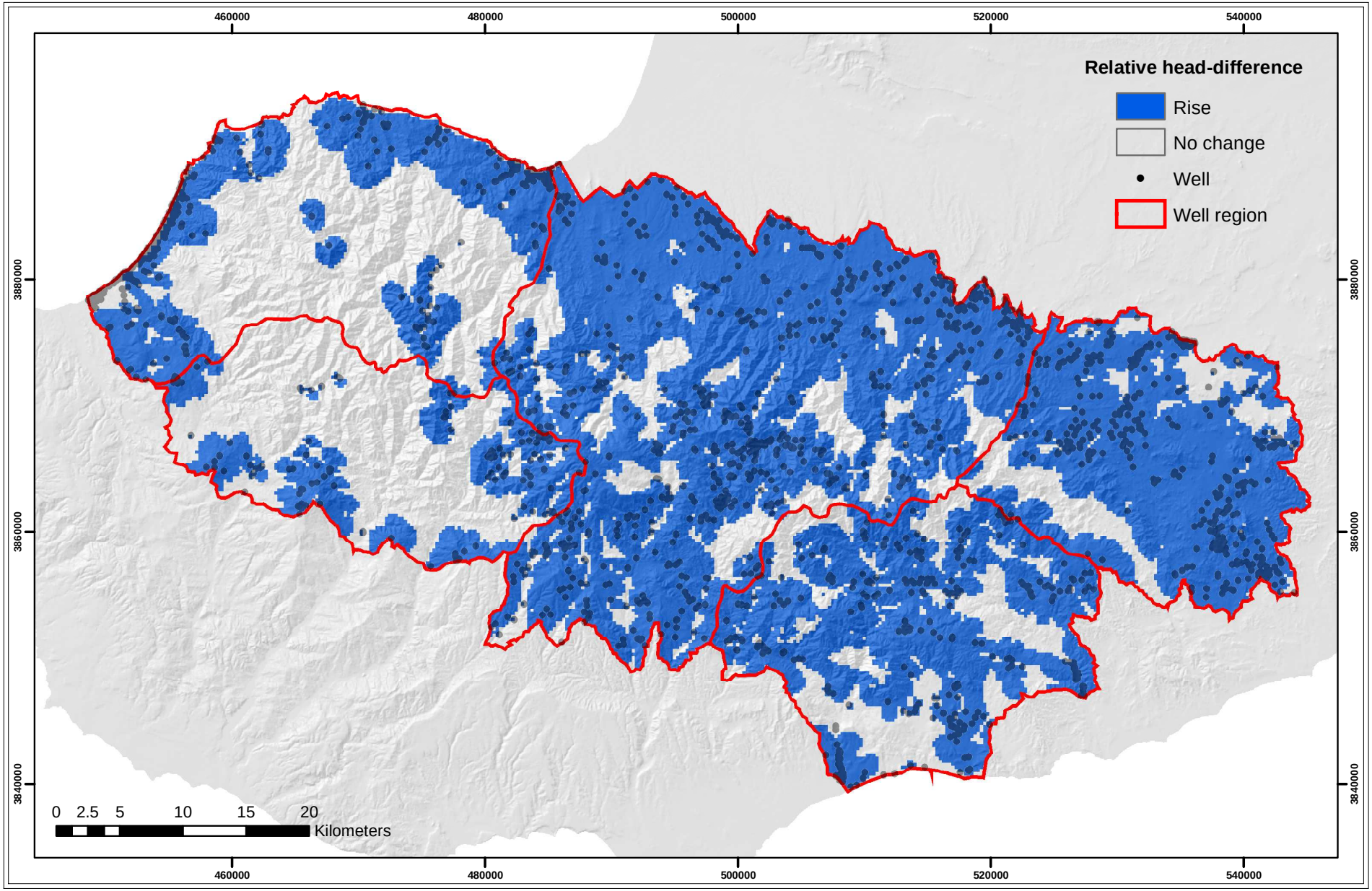

Fig. 44: Relative head-difference between the calibration run and natural scenario.

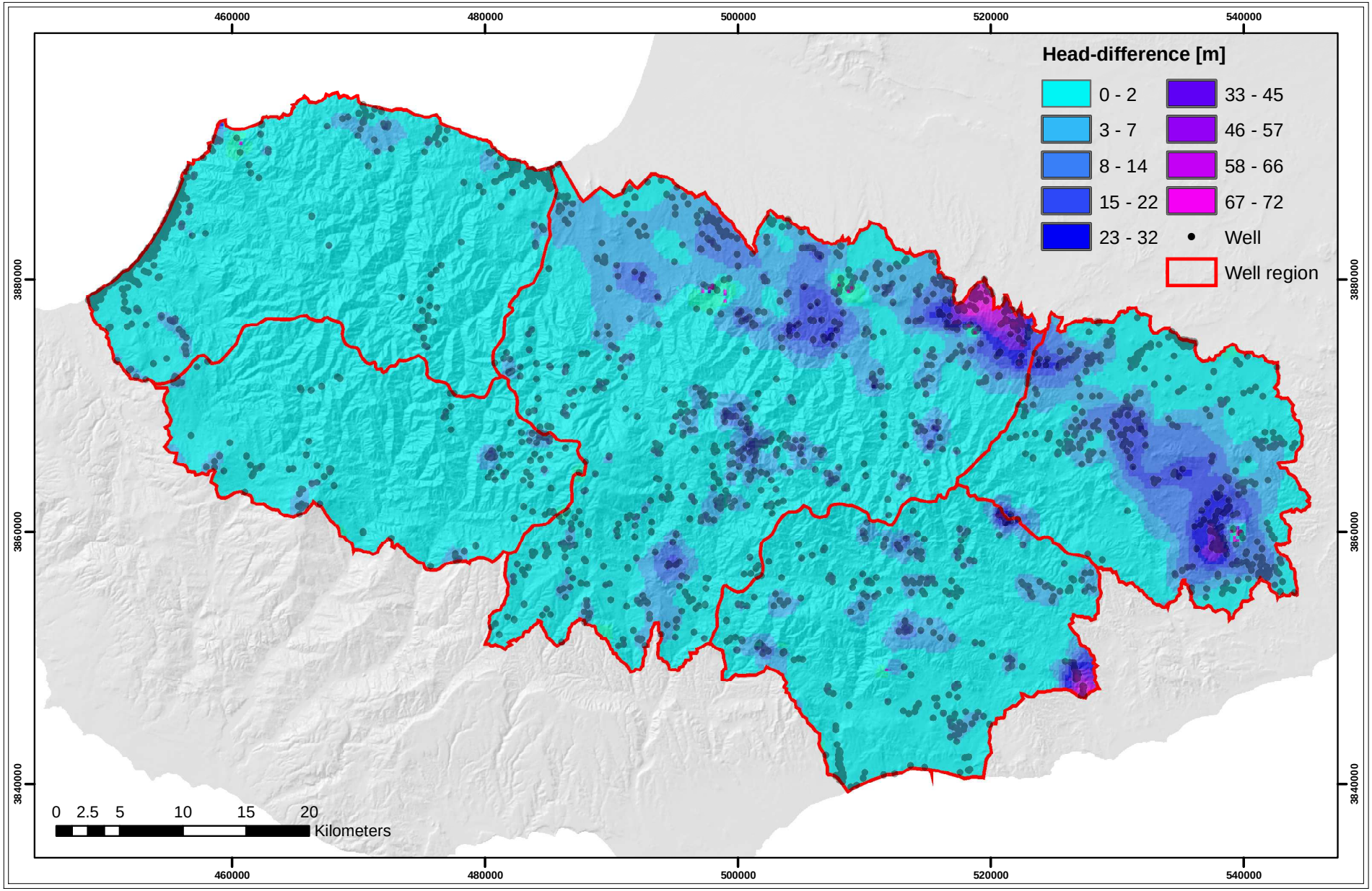

Fig. 45: Absolute head-difference between calibration run and increased abstraction scenario.

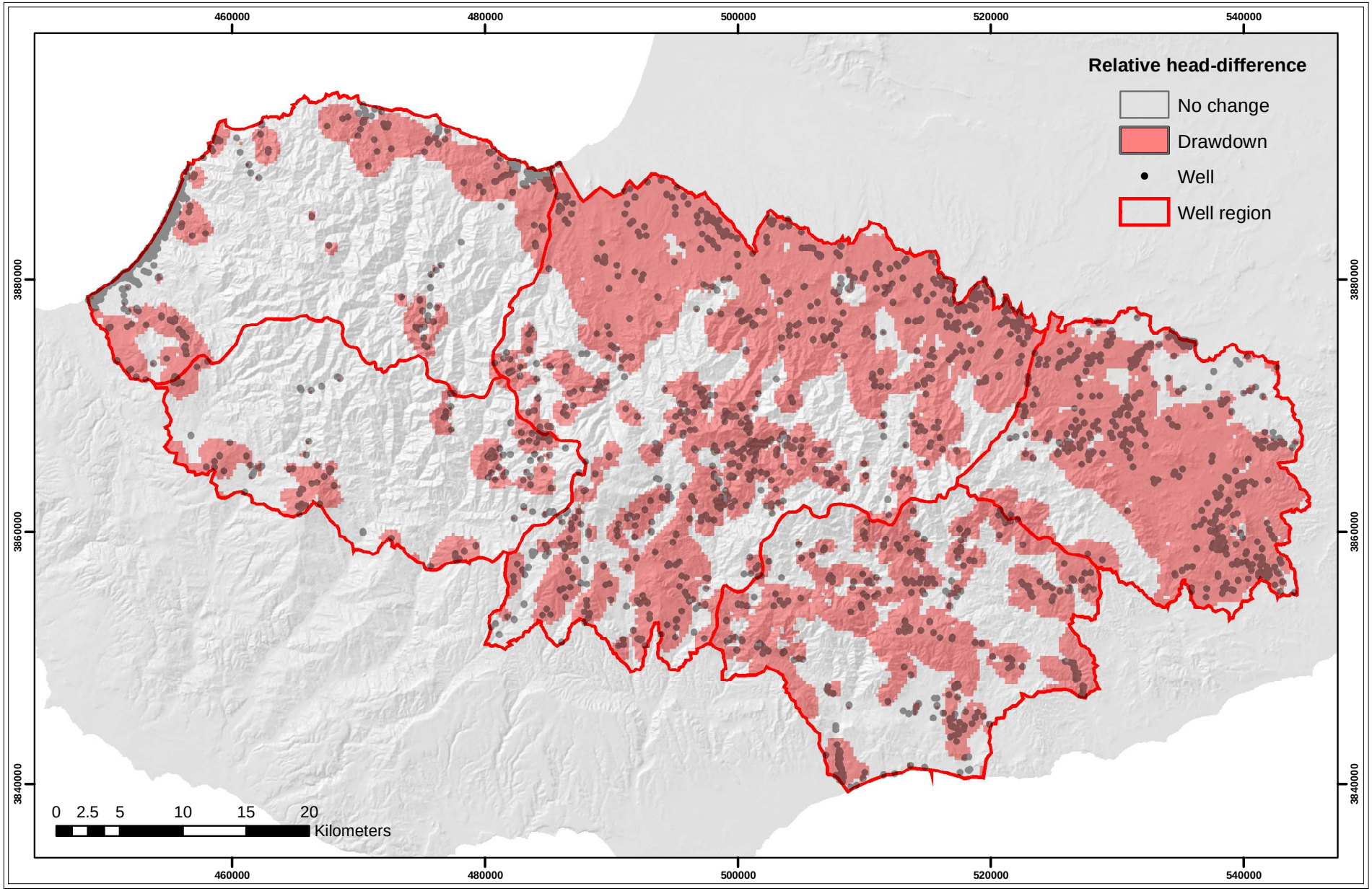

Fig. 46: Relative head-difference between the calibration and increased abstraction run.

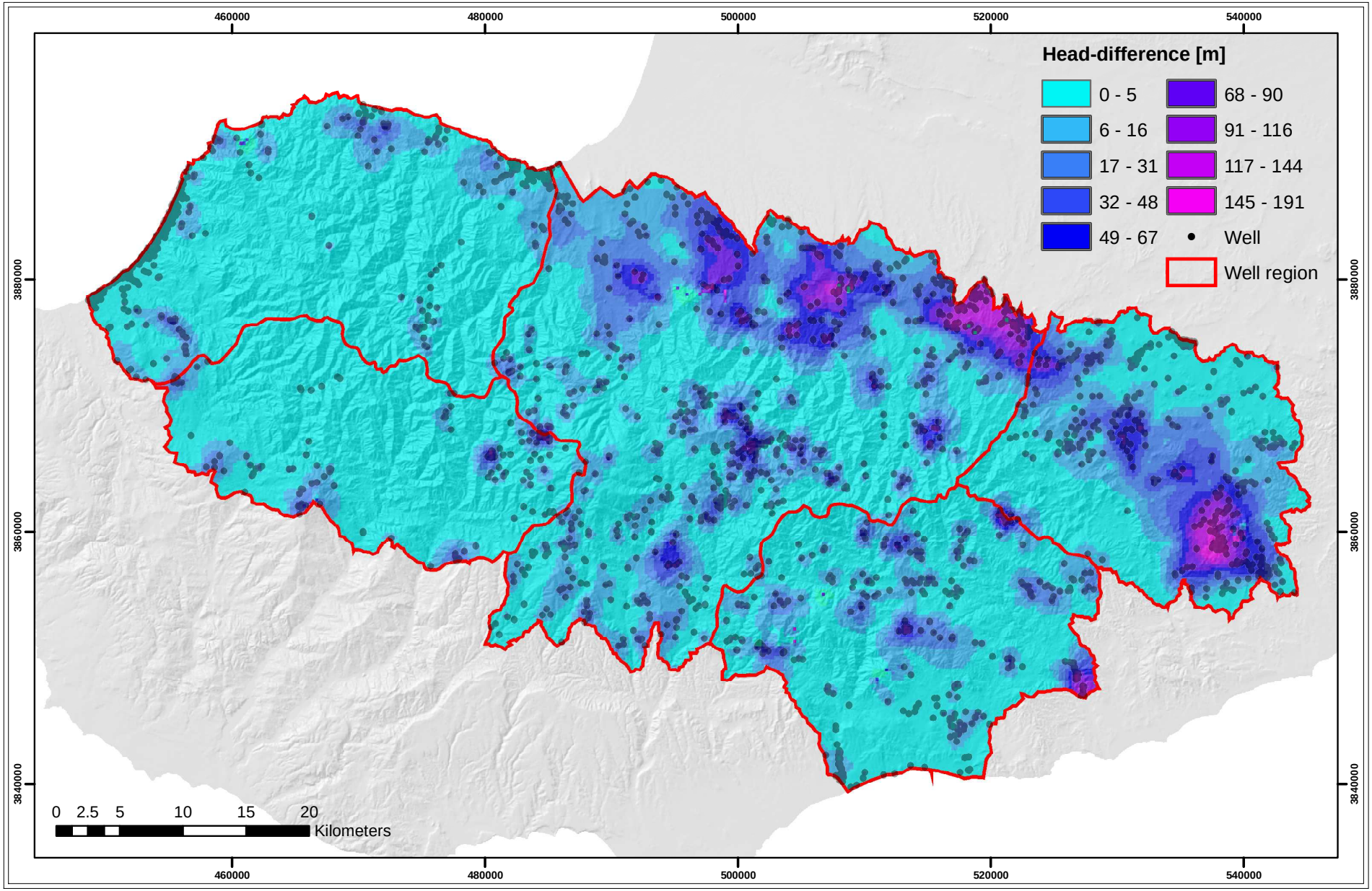

Fig. 47: Absolute head-difference between natural and increased abstraction scenario.

4.2.2.3.4 Lateral flow studies in the pilot catchments

The groundwater flow investigations in the pilot catchments outline the small scale flow characteristics, identify zones of lateral in- and outflow, and the influence on the local water balance. In the study area, well regions and pilot catchment are bordered by topographic watersheds. This is reasonable as the topographic watershed is – unlike the dynamic groundwater divide - a constant feature suitable for water management purposes. Nevertheless, they might show large deviations to the actual groundwatersheds, especially in lowlands or areas of complex hydrogeological conditions. In areas with a distinct topography, the deviations are generally lower. This applies basically to the study area too. Nevertheless, investigations within the GRC-project and results of the regional flow modelling within the present study indicate, that lateral fluxes occur between the catchments. In the study area, not all river-reaches act as receiving waters. Especially smaller tributaries show influent conditions and are sub-flown by groundwater. Close to the watershed, adjacent catchments might receive groundwater from these tributaries. This happens, if the neighbouring catchment is more deeply incised, which is generally the case for the north facing catchments in the Troodos. Even if the areal extent of these lateral flow zones is rather small, the flow volumes might be significant, due to the high groundwater turnover rates in the upper Troodos.

Additionally, physical models need clearly defined boundary conditions. Unknown lateral fluxes aggravate the calibration of water balance or groundwater flow models. Thus, the in- and outflow volumes of the pilot catchments in the calibration run are studied to assess the calibration quality.
Lateral in- and outflow volumes are quantified using the zone flow information of the MODFLOW budget for the single pilot catchments (Table 28, Table 30, Table 32 and Table 34; Appendix C). The zone flow information is summarised in Table 20. The quality and location of the lateral flow is visualized using the raster flow vector field display for the single pilot catchments (Fig. 48 to Fig. 51).

The lateral flow volumes range between 9 and 22 mm/a and reach a maximum of 16 % of the total and 70 % of the net groundwater recharge (Table 20). The difference between lateral in- and outflow and thus the effect on the catchments' water balances is much lower. It ranges from -3 mm/a in the Kargotis to 6 mm/a in the Limnatis pilot catchment.
The inflow volumes exceed - with exception of the Kargotis - the outflow volumes, which might indicate favourable groundwater drainage conditions of these catchments.
Fig. 48 shows the importance of the Diarizos as the major drain of the western part of the upper Troodos and the relief dependency of the groundwater flow. Unlike the calculation result (Table 20) no greater in- or outflow locations are visible, except for small inflow areas along the middle third of the eastern part of the watershed. Even these small zones of lateral flow yield detectable volumes due to high groundwater recharge rates in the upper Troodos.

In the Limnatis catchment, groundwater inflow is visible in a zone along the eastern watershed in the lower third of the catchment (Fig. 49). A large part of an upstream reach of the neighbouring Garyllis River is drained by the Limnatis.
River reaches with non-converging flow vectors are visible in the Pyrgos catchment, indicating influent river flow conditions (Fig. 50). This catchment loses groundwater on the south-eastern border and gains groundwater from the north-west.
The Kargotis drains the northern part of the upper Troodos (Fig. 51). The deeply incised upstream reaches in the south-eastern part of the catchment gain groundwater from the neighbouring Kouris River, as presumed by UDLUFT ET AL. (2003) within the GRC project. Additionally, inflow occurs on the north-western part of the catchment. Several reaches in the middle part show influent flow conditions. The dominant visible features are the large and thick flow vectors in the northern third of the catchment. They mark cells with high groundwater turnover rates bound to the inset of the Alluvium, overlying the low permeable Pillow Lava series (Fig. 5). A flow budget analysis of single raster cells at the downstream border of the Kargotis watershed yield 12 mm/a of groundwater outflow through the Alluvium. This is important as it could indicate that a considerable amount of groundwater sub-flows the gauge and might not be measured.

Table 20: Lateral groundwater flow volumes compared to the total flow volumes of the single pilot catchment areas.

Pilot catchment	Lateral inflow [mm/a]	Lateral outflow [mm/a]	Total groundwater recharge [mm/a]	Net* groundwater recharge [mm/a]
Diarizos	13	9	172	109
Limnatis	13	7	165	67
Pyrgos	16	13	138	100
Kargotis	19	22	139	31

*) Net groundwater recharge is MODBIL calc. groundwater recharge diminished by sec. evapotranspiration (Chapter 4.1.3.2)

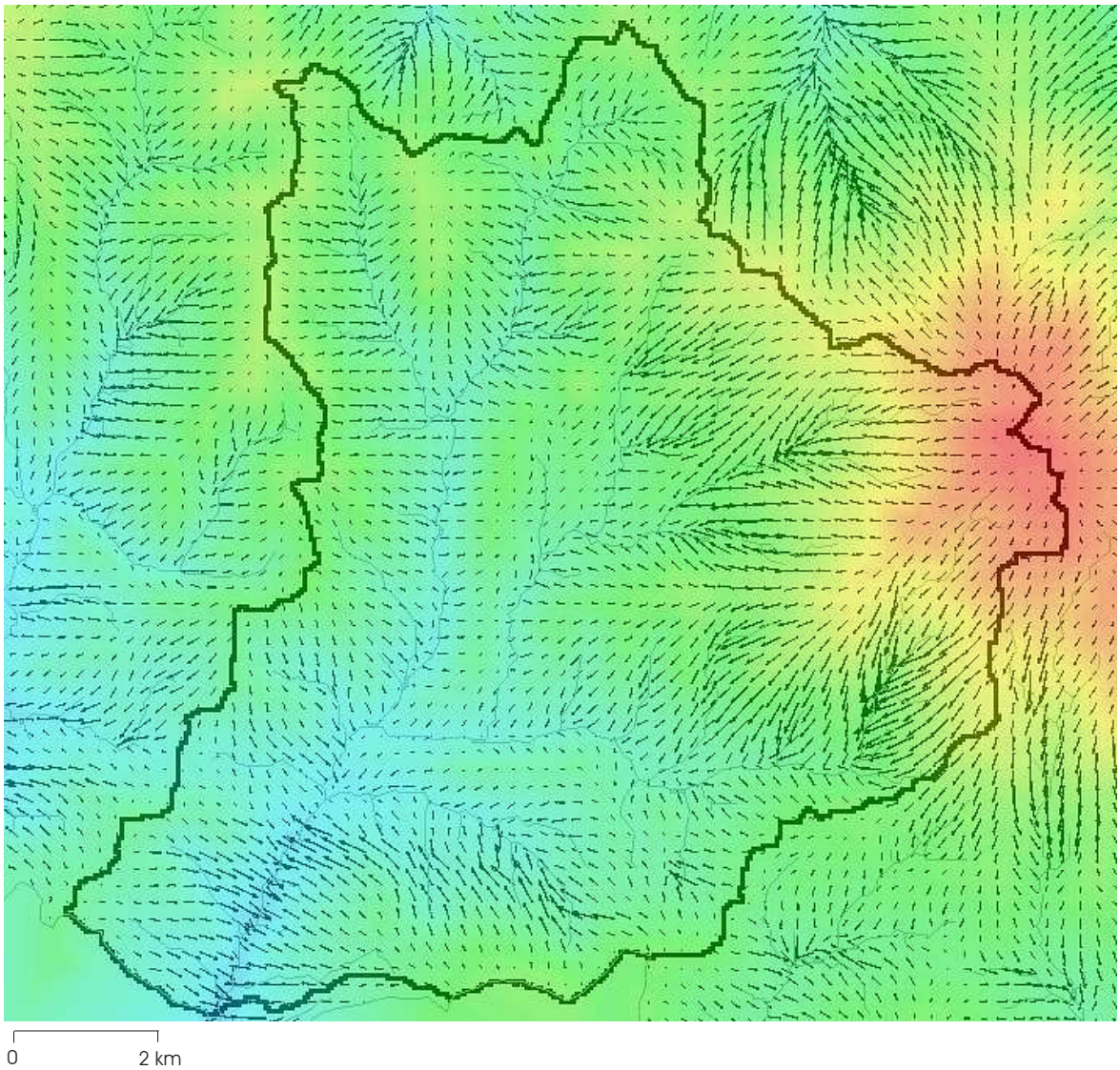

Fig. 48: Groundwater flow vector display of the Diarizos pilot catchment (Fig. 6), underlain by the digital elevation model. Length and thickness of the vector arrows are proportional to the flow volume. Small lateral flow zones are visible in the middle part of the eastern watershed close to the high peak of the upper Troodos (reddish colours), and along the southern border of the watershed.

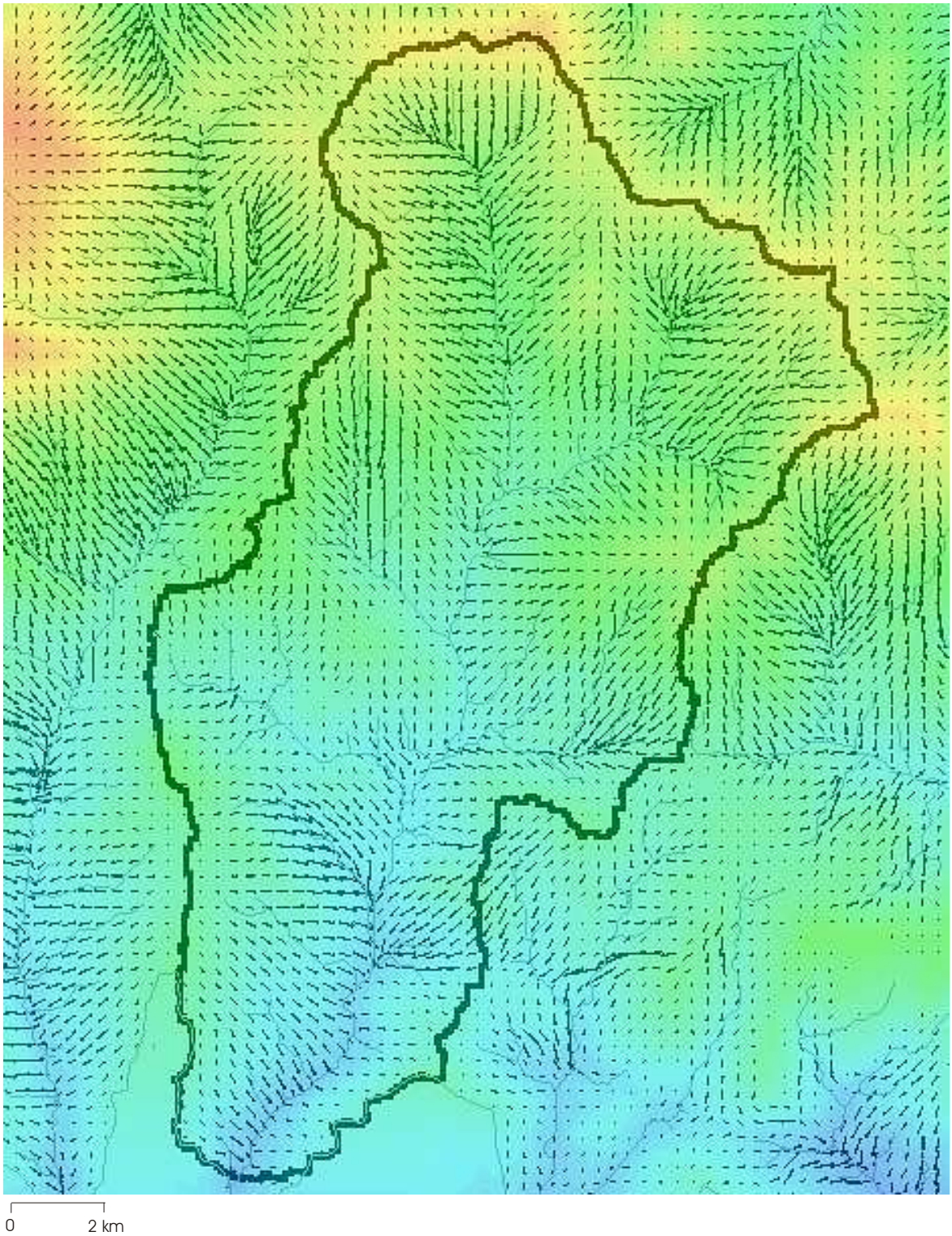

Fig. 49: Groundwater flow vector display of the Limnatis pilot catchment (Fig. 6), underlain by the digital elevation model. Length and thickness of the vector arrows are proportional to the flow volume. Remarkable lateral inflow occurs along the lower third of the eastern border of the watershed, where a complete tributary of the adjacent Garyllis River loses water to the Limnatis catchment.

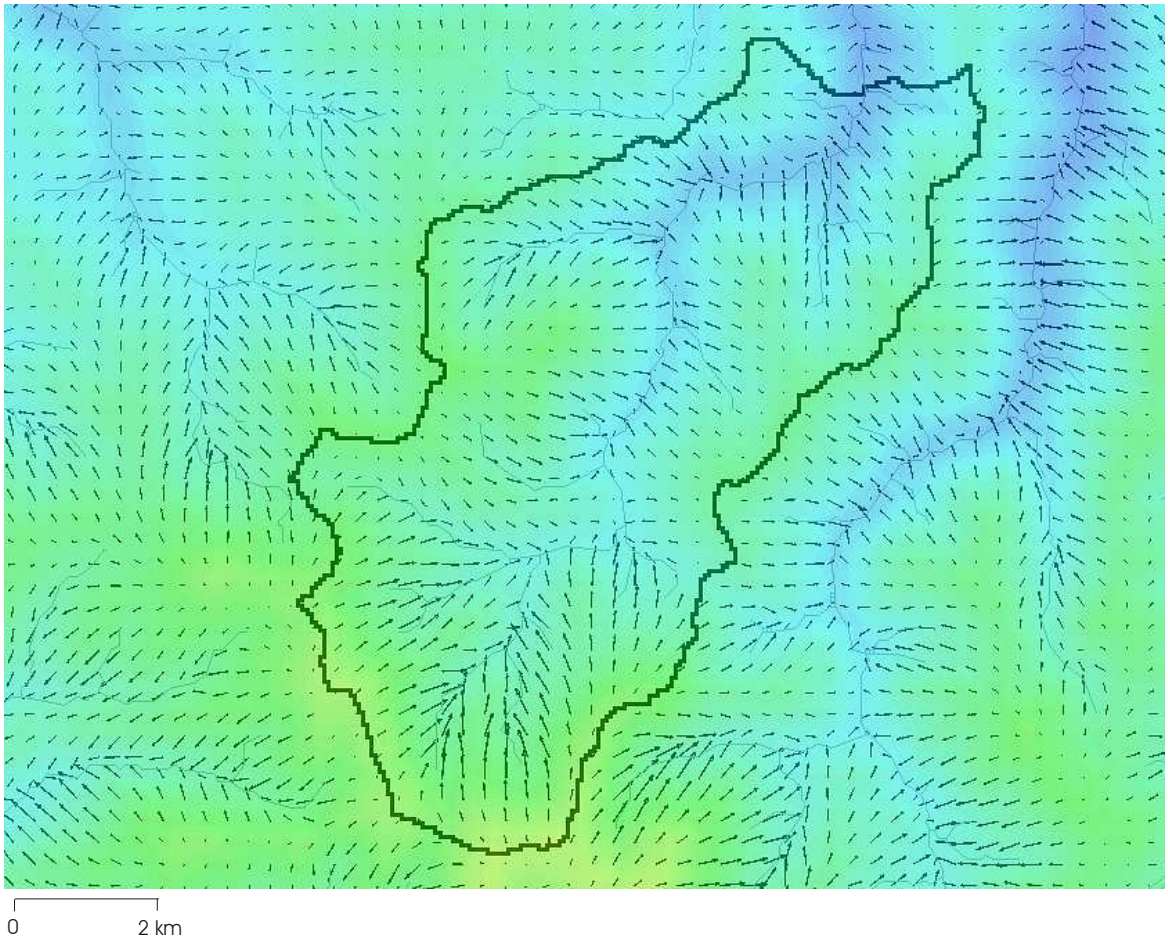

Fig. 50: Groundwater flow vector display of the Pyrgos pilot catchment (Fig. 6), underlain by the digital elevation model. Length and thickness of the vector arrows are proportional to the flow volume. River reaches in the middle part of the catchment with non-converging flow vectors are visible, indicating local influent flow conditions.

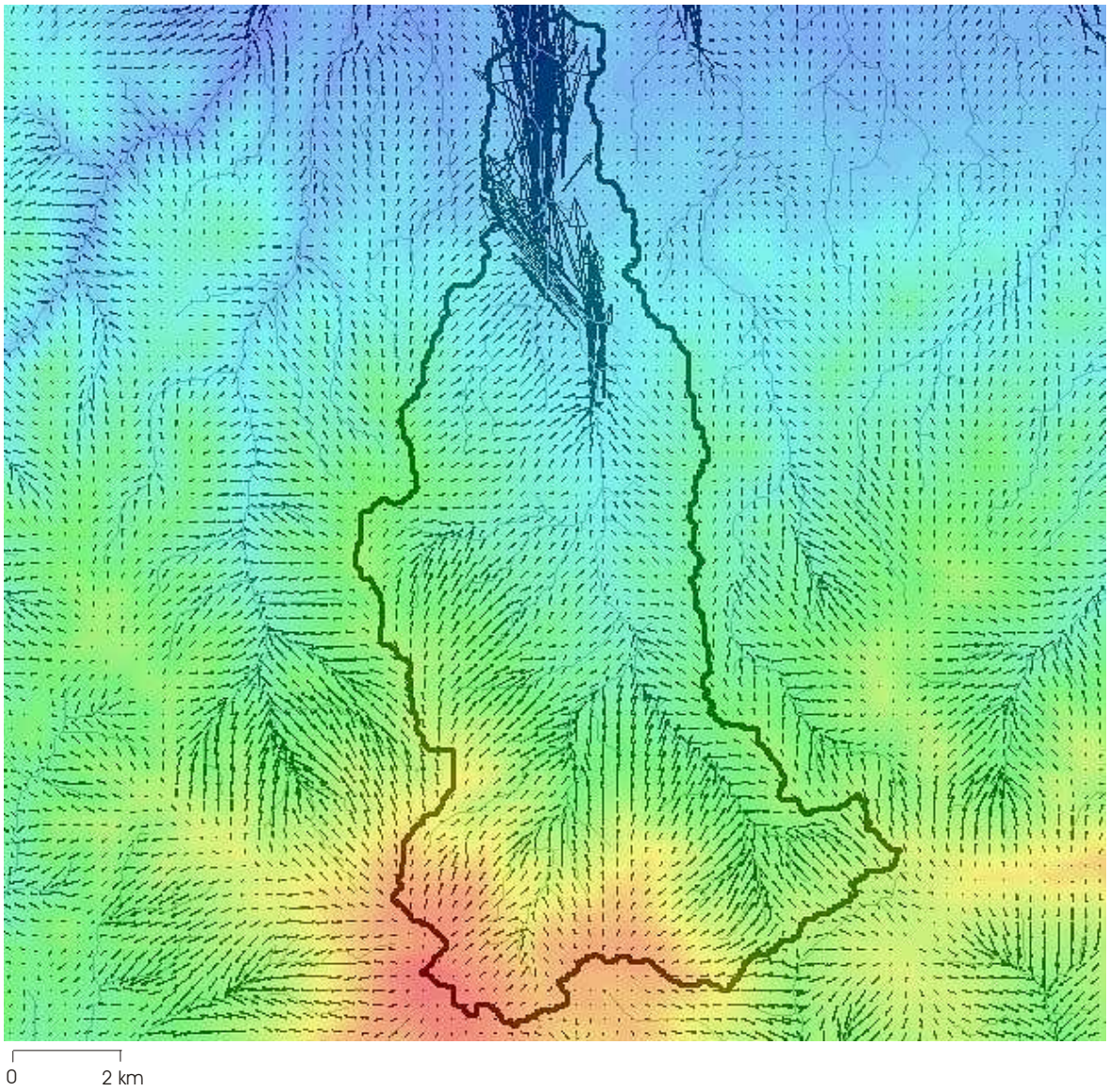

Fig. 51: Groundwater flow vector display of the Kargotis pilot catchment (Fig. 6), underlain by the digital elevation model. Length and thickness of the vector arrows are proportional to the flow volume. Several reaches in the middle part show influent flow conditions. Local inflow occurs along the south eastern segment of the watershed from the uppermost reaches of the Kouris River. Long and thick arrows indicate the inset of the Alluvium close to the gauging station, bordering the catchment to the north.

4.2.2.4 Sensitivity analysis

Sensitivity analysis is a procedure to quantify the impact on an aquifer's response due to an incremental variation in model parameters or model stresses. Its purpose is to identify the influence of different parameters on model behaviour and the range of dynamic parameter values, the model can handle. Of special importance for the groundwater models are hydraulic conductivity, recharge and groundwater abstraction, as these parameters are subject to calibration. The impact of abstraction rate changes on the groundwater head is being discussed in Chapter 4.2.2.3.2 and 4.2.2.3.3. An abstraction decrease of 100 % (no abstraction in the natural run) leads to several tens to 100 m of groundwater rise in the main abstraction zones. An 18 % increase of abstraction, as simulated in the increased abstractions scenario, yields a few tens up to 40 m drawdown in the abstraction areas.

The sensitivity to hydraulic conductivity and recharge rate changes is investigated by incremental parameter rate changes within a range of approx. ±100 % of the calibrated values.
Fig. 52 shows the response of groundwater heads to different parameter rate increments. The larger the parameter values differ from calibrated values (100 %) the larger the mean head deviations and variances get. The head deviations for the increments 90 %, 110 % and 120 % are larger for recharge changes, but the maximum deviation is larger for hydraulic conductivity changes. Including the whole range of ±100 % of the calibrated values, the head deviations for all parameters lie within several tens of meters for hydraulic conductivity and recharge, reaching the order of magnitude of the abstraction rate changes mentioned above.

The sensitivity analysis show the limitations of the groundwater model. The model is very sensitive to parameter changes lowering the groundwater heads. For hydraulic conductivities, the model tolerates an increase of 20 %. For higher values, the model does not converge. The sensitivity to recharge changes is even higher. For mean recharge rates reaching 80 % of the calibrated value or less the model does not converge. The sensitivity analysis is based on mean values and does not reflect the spatial heterogeneity of the analysed parameters. Thus, the actual limitations of the model might deviate and the tolerable parameter range might be larger.

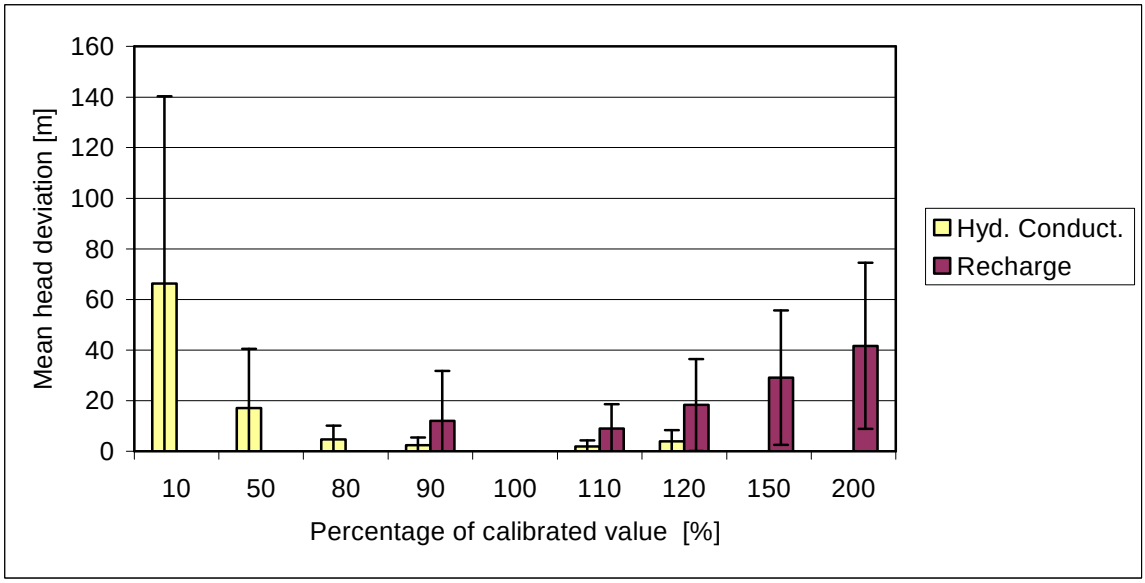

Fig. 52: Sensitivity of the model to hydraulic conductivity or recharge changes, displayed as mean deviations of the observed groundwater heads including standard deviation. The 100 % step represents the reference values of the calibration run. For 150 % and 200 % runs (hydraulic conductivity) as well as 80 % and smaller recharge runs, the groundwater model does not converge.

5 Conclusions and outlook

The coupled water balance and groundwater flow modelling approach forms an advanced method to investigate the Troodos fractured aquifer-system. Input parameters are pre-processed in a sophisticated and high resolution way before they are incorporated into the groundwater models. By modelling the Troodos Mountains as a single basin, disturbing inter basin fluxes are negligible. However, the large extent of the models diminishes the accuracy locally and increases the sensitivity.

Very good input data quantity and quality set the base for a high resolution simulation of groundwater recharge and evapotranspiration with the water balance modelling program MODBIL. Highest recharge rates (390 mm/a) are observed in areas of high precipitation, high soil and subsoil conductivities, low evapotranspiration and low slopes, typical of the Gabbro and Sheeted Dyke formations in the upper Troodos. MODBIL allows the location and quantification of groundwater abstraction needs for irrigation and evapotranspiration of moist areas. This split secondary evapotranspiration concept enables the regional quantification of groundwater abstraction rates, as well as a water balance consistent groundwater flow modelling. The secondary evapotranspiration (mean: 69 mm/a) reaches the order of magnitude of the total runoff (mean: 76 mm/a). Irrigated areas agglomerate close to settlements and on floodplains of the major Troodos rivers. The calculated groundwater abstraction rate, satisfying the secondary evapotranspiration need for irrigation, yields 18 mm/a, leading to regional mean abstraction rates of 0.5 to 0.92 l/s per well. As the abstraction rates are averaged over time for all wells within defined areas under review, the actual rates for single wells might deviate. The groundwater need for the evapotranspiration of moist areas, basically riparian vegetation and open waters, is approximately three times higher, yielding 51 mm/a. An exact calibration of the single secondary evapotranspiration components is not possible with the used methodology. A more detailed separation of groundwater needs for irrigation from needs for moist area and open water evapotranspiration could be achieved using small-scale, transient groundwater models of defined catchments, incorporating irrigation times. Validation of these results using different approaches would be helpful. Especially as the assessment of the well abstraction rates are not merely a scientific task, but rather a political issue in the frame of integrated water resources management.

The results of the water balance investigations indicate that approx. 15 % of the total groundwater recharge of the study area are abstracted for irrigation purposes, 44 % are consumed by transpiration of riparian vegetation and evaporation of open waters, 37 % discharge to rivers or lakes, and 4 % to the sea.

The high resolution distribution of groundwater recharge and evapotranspiration enhances the accuracy of the groundwater flow models. The cross-section-models complement the regional flow model as they emphasise the vertical, deeply percolating groundwater component and visualise general groundwater flow characteristics. They indicate a

dominant vertical flow system in the upper Troodos, quasi “stratiform” flow in the Gabbro and Sheeted Dyke regions, and relative groundwater rise and outflow in the vicinity of the low pervious Pillow Lava promontories. They show inter catchment flow and indirect recharge of the Sedimentary Successions, which might influence the regional water balance and increase the water availability locally, especially in the eastern Troodos. Due to the large modelling depth, supraregional flow phenomena can be simulated. Groundwater flow systems are identified several hundred metres below surface, which originate in the upper Troodos and end up in the promontories of the eastern Troodos. The flow quantities of this deep percolation system are comparably small due to decreasing hydraulic conductivities and porosities with depth. Nevertheless, important influences on local water balances can not be excluded and thus additional isotope investigations and detail groundwater models are recommended.

The regional horizontal model simulates the active water exchange part of the Troodos fractured aquifer-system. This part is characterised by small distances to receiving waters, high turnover rates in the uppermost 100 to 150 metres below surface, and young groundwater ages of generally less than 25 years (UDLUFT ET AL., 2003; BORONINA ET AL., 2005). Additionally, relatively high soil and subsoil conductivities imply a vulnerability potential for contamination (UDLUFT & KÜLLS, 2004).

The groundwater heads in the study area follow the terrain surface in a depth of several tens of metres, decreasing in the vicinity of the receiving waters, increasing up to more then 200 m below the Sheeted Dyke ridges and in the irrigation areas of the eastern Troodos. Due to the high turnover rates, the recovery potential of the groundwater heads is high. The natural scenario, where the abstraction rates are set to zero, indicates a groundwater rise of a few tens of metres in the main abstraction areas, yielding locally more than 100 m in the foothills. The heads of the increased abstraction scenario reveal a reciprocal pattern. Compared to the calibration run, the heads in the abstraction areas descent mostly for a few metres and reach values of more than 50 m in the Pillow Lavas of the northern and eastern Troodos. Discharge dynamics of the major springs show a similar trend.

The scenarios indicate that especially the foothills in the northern and eastern Troodos with low pervious lithologies and low recharge amounts are very sensitive to abstraction rate changes. Here, the groundwater heads are influenced far beyond the abstraction areas. The same is assumed for the less developed Anti-Troodos with its low permeable lithologies of the Arakapas Sequence. The Pitsilia area, the main abstraction zone of the upper Troodos in the Gabbros, shows a smaller sensitivity to abstraction changes although the single well abstraction rates are even higher. Here, the drawdown does not exceed 10 to 15 m. Possibly, the abstraction rate changes are “buffered” by favourable aquiferous properties of the Gabbros and high groundwater recharge rates.

The GRC-project water balance studies assumed inter-catchment flow in the Troodos. Especially the steeply inclined, north-facing valleys in the upper Troodos seem to receive groundwater from adjacent, south-facing catchments. In the present study, lateral groundwater fluxes are analysed in the pilot catchments exemplarily to identify indirect

recharge, which might influence the catchments' water balances and thus the quality of the calibration process of the models. In detail, lateral flow could be detected for all pilot catchments. Mostly, reaches of neighbouring catchments release or receive water. In the Kargotis catchment, a considerable amount of groundwater (12 mm/a) is detected sub-flowing the gauge in the Alluvium. Influent and effluent flow conditions of the reaches could be identified. Locally, the inter catchment flow volumes reached the order of magnitude of the calculated baseflow content but the balance of lateral in- and outflow volumes of the single pilot catchments turned out to be rather small (max.: 6 mm/a for the Kargotis). The influence on the water balance of the pilot catchments and thus on the calibration process can be considered as small but should be beard in mind for future studies.

The presented balanced regional groundwater model forms a comprehensive modelling system, supporting further detail investigations. It is recommended to model the abstraction areas in a higher areal, depth or temporal resolution, using the lateral fluxes calculated by the regional model as boundary conditions. That way, calibration parameters influencing secondary evapotranspiration could be fine tuned and abstraction rates simulated on a local level. Lateral groundwater fluxes forming indirect recharge for the first class porous aquifers of the lowlands (e.g. Western Mesaoria Upper Aquifer (WMUA)) can be quantified. In this case it is recommended to link the Troodos groundwater model (or part of it) to the groundwater model of the WMUA, developed within the GRC-project (UDLUFT ET AL., 2004B).
In combination with MODBIL, future changes in landuse and water management conditions - or scenarios of a potential climate change (DÜNKELOH, 2009) - can be pre-processed and incorporated into the groundwater models to simulate their impact on the igneous aquifer-system, and thus on the groundwater resources of the Troodos Mountains.

6 References

ANDERSON, M. & WOESSNER, W. (1991): Applied Groundwater Modeling. - Academic Press: 381 p., Orlando.

AFRODISIS, S., AVRAAMIDES, C., FISCHBACH, P., HAHN, J., UDLUFT, P. & WAGNER, W. (1986): Hydrogeological and hydrochemical studies in the Troodos region. - Technical Report N6 in Cyprus — German Geological and Pedological Project No. 81.2224.4, Ministry of Agriculture and Natural Resources, Geological Survey Department of Cyprus: 101 p., Nicosia.

AFRODISIS, S. & FISCHBACH, P. (1988): Mineral waters in the Troodos region. - In: Ministry of Agriculture and Natural Resources, Cyprus (ed.) Proceedings, workshop on conservation and development of natural resources in Cyprus, case studies, 13th - 18th October 1986: 185-186, Nicosia.

AG BODEN (1994): Bodenkundliche Kartieranleitung. 4. Auflage. - Bundesanstalt für Geowissenschaften und Rohstoffe und Geologische Landesämter: 392 p., Hannover.

AL-ALAMI, H. (1999): Watershed Management in Wadi Hadi (Jordan). - Hydrogeologie und Umwelt, 18: 1-160, Würzburg.

ALBERT, K. (1994): Hydrogeologische Untersuchungen in den Einzugsgebieten des Grünbaches, Gerchsheimer Grabens und Rödersteingrabens auf Blatt 6324 Tauberbischofsheim-Ost. - Hydrogeologie und Umwelt, 8: 158 p., Würzburg.

AL-FARAJAT, M. (2003): Hydrogeo-Eco-Systems in Aquaba/Jordan - Coasts and Region. - Hydrogeologie und Umwelt, 30: 220 p., Würzburg.

ALLEN, R.G., PEREIRA, L.S., RAES, D. & SMITH, M. (1998): Crop evapotranspiration: guidelines for computing crop water requirements. - Irrigation and Drainage Paper, 56, FAO: 300 p., Rome.

BEAR, J. & VERRUIJT, A. (1987). Modeling Groundwater Flow and Pollution. In: J. Bear (ed.): Theory and Applications of Transport in Porous Media, Vol. 2, Reidel Publishing Company: 432 p., Dordrecht.

BORGSTEDT, A. (2004): Grundwasserneubildung im Einzugsbereich des Ouham, Zentralafrikanische Republik. - Hydrogeologie und Umwelt, 32: 132 p., Würzburg.

BORONINA, A., RENARD, P., BALDERER, W. & CHRISTODOULIDES, A. (2003): Groundwater resources in the Kouris catchment (Cyprus): data analysis and numerical modelling. - Journal of Hydrology, Volume 271, Issues 1-4: 130-149, Amsterdam (Elsevier).

BORONINA, A., BALDERER, W., RENARD, P. & STICHLER, W. (2005): Study of stable isotopes in the Kouris catchment (Cyprus) for the description of the regional groundwater flow. - Journal of Hydrology, Volume 308, Issues 1-4: 214-226. Amsterdam (Elsevier).

BURDON, D.J. (1955): Groundwater in the island of Cyprus. - In: Association Int. Hydrol. Sci. (ed.): Assemblee Gen.: 315-323 p., Rome.

CHARALAMBIDES, A., KYRIACOU, E., CONSTANTINOU, C., BAKER, J., VAN OS, B., GURNARI, G., SHIATHAS, A., VAN DIJK, P.& VAN DER MEER, F. (1998): Mining Waste Management on Cyprus. - Final report, LIFE project, ITC, Enschede.

CHIANG, W.H. & KINZELBACH, W. (2001): 3D-Groundwater Modeling with PMWIN. – Springer: 346 p., Berlin.

DAVIS, J.C. (1986): Statistics and Data Analysis in Geology. - John Wiley and Sons, New York.

DOHERTY, J. (2004): PEST Model-Independent Parameter Estimation. - User Manual. 5th ed., Watermark Computing, Corinda.

DÜNKELOH, A., UDLUFT, P. & JACOBEIT, J. (2003): Physikalische Wasserhaushalts-modellierung für ein typisches Einzugsgebiet des Troodos - Gebirges (Zypern). – In: Tagungsband der 22. Jahrestagung des AK Klima der DGfG, Gladenbach, 2003.

DÜNKELOH, A. & UDLUFT, P. (2004A): Water balance dynamics of Cyprus – Part 2: Model application for the assessment of the natural groundwater resources and the construction of scenario models. - In: Chatzipetros, A. & Pavlides, S. (eds.): Proc. of the 5th International Symposium on Eastern Mediterranean Geology: 1495-1497, Thessaloniki.

DÜNKELOH, A. & UDLUFT, P. (2004B): Anwendung physikalischer Wasserhaushaltsmodellierung auf Zypern - Teil 2: Modelleinsatz zur Abschätzung natürlicher Wasserressourcen und die Entwicklung von Szenarien. In: Schiedek, T. & Kaufmann Knoke, R. (eds.): Hydrogeologie regionaler Aquifersysteme. Schriftenreihe der Deutschen Geologischen Gesellschaft, Heft 32: 175.

DÜNKELOH, A., UDLUFT, P. & JACOBEIT, J. (2004): Modellierung der Wasserhaushaltsdynamik von Zypern. In: Tagungsband der 23. Jahrestagung des AK Klima der DGfG in Eltville/Rhein: 42.

DÜNKELOH, A. (2005A): Water budget of the upper Diarizos catchment, Troodos, Cyprus. - Hydrogeologie und Umwelt, 33(15): 1-24, Würzburg.

DÜNKELOH, A. (2005B): Physical water balance modelling for the sustainable management of the natural groundwater resources: Case studies from Cyprus. In: Freiwald, A., Röhling, H.G. & Löffler, S.B. (eds): GeoErlangen 2005: System Earth – Biosphere Coupling, Regional Geology of Central Europe. Schriftenreihe der Deutschen Gesellschaft für Geowissenschaften, Heft 39: 86.

DÜNKELOH, A. (2009): Water balance dynamics of Cyprus - Actual state and impacts of potential climate change. - Doctoral Thesis Universität Würzburg, Würzburg (accepted).

GASS, I.G., MACLEOD, C.J., MURTON, B.J., PANAYIOTOU, A., SIMONIAN, K.O. & XENOPHONTOS, C. (1994): The geology of the Southern Troodos transform fault zone. - Memoir No. 9, Geological Survey Department, Ministry of Agriculture, Natural Resources and Environment of Cyprus: 218 p., Nicosia.

GEOLOGICAL SURVEY DEPARTMENT, (1995): Geological Map of Cyprus, Revised Edition 1995, Scale 1:250 000. – Geological Survey Department, Ministry of Agriculture, Natural Resources and Environment of Cyprus, Nicosia.

HARBAUGH, A.W., BANTA, E.R., HILL, M.C., & MCDONALD, M.G. (2000): MODFLOW-2000, the U.S. Geological Survey modular ground-water model - user guide to modularization concepts and the ground-water flow process. - U.S. Geological Survey Open-File Report 00-92: 121 p.

HAUDE, W. (1959): Verdunstung und Strahlungsbilanz in einem warmen Trockenklima. – Meteorologische Rundschau, 12: 11-17.

IACOVIDES, S.J. (1979): Environmental isotope survey (Cyprus). - In: Water Development Department Cyprus (ed.): Rep. on IAEA research contract no. 1039/RB, Nicosia (unpublished).

KAMPANELLAS, C., OMORFOS, C., IOANNOU, E., FRAGHKESCOU, T. & KOKOTI, V. (EDS.) (2003): Development of water resources in Cyprus – a historical review. - Water Development Department, Press and Information Office, Republic of Cyprus: 28 p., Nicosia.

KINZELBACH, W. & RAUSCH, R. (1995): Grundwassermodellierung. Eine Einführung mit Übungen. - Gebrüder Borntraeger: 283 p., Berlin.

KLOHN, W. (2002): Reassessment of the Island's Water Resources and Demand. - Synthesis Report (Project No. FAO/WDD TCP/CYP/2801). Water Development Department of Cyprus: 23 p., Nicosia.

KÖNIG, R. (1993): Quantifizierung der Bodenwasserbewegungen im Hinblick auf die Grundwasserneubildung mit Hilfe deckschichtenphysikalischer Kenngrößen. - Hydrogeologie und Umwelt, 6: 156 p., Würzburg.

KÜLLS, C., ZAGANA, E., UDLUFT, P. (1998): Integrated evaluation of quantitative and qualitative groundwater potential in the Eastern Mediterranean Region. - In: Weaver, T.R. & Lawrence, C.R. (eds.): Groundwater Sustainable Solutions: 683-688.

KÜLLS, C., CONSTANTINOU, C., PETRIDES, G. & UDLUFT, P. (2000A): Dynamics of groundwater recharge in natural environments and mining areas: Case studies from Cyprus. - Proc. of the 3rd Mineral Wealth Conference, Athens, Nov. 2000.

KÜLLS, C., CONSTANTINOU, C. & UDLUFT, P. (2000B): Mapping the availability and dynamics of groundwater recharge - II: Case studies from Mediterranean Basins. - Proceedings of the Third Congress on Regional Geological Cartography and Information Systems: 163-168, München.

MAILLET, E. (1905): Mécanique et physique du globe. - Essais d'hydraulique souterrain et fluviale: 218 p., Paris.

MAINARDY, H. (1999): Grundwasserneubildung in der Übergangszone zwischen Festgesteinsrücken und Kalahari-Lockersedimentüberdeckung (Namibia). - Hydrogeologie und Umwelt, 17: 145 p., Würzburg.

MALPAS, J., MOORES, E.M., PANAYIOTOU, A. & XENOPHONTOS, C. (EDS.) (1990): Ophiolites. Oceanic Crustal Analogues. - Proceeding of the 'Troodos 87' Symposium, Cyprus, Geological Survey Department, Nicosia.

MCCALLUM, J.E. & ROBERTSON, A.H.F. (1990): Pulsed uplift of the Troodos Massif – evidence from the Plio – Pleistocene Mesaorai basin. In: Malpas, J., Moores, E.M., Panayiotou, A. & Xenophontos, C. (eds.): Ophiolites. Oceanic Crustal Analogues. - Proceeding of the 'Troodos 87' Symposium, Cyprus: 217-234, Nicosia..

MCDONALD, M.G. & HARBAUGH, A.W. (1983): A modular three-dimensional finite-difference ground-water flow model. - Open-File Report 83-875. U.S. Geological Survey: 528 p.

MEDERER, J. (2003): Hydrogeologische, hydrochemische und bodenphysikalische Untersuchungen im Einzugsgebiet des Limnatis, Troodos-Gebirge, Zypern. – Diploma Thesis, Universität Würzburg: 98 p., Würzburg (unpublished; in German).

MEDERER, J. & UDLUFT, P. (2004A):Bilanzierte Grundwasserfließmodelle des Troodos Gebirges, Zypern. In: Schiedek, T. & Kaufmann-Knoke, R. (eds.): Hydrogeologie regionaler Aquifersysteme, Schriftenreihe der Deutschen Geologischen Gesellschaft, Heft 32: 175.

MEDERER, J. & UDLUFT, P. (2004B): Balanced groundwater flow models of the Troodos Mountains, Cyprus. - In: Chatzipetros, A. & Pavlides, S. (eds.): Proceedings of the 5th International Symposium on Eastern Mediterranean Geology: 1533-1535, Thessaloniki.

MEDERER, J. (2005): Groundwater resources of the Limnatis catchment in Cyprus: Application of the water balance modelling program MODBIL in an area of irrigation. - Hydrogeologie und Umwelt, 33(4): 1-13, Würzburg.

MONTEITH, J.L. (1965): Evaporation and environment. - In: Proceedings of the Symposium of the Society for Experimental Biology 19, Cambridge University Press: 205-234, Cambridge.

NATERMANN, E. (1951): Die Linie des langfristigen Grundwassers (AuL) und die Trockenwetterabflusslinie (TWL).- Wasserwirtschaft 1951, Tagung in München 1950: 12-, Stuttgart.

NATIONAL RESEARCH COUNCIL (NRC), (1996): Rock fractures and fluid flow. - National Academy Press, Washington DC.

OBEIDAT, M. (2001): Hydrochemistry and Isotope Hydrology of Groundwater Resources in the Hammad Basin (Jordan). - Hydrogeologie und Umwelt, 26: 177 p., Würzburg.

POLLOCK, D.W. (1994): User's Guide for MODPATH/MODPATH-PLOT, Version 3: A particle tracking post-processing package for MODFLOW, the U.S. Geological Survey finite-difference ground-water flow model. - Of 94-464, U.S. Geol. Survey, Washington, D.C.

RENGER, M., STREBEL, O. & GIESEL, W. (1974): Beurteilung bodenkundlicher, kulturtechnischer und hydrologischer Fragen mit Hilfe von klimatischer Wasserbilanz und bodenphysikalischen Kennwerten. - Z. Kulturtech. Flurbereinig., 15: 148-160.

ROBERTSON, A.H.F. (1990): Tectonic evolution of Cyprus. – In: MALPAS, J., MOORES, E.M., PANAYIOTOU, A. & XENOPHONTOS, C. (EDS.): Ophiolites. Oceanic Crustal Analogues. - Proceeding of the 'Troodos 87' Symposium, Cyprus: 235–250; Nicosia (Geological Survey Department).

ROSA FILHO, E.F. (1991): Umweltgeologische Untersuchungen und Hydrogeologische Modellrechnungen im Einzugsgebiet der Trinkwassertalsperre Passaúna (Curitiba, Paraná, Brasilien). – Doctoral Thesis Universität Würzburg, Würzburg.

RUTLEDGE, A.T. (1998): Computer programs for describing the recession of groundwater discharge and for estimating mean groundwater recharge and discharge from streamflow data – update. – U.S. Geological Survey Water Resources Investigations Report 98-4148: 43 p.

SAVVIDES, L., DÖRFLINGER, G. & ALEXANDROU, K. (2001): The Assessment of Water Demand of Cyprus. - WDD-FAO report Vol. II., Water Development Department of Cyprus, Nicosia.

SAXTON, K. E., RAWLS, W. J., ROMBERGER, J. S. & PAPENDICK, R. I. (1986): Estimating generalized soil-water characteristics from texture. - Soil Sci. Soc. Am. J., 50: 1031-1036. http://www.bsyse.wsu.edu/saxton/soilwater/Article.htm.

SHEPARD, D. (1968): A two-dimensional interpolation function for irregularly-spaced data. -Proceedings of the 1968 ACM National Conference: 517–524.

SPONAGEL, H. (1980): Zur Bestimmung der realen Evapotranspiration landwirtschaftlicher Kulturpflanzen. - Geologisches Jahrbuch F 9: 3-87.

UDLUFT, P. (1972): Bestimmung des entwässerbaren Kluftraumes mit Hilfe des Austrocknungkoeffizienten nach MAILLET, dargestellt am Einzugsgebiet der Lohr (Nord-Ost-Spessart). - Z. Dtsch. Geol. Ges., 123: 53-63, Hannover.

UDLUFT, P. & ZAGANA, E. (1994): Calculation of the Water Budget of the Venetikos Catchment Area. - Bulletin of the Geological Society of Greece, XXX/4: 267-274.

UDLUFT, P. & KÜLLS, C. (2000): Mapping the availability and dynamics of groundwater recharge. Part I: Modelling techniques. Proceedings of the Congress Regional Geological Cartography and Information Systems: 337-340, München.

UDLUFT, P. (2002A): Groundwater Recharge in the Eastern Mediterranean (GREM) – A comparative study on integrated evaluation techniques for groundwater resources - final report. - Science Research Development, European Commission, Office for Official Publications, Luxembourg.

UDLUFT, P. (2002B): Computer Database and Geographic Information System (GIS). - GRC-Project Report Task 2, Geological Survey Department of Cyprus: 363 p., Nicosia.

UDLUFT, P., DÜNKELOH, A., MEDERER, J., KÜLLS, C. & SCHALLER, J. (2002): Data collection and collation. - GRC-Project Report Task 3, Geological Survey Department of Cyprus: 215 p., Nicosia.

UDLUFT, P., DÜNKELOH, A., MEDERER, J., KÜLLS, C. & SCHALLER, J. (2003): Water balances for catchments and the whole island. - GRC-Project Report Task 6/7, Geological Survey Department of Cyprus: 363 p., Nicosia.

UDLUFT, P.& KÜLLS, C. (2003): New Investigations. - GRC-Project Report Task 4, Geological Survey Department of Cyprus: 38 p., Nicosia.

UDLUFT, P. & DÜNKELOH, A. (2004A): Water balance dynamics of Cyprus – Part 1: Modelling techniques. - In: Chatzipetros, A. & Pavlides, S. (eds.): Proceedings of the 5th International Symposium on Eastern Mediterranean Geology: 1578-1580, Thessaloniki.

UDLUFT, P. & DÜNKELOH, A. (2004B): Anwendung physikalischer Wasserhaushaltsmodellierung auf Zypern - Teil 1: Modelliertechnik. In: Schiedek, T. & Kaufmann Knoke, R. (eds.): Hydrogeologie regionaler Aquifersysteme. Schriftenreihe der Deutschen Geologischen Gesellschaft, Heft 32: 54.

UDLUFT, P., DÜNKELOH, A., MEDERER, J., KÜLLS, C. & SCHALLER, J. (2004A): Final Report. - GRC-Project Report, Geological Survey Department of Cyprus: 181 p., Nicosia.

UDLUFT, P. & KÜLLS, C. (2004): Analyses proposed within TASK 10 “Re-evaluation of Groundwater Resources Quality-wise”. - GRC-Project Report Task 10, Geological Survey Department of Cyprus: 56 p., Nicosia.

UDLUFT, P., KÜLLS, C., DÜNKELOH, A. & MEDERER, J. (2004B): Groundwater Modelling on Selected Areas. - GRC-Project Report Task 8, Geological Survey Department of Cyprus: 118 p., Nicosia.

UDLUFT, P., KÜLLS, C. & SCHALLER, J. (2004C): Recommendations. - GRC-Project Report Task 11, Geological Survey Department of Cyprus: 31 p., Nicosia.

UDLUFT, P. & DÜNKELOH, A. (2005): MODBIL – A numerical water balance model. - Program and manual. Vers. 4.7 (December 2005), Würzburg (unpublished).

UNITED NATIONS (ED.) (1970): UNDP - Survey of groundwater and mineral resources. – United Nations: 231 p., New York.

VARGA, R., GEE, J.S., BETTISON-VARGA, L., ANDERSON, R.S. & JOHNSON, C.L. (1999): Early establishment of seafloor hydrothermal systems during structural extension: paleomagnetic evidence from the Troodos ophiolite Cyprus. - Earth and Planetary Science Letters ,171 (2): 221–235.

VERHAGEN, B. T., GEYH, M. A., FRÖHLICH, K. & WIRTH, K. (1991): Isotope hydrological methods for the quantitative evaluation of groundwater resources in arid and semi-arid areas - development of a methodology. - Federal Ministry of Economic Cooperation, Fed. Rep. of Germany: 164 p., Bonn (Weltforum).

WAGNER, W., ZOMENIS, S. & PLOETHNER, D. (1987): Technical cooperation project – groundwater quality investigations in Cyprus, main results and conclusions – project report hydrochemistry 14. – In: Bundesanstalt für Geowissenschaften und Rohstoffe (ed.): BGR arch. no. 101301: 60 p., Hannover.

WAGNER, W., ZOMENIS, S. & PLOETHNER, D. (1990): Groundwater quality in the region between Nicosia, Larnaca and Limassol. – In: Bundesanstalt für Geowissenschaften und Rohstoffe (ed.): Geologisches Jahrbuch, C 54: 3-56, Hannover.

WANG & JÄTZOLD IN: SCULTETUS, H.R. (1969): Klimatologie – Das Geographische Seminar- Praktische Arbeitsweisen. – Westermann: 163 p., Braunschweig.

WEIGAND, S. (2001): Entwicklung und Validierung des Computerprogramms MODTRANS - Ein Computerprogramm zur Berechnung des Stofftransports in der ungesättigten Bodenzone. - Hydrogeologie und Umwelt, 25: 158 p., Würzburg.

WIJNEN, J. (2002): A groundwater flow and particle tracking model for the Iraíbasin, Paraná, Brazil. – Doctoral Thesis, Univeristät Würzburg, OPUS Onlinepublikation Universität Würzburg http://opus.bibliothek.uni-wuerzburg.de/opus/volltexte/2002/53/.

WITTENBERG, H. (1999): Baseflow recession and recharge as nonlinear storage processes. - Hydrological Processes, 13: 715-726.

WUNDT, W. (1953): Die Niedrigwasserführung in Baden Württemberg als Maß für die verfügbaren Grundwassermengen. – Gas- u. Wasserf., 24: 719-722.

ZAGANA, E., KÜLLS, C. & UDLUFT, P. (1999): Hydrochemie und Wasserhaushalt des Aliakmonas, Nordgriechenland. - Vom Wasser, 94: 29-39.

ZAGANA, E. & UDLUFT, P. (1999): Wasserhaushalt im Aliakmonas-Gebiet (Griechenland); Bilanzierung und Modellierung. - Hydrogeologie und Umwelt, 18: 258-288, Würzburg.

ZAGANA, E. (2001): Wasserhaushalt und Stofftransport im Aliakmonasgebiet (Nordwest-Griechenland). - Hydrogeologie und Umwelt, 24: 236 p., Würzburg.

ZAGANA, E., KÜLLS, C., UDLUFT, P. & CONSTANTINOU, C. (2007): Methods of groundwater recharge estimation in eastern Mediterranean - a water balance model application in Greece, Cyprus and Jordan. - Hydrological Processes, Vol. 21, No. 18: 2405-2414.

ZOMENIS, S.L., WAGNER, W. & PLOETHNER, D. (1988): Groundwater quality investigations in Cyprus – main results of a project of technical cooperation in applied sciences. – In: Republic of Cyprus (ed.): Geological survey department, bulletin no. 8: 39 p., Nicosia.

Appendices

Appendix A: Meteorological stations

Table 21: Meteorological stations with precipitation data (10/1987-09/1997).

Station number	UTM East WGS 84	UTM North WGS 84	Days with valid data
040-6270	447354	3877190	3653
041-6272	448422	3877555	3653
063-2310	451638	3870596	3653
070-4241	450335	3879370	3653
085-661	452100	3880660	3653
090-8752	454578	3884428	3653
093-2071	457031	3863948	3653
101-360	462344	3853585	3653
105-2910	461031	3863683	3653
106-6300	461271	3889270	3653
108-6020	463206	3881540	3653
110-990	465722	3870847	3653
120-5560	466382	3864476	3653
130-7300	466320	3875850	3653
135-8190	468855	3861059	3653
151-7830	469950	3873230	3653
160-6540	470693	3893732	3653
164-2030	470770	3875170	3653
168-4260	473617	3882307	3653
171-340	472705	3865265	3653
174-5565	474435	3867650	3653
175-5980	475233	3857435	3653
180-3860	476453	3871183	3653
203-4480	480361	3852649	3653
204-2871	480314	3865045	3653
205-5440	481115	3848442	3653
211-2792	484146	3873743	3653
220-5640	484482	3869253	3653
225-6430	484399	3867846	3653
250-6230	487651	3860747	3653
260-3320	487233	3855742	3653
270-7861	489173	3864574	3653
288-2391	490686	3872993	3653
289-3090	489698	3881833	3653
290-2320	491019	3877742	3653
291-2670	491147	3871890	3653
295-2050	491824	3852825	3653
301-401	492440	3865057	3653
310-6180	493226	3867263	3653
311-3171	493367	3846997	3653
320-7000	492628	3858755	3653
337-3880	497925	3866270	3653
338-6261	499126	3841856	3653

Station number	UTM East WGS 84	UTM North WGS 84	Days with valid data
347-540	497858	3849743	3653
370-2950	500550	3874494	3653
373-8130	501234	3881940	3653
377-91	501434	3863595	3653
388-4222	501427	3834913	3653
410-1641	503118	3861327	3653
415-891	504288	3888751	3653
421-332	503518	3865932	3653
429-8710	507535	3844593	3653
430-5780	507577	3877536	3653
440-5550	507522	3875003	3653
450-5462	508533	3864579	3653
460-1340	510863	3872705	3653
462-570	510330	3865446	3653
464-4850	513401	3885642	3653
467-2510	514460	3868500	3653
491-3471	516233	3875490	3653
493-1401	516889	3880409	3653
500-4460	517527	3864492	3653
510-3370	518069	3863806	3653
530-5351	517885	3857860	3653
540-5020	518554	3842644	3653
550-4540	520682	3867871	3653
565-6280	522256	3876114	3653
572-2692	524090	3851397	3653
580-1930	525337	3882527	3653
583-7910	529593	3881198	3653
592-4130	527345	3861669	3653
596-8100	524640	3855824	3653
597-420	526562	3874143	3653
598-3051	528018	3856888	3653
600-4151	527878	3858644	3653
628-7150	532750	3853287	3653
630-9061	529996	3844449	3653
632-4710	530630	3868756	3653
648-3610	535992	3854310	3653
650-5720	535845	3874555	3653
652-3651	536629	3864901	3653
660-3650	536666	3862696	3653
674-1161	538952	3861535	3653
675-7310	539768	3860497	3653
676-240	539691	3851754	3653
678-6481	542432	3867635	3653
710-3410	552368	3856212	3653
713-620	553776	3867458	3653
718-941	551946	3874201	3653

Table 22: Meteorological stations with temperature data (10/1987-09/1997).

Station number	UTM East WGS 84	UTM North WGS 84	Days with valid data
032-3041	447708	3863204	3653
041-6272	448422	3877555	3630
120-5560	466382	3864476	3645
130-7300	466320	3875850	3653
203-4480	480361	3852649	3653
225-6430	484399	3867846	3653
301-401	492440	3865057	3653
310-6180	493226	3867263	3653
320-7000	492628	3858755	3653
377-91	501434	3863595	3653
388-4222	501427	3834913	3636
415-891	504288	3888751	3653
429-8710	507535	3844593	3645
440-5550	507522	3875003	3644
493-1401	516889	3880409	3651
565-6280	522256	3876114	3653
572-2692	524090	3851397	3633
592-4130	527345	3861669	3560
630-9061	529996	3844449	3650
660-3650	536666	3862696	3653
690-920	549023	3880336	3635
731-4044	557137	3859947	3653

Table 23: Meteorological stations with relative humidity data (10/1987-09/1997).

Station number	UTM East WGS 84	UTM North WGS 84	Days with valid data
032-3041	447708	3863204	3648
041-6272	448422	3877555	3624
203-4480	480361	3852649	3653
225-6430	484399	3867846	3653
301-401	492440	3865057	3588
320-7000	492628	3858755	3649
377-91	501434	3863595	3612
415-891	504288	3888751	3651
493-1401	516889	3880409	3653
630-9061	529996	3844449	3637
731-4044	557137	3859947	3652

Appendix B: Pumping test, spring flow and observation point data

Table 24: Results of pumping test of selected boreholes in the study area (Chapter 3.3).

Borehole	Formation	Region	Saturated aquifer thickness [m]	Conductivity [m/s]	Transmissivity [m²/s]
1977-031	Ultramafics	Upper Troodos	50	2.10E-05	1.05E-03
1977-031PT2	Ultramafics	Upper Troodos	50	5.89E-06	2.95E-04
1977-042	Ultramafics	Upper Troodos	25	2.91E-06	7.28E-05
1989-063	Ultramafics	Upper Troodos	20	7.65E-05	1.53E-03
1996-040 Kyperounta	Gabbro	Pitsilia	10	1.04E-05	1.04E-04
1997-067_Agridia	Gabbro	Pitsilia	10	1.20E-05	1.20E-04
1997-070_Agridia	Gabbro	Pitsilia	10	1.19E-05	1.19E-04
1997-061_KatoMylos	Gabbro	Pitsilia	80	9.00E-07	7.20E-05
1997-078_Agridia	Gabbro	Pitsilia	70	1.49E-06	1.04E-04
1988-084_Agros	Gabbro	Pitsilia	70	1.57E-06	1.10E-04
1990-103_Fterikoudi	Gabbro	Troodos E	40	3.75E-06	1.50E-04
1997-006_Kaminaria	Sheeted Dykes	Troodos W	50	1.54E-06	7.70E-05
2000-030_Pyrga	Sheeted Dykes	Troodos E	110	3.64E-06	4.00E-04
1999-036_Alona	Sheeted Dykes	Pitsilia	20	1.30E-06	2.60E-05
2000-101_Solea	Sheeted Dykes	Troodos N	50	1.08E-06	5.40E-05
1997-058_Pyrgos	Sheeted Dykes	Troodos E	70	6.00E-07	4.20E-05
1996-088_TreisElies	Sheeted Dykes	Troodos W	60	1.50E-06	9.00E-05
1996-006_Apliki	Sheeted Dykes	Troodos E	100	1.95E-07	1.95E-05
1997-043_Mandria	Sheeted Dykes	Troodos S	60	9.00E-06	5.40E-04
1989-010_Vavatsina	Sheeted Dykes	Troodos E	100	1.50E-06	1.50E-04
1991-063_Sykopetria	Sheeted Dykes	Troodos E	80	5.25E-07	4.20E-05
1984-146_TreisElies	Sheeted Dykes	Troodos W	70	6.29E-06	4.40E-04
1988-015_Odou	Sheeted Dykes	Troodos E	60	3.25E-06	1.95E-04
1982-003_Fikardou	Sheeted Dykes	Troodos E	175	1.14E-07	2.00E-05
1985-156_AgiosMamas	Sheeted Dykes	Troodos S	40	2.00E-05	8.00E-04
1991-005_Arakapas	Sheeted Dykes	Troodos S	50	4.00E-06	2.00E-04
1990-132_Foini	Sheeted Dykes	Troodos W	80	3.75E-07	3.00E-05
1968-043_Palaichorio	Sheeted Dykes	Troodos E	120	6.88E-07	8.25E-05
1982-150_Soleas	Sheeted Dykes	Troodos N	100	3.00E-06	3.00E-04
1981-035_AgVavatsina	Sheeted Dykes	Troodos E	80	2.50E-06	2.00E-04
1993-046_Arakapas	Sheeted Dykes	Troodos S	100	2.25E-07	2.25E-05
1993-088_Solea	Sheeted Dykes	Troodos N	110	1.55E-07	1.70E-05
1994-036_Vavatsina	Sheeted Dykes	Troodos E	100	1.14E-07	1.14E-05
1999-006_Flasou	Basal Group	TroodosN	10	1.25E-05	1.25E-04
1997-064_Klirou	Basal Group	Troodos NE	50	4.50E-07	2.25E-05
2000-057_Pyrga	Basal Group	Troodos E	80	6.88E-05	5.50E-03
2000-050_Pyrga	Basal Group	Troodos E	10	6.00E-05	6.00E-04
2000-069_Kampi	Basal Group	Troodos E	40	2.25E-06	9.00E-05
1996-017_Klirou	Basal Group	Troodos NE	40	2.50E-06	1.00E-04
1999-084_Nikitaria	Basal Group	Troodos N	120	1.77E-07	2.13E-05
1982-042_Pyrga	Basal Group	Troodos E	80	5.00E-05	4.00E-03
1982-029_Pyrga	Basal Group	Troodos E	50	6.00E-06	3.00E-04
1982-042_Pyrga2	Basal Group	Troodos E	80	5.00E-06	4.00E-04
1983-141_Menogeia	Basal Group	Troodos E	20	1.50E-05	3.00E-04
1983-178_Kofinou LPL	Basal Group	Troodos E	90	1.33E-05	1.20E-03
1993-053_Linou	Basal Group	Troodos N	70	2.14E-07	1.50E-05

Borehole	Formation	Region	Saturated aquifer thickness [m]	Conductivity [m/s]	Transmissivity [m²/s]
1993-017_KaloChorio	Basal Group	Troodos NE	30	6.67E-06	2.00E-04
1984-023_Nikitaria	Basal Group	Troodos N	40	4.50E-06	1.80E-04
1984-028_Pyrga	Basal Group	Troodos E	40	9.00E-05	3.60E-03
1991-082_Pyrga	Basal Group	Troodos E	40	2.63E-05	1.05E-03
1994-055_Mandria	Basal Group	Troodos S	80	1.25E-06	1.00E-04
1986-064_Argaka	Basal Group	Troodos W	150	9.00E-07	1.35E-04
1991-105_Pyrga	Basal Group	Troodos E	5	3.60E-05	1.80E-04
1996-044_Kampia	Pillow Lavas	Troodos NE	50	1.20E-06	6.00E-05
1983-181_Lythrodontas	Pillow Lavas	Troodos E	30	3.00E-06	9.00E-05
1985-013_Mitsero	Pillow Lavas	Troodos NE	30	1.25E-05	3.75E-04
1985-013_Klirou	Pillow Lavas	Troodos NE	50	2.00E-06	1.00E-04
1977-092_Omodos	Lefkara chalks	Troodos S	100	1.00E-06	1.00E-04
1987-160_Limnatis	Lefkara chalks	TroodosS	110	8.25E-07	9.08E-05
1998-092-Paramali	Pakhna chalks	NW Lemesos	30	8.00E-07	2.40E-05
1999-080_Platanistea	Pakhna chalks	NW Lemesos	60	2.00E-06	1.20E-04
1999-080_Platanistea	Pakhna chalks	NW Lemesos	60	2.00E-07	1.20E-05
2001-029_Kilani-	Pakhna chalks	Troodos S	20	5.00E-06	1.00E-04
1982-008_Paramytha	Pakhna chalks	NW Lemesos	100	1.50E-06	1.50E-04
1994-032_Koilani	Pakhna chalks	Troodos S	165	2.00E-06	3.30E-04
1972-005	Gravel	Kouris Episkopi	30	3.44E-05	1.03E-03
1973-105	Gravel	Kouris Episkopi	40	1.32E-04	5.28E-03
1978-051	Gravel	Kouris Episkopi	25	9.72E-05	2.43E-03
1984-073	Gravel	Kouris Episkopi	80	8.10E-07	6.48E-05
1984-130	Gravel	Kouris Episkopi	45	2.27E-05	1.02E-03
1973-057	Gravel	TroodosN	30	3.85E-05	1.16E-03
1973-013	Gravel	TroodosN	25	3.74E-05	9.35E-04
1973-013PT2	Gravel	TroodosN	30	6.59E-05	1.98E-03
1973-013PT3	Gravel	TroodosN	25	1.01E-04	2.53E-03
1973-040	Gravel	TroodosN	25	6.45E-05	1.61E-03

Table 25: Location, calibrated elevation and yields of springs used in the regional groundwater flow model (10/1987-09/1997).

Site id	UTM East WGS 84	UTM North WGS 84	Calibrated elevation [m.a.m.s.l.]	Spring yield [l/s] in different scenarios		
				Calibration	Natural	Increased abstraction
1-2-2-20	486200	3865900	1600	1.48	1.54	1.48
1-2-2-21	486100	3865900	1540	1.43	1.45	1.43
1-2-2-25	485600	3865900	1420	1.06	1.09	1.06
1-4-4-40	465000	3863000	735	0.00	0.74	0.00
1-4-4-45	465100	3862000	795	0.00	0.00	0.00
2-9-2-05	476400	3881100	490	0.42	0.51	0.39
3-1-1-10	479800	3873000	695	1.72	1.75	1.71
3-2-1-10	485600	3868500	1285	1.01	1.32	1.00
3-2-1-11	485500	3868900	1220	0.25	0.39	0.22
3-2-1-16	487200	3869900	1210	1.13	1.61	1.03
3-2-1-17	487200	3869000	1350	0.13	0.25	0.10
3-3-1-20	489000	3867000	1420	5.62	5.66	5.62
3-3-1-29	487900	3868200	1460	1.15	1.19	1.15
3-3-1-30	487800	3868400	1380	2.47	2.50	2.47
3-3-1-60	489200	3870100	975	0.29	0.37	0.27
3-3-1-80	489800	3870200	855	5.78	5.80	5.78
3-3-4-85	489300	3882300	195	0.37	4.35	0.00
3-3-4-90	489400	3883500	175	0.56	3.88	0.00
3-4-2-30	493600	3877800	390	0.23	1.13	0.02
3-7-3-10	512500	3863200	930	1.34	1.75	1.26
3-7-3-85	517300	3874500	460	0.22	1.33	0.00
8-7-3-50	532800	3862600	200	0.12	0.84	0.00
9-4-3-15	499200	3848300	320	0.00	0.00	0.00
9-6-1-30	487600	3862300	1300	5.09	5.51	5.02
9-6-3-10	489400	3865200	1630	0.93	1.44	0.87
9-6-3-11	489500	3864600	1560	2.52	2.68	0.96
9-6-3-12	489600	3864300	1580	0.98	1.12	0.96
9-6-3-48	494300	3862100	820	6.98	7.44	6.89
9-6-3-50	491300	3861800	1120	0.75	1.04	0.68
9-6-4-15	491000	3854900	510	2.53	2.58	2.52
9-9-9-2	528200	3858250	445	0.01	0.47	0.00
9-9-9-3	532000	3864700	225	0.07	0.96	0.00
9-9-9-4	542180	3859910	170	0.55	1.80	0.26
9-9-9-5	542420	3859650	165	0.17	1.38	0.00

Table 26: Observation points with observed and computed groundwater heads used for the calibration of the regional groundwater flow model.

site id	UTM East WGS 84	UTM North	elevation [m.a.m.s.l.]	observed head [m.a.m.s.l.]	computed head [m.a.m.s.l.]	head diff. [m]
1987/034	537822	3859861	334	309	267.2498	-41.7502
1987/042	498657	3877281	608	543	503.1375	-39.8625
1987/042	498657	3877281	608	543	503.1375	-39.8625
1987/065	475232	3876261	740	693	766.9323	73.9323
1987/084	526542	3856221	380	373	401.5146	28.5146
1987/086	498192	3870821	850	809	851.2712	42.2712
1987/118	517322	3876061	422	388	395.6129	7.6129
1987/119	522132	3875986	394	381	367.9023	-13.0977
1987/137	497507	3855551	468	455	470.1993	15.1993
1987/140	485232	3868336	1317	1236	1279.975	43.975
1987/140	485232	3868336	1317	1236	1279.975	43.975
1987/160	495132	3852991	533	518	519.1694	1.1694
1988/002	467742	3865031	740	700	696.9504	-3.0496
1988/031	457012	3888141	92	63	43.53666	-19.46334
1988/040	508322	3877381	466	448	415.3811	-32.6189
1988/055	531377	3873201	298	296	285.4492	-10.5508
1988/057	532902	3863871	283	280	250.8831	-29.1169
1988/063	541372	3857606	180	164	163.7106	-0.2894
1988/069	540522	3871201	200	186	215.9114	29.9114
1988/079	507777	3864241	1065	1035	972.576	-62.424
1988/080	542412	3855811	133	107	134.1585	27.1585
1988/087	476222	3877811	683	666	686.4464	20.4464
1988/089	499977	3866226	1260	1205	1156.901	-48.099
1988/090	540572	3856986	161	144	158.0035	14.0035
1988/105	513852	3861681	1070	1061	1052.223	-8.777
1988/106	514217	3879126	359	330	296.7601	-33.2399
1988/119	535737	3875031	240	225	240.7311	15.7311
1988/161	514392	3879486	360	332	296.5084	-35.4916
1988/164	508932	3853681	640	594	521.397	-72.603
1989/010	521142	3860711	795	776	726.9731	-49.0269
1989/016B	516957	3879306	363	267	298.3379	31.3379
1989/016B	516957	3879306	363	267	298.3379	31.3379
1989/018	502552	3884561	215	168	213.3201	45.3201
1989/020	515172	3852911	595	589	572.3745	-16.6255
1989/058	499112	3883881	202	187	167.6019	-19.3981
1989/060	500892	3877066	460	430	421.1503	-8.8497
1989/069	499302	3869326	1125	1121	1116.213	-4.787
1989/243	496222	3861021	892	851	852.5643	1.5643
1989/259	503072	3866106	1100	1080	1049.862	-30.138
1989/260	516112	3879536	345	266	299.0063	33.0063
1989/260	516112	3879536	345	266	299.0063	33.0063
1989/271	498242	3884506	186	168	154.7073	-13.2927
1989/281	530747	3866386	360	321	353.0123	32.0123
1990/003	513197	3852101	500	486	453.0654	-32.9346
1990/010	509892	3880121	360	321	313.627	-7.373
1990/015	529817	3869336	360	352	355.5615	3.5615
1990/015	529817	3869336	360	352	355.5615	3.5615
1990/041	541432	3866621	200	197	186.4274	-10.5726
1990/045	542532	3866911	180	175	174.4085	-0.5915
1990/084	455422	3871881	580	542	476.4216	-65.5784
1990/085	480512	3864721	741	681	755.0726	74.0726
1990/093	518872	3875946	400	386	357.3786	-28.6214

site id	UTM East WGS 84	UTM North	elevation [m.a.m.s.l.]	observed head [m.a.m.s.l.]	computed head [m.a.m.s.l.]	head diff. [m]
1990/110	502232	3867111	987	920	985.6661	65.6661
1990/111	455422	3872071	574	538	473.3757	-64.6243
1990/112	522422	3873961	420	420	418.7242	-1.2758
1990/132	485142	3861651	938	920	958.752	38.752
1990/139	510382	3856151	424	369	384.4903	15.4903
1991/005	510942	3856426	440	392	422.955	30.955
1991/040	489712	3876316	480	453	464.946	11.946
1991/048	535202	3871401	280	268	280.9387	12.9387
1991/055	534792	3871111	288	262	277.6273	15.6273
1991/060	485942	3855401	882	846	862.7763	16.7763
1991/082	537462	3858771	239	191	221.9882	30.9882
1991/094	510827	3871631	680	614	532.1509	-81.8491
1991/094	510827	3871631	680	614	532.1509	-81.8491
1991/105	538322	3859571	370	279	253.923	-25.077
1991/105	538322	3859571	370	279	253.923	-25.077
1991/111	498922	3869146	1232	1181	1132.99	-48.01
1991/114	531057	3873001	281	272	298.5351	26.5351
1991/116	509752	3854236	508	426	443.5117	17.5117
1991/123	537852	3858621	251	224	210.5835	-13.4165
1991/133	485127	3873156	748	716	765.7637	49.7637
1991/141	539802	3857571	264	184	176.5105	-7.4895
1991/154	538542	3858711	276	195	217.2697	22.2697
1992/006	509882	3856701	513	475	453.1261	-21.8739
1992/007	540122	3858281	280	243	196.1202	-46.8798
1992/020	480442	3866226	882	833	793.5322	-39.4678
1992/032	511552	3868491	616	616	626.9122	10.9122
1992/043	508002	3842476	28	10	39.13373	29.13373
1992/059	486872	3860221	1017	994	1041.702	47.702
1992/063	499097	3862761	820	802	837.4604	35.4604
1992/076	498782	3862331	847	808	837.8705	29.8705
1992/090	490887	3873701	611	567	595.2429	28.2429
1992/091	493707	3866221	1142	1109	1162.23	53.23
1992/093	483622	3864421	1050	1003	1055.486	52.486
1992/V01	490532	3880286	345	335	292.6134	-42.3866
1993/018	500282	3854251	649	569	575.7549	6.7549
1993/018	500282	3854251	649	569	575.7549	6.7549
1993/027	456272	3874621	440	401	375.2341	-25.7659
1993/033	504992	3854746	760	710	643.9891	-66.0109
1993/035	503002	3855111	755	714	718.7786	4.7786
1993/039	454872	3873771	362	313	387.1359	74.1359
1993/050	493222	3860781	797	770	814.4183	44.4183
1993/053	490432	3881166	313	307	263.0523	-43.9477
1993/063	499762	3862451	925	924	865.3883	-58.6117
1993/079	502662	3867361	980	952	953.3066	1.3066
1993/082	500322	3876691	505	505	459.9604	-45.0396
1994/027	486632	3856941	960	811	881.7672	70.7672
1994/032	486962	3856371	830	791	841.0689	50.0689
1994/057	485412	3861631	955	955	999.0641	44.0641
1994/062	531777	3868456	380	368	328.7096	-39.2904
1994/V08	502712	3884431	220	162	215.6058	53.6058
1994/V26	489042	3871956	880	833	839.8514	6.8514
1995/041	490562	3860621	1039	1008	1016.418	8.418
1995/050	523322	3865871	589	554	583.4429	29.4429
1995/052	522727	3866196	680	628	602.1934	-25.8066

site id	UTM East WGS 84	UTM North	elevation [m.a.m.s.l.]	observed head [m.a.m.s.l.]	computed head [m.a.m.s.l.]	head diff. [m]
1995/054	495512	3869461	1100	1088	1065.857	-22.143
1995/057	497172	3870741	917	890	911.4265	21.4265
1995/060	501382	3869821	878	809	882.3416	73.3416
1995/062	497282	3871221	891	889	871.066	-17.934
1995/064	483942	3869651	1126	1050	1057.03	7.03
1995/065	461742	3864641	360	351	368.8086	17.8086
1995/065	461742	3864641	360	351	368.8086	17.8086
1996/004	522952	3872181	500	468	477.1254	9.1254
1996/006	510107	3864476	800	748	795.6323	47.6323
1996/017	518182	3873351	505	498	520.413	22.413
1996/030	513462	3876711	440	410	433.0426	23.0426
1996/039	519472	3880021	300	255	317.9847	62.9847
1996/058	501032	3864381	1100	1088	1070.248	-17.752
1996/084	482912	3867871	1151	1116	1117.593	1.593
1996/085	498112	3863516	1040	993	986.5395	-6.4605
1996/086	508072	3841966	28	5	30.55989	25.55989
1996/087	518322	3877956	360	330	333.1766	3.1766
1996/088	481472	3866101	821	791	837.8677	46.8677
1996/089	489052	3871531	849	796	853.413	57.413
1996/098	516982	3878401	368	352	315.8532	-36.1468
1996/V02	452042	3872921	192	113	133.6955	20.6955
1996/V02	452042	3872921	192	113	133.6955	20.6955
1997/006	480822	3864131	778	739	771.1245	32.1245
1997/013	529472	3875001	320	312	320.6961	8.6961
1997/024	517302	3854871	360	344	364.323	20.323
1997/028	513582	3852231	540	390	472.7217	82.7217
1997/029	510222	3854861	372	345	387.7161	42.7161
1997/036	543022	3866971	180	149	165.2331	16.2331
1997/041	484092	3867081	1240	1200	1193.733	-6.267
1997/046	494492	3863576	946	935	961.9056	26.9056
1997/050	496612	3868111	1320	1185	1243.321	58.321
1997/056	495652	3867681	1219	1181	1223.676	42.676
1997/064	515342	3872131	607	600	550.4448	-49.5552
1997/065	502072	3866871	1002	941	997.0999	56.0999
1997/067	499392	3864321	1010	918	958.5752	40.5752
1997/067	499392	3864321	1010	918	958.5752	40.5752
1997/070	499382	3865391	1060	1043	1058.271	15.271
1997/071	531562	3874111	280	269	279.2441	10.2441
1997/076	511102	3855111	380	357	388.2882	31.2882
1997/081	475972	3876651	789	753	731.7085	-21.2915
1997/085	508432	3873961	501	494	523.7912	29.7912
1997/V01	501287	3864856	1151	1147	1103.153	-43.847
1997/V02	461942	3865021	374	362	374.479	12.479
1997/V08	454312	3880221	126	124	45.52694	-78.47306

Appendix C: Pilot catchment and well region results

Table 27: Modbil water balance of the Diarizos pilot catchment (Area: 129 km²; 10/1987-09/1997). Secondary Evapotranspiration (Sec. ET) is described in detail in Chapter 4.1.3.2.

	mm/a	m³/s
Precipitation	688	2.814
Groundwater Recharge	172	0.704
Interflow	51	0.209
Actual ET	532	2.176
Sec. ET total	63	0.258
Sec. ET irrigated areas/ settlements	4	0.017
Sec. ET moist areas/waters	59	0.240
Total Runoff modelled	160	0.654
Total Runoff gauged	166	0.679

Table 28: Modflow flow budget of the Diarizos pilot catchment (Area: 129 km²; 10/1987-09/1997).

	In		Out	
	mm/a	m³/s	mm/a	m³/s
Constant heads	0	0.000	0	0.000
Drains	0	0.000	-1	-0.004
General heads	0	0.000	0	0.000
Rivers	5	0.021	-112	-0.459
Wells	0	0.000	-11	-0.044
Recharge	171	0.701	0	0.000
Evapotranspiration	0	0.000	-57	-0.233
Total Source/Sink	177	0.723	-181	-0.739
Zone Flow				
Top	0	0.000	0	0.000
Bottom	0	0.000	0	0.000
Left	4	0.015	-1	-0.004
Right	5	0.019	-1	-0.006
Front	3	0.012	-3	-0.012
Back	1	0.006	-3	-0.013
Total Zone Flow	13	0.052	-9	-0.035
Total Flow	189	0.774	-189	-0.774

Table 29: Modbil water balance of the Limnatis pilot catchment (Area: 112.5 km²; 10/1987-09/1997). Secondary Evapotranspiration (Sec. ET) is described in detail in Chapter 4.1.3.2. *) Does not include estimated transmission losses of 10 to 15 mm/a.

	mm/a	m³/s
Precipitation	653	2.329
Groundwater Recharge	165	0.589
Interflow	44	0.157
Actual ET	545	1.944
Sec. ET	98	0.350
Sec. ET irrigated areas/settlements	26	0.091
Sec. ET moist areas/waters	74	0.262
Total Runoff modelled	111	0.396
Total Runoff gauged*	115	0.410

Table 30: Modflow flow budget of the Limnatis pilot catchment (Area: 112.5 km²; 10/1987-09/1997).

	In		Out	
	mm/a	m³/s	mm/a	m³/s
Constant heads	0	0.000	0	0.000
Drains	0	0.000	0	0.000
General heads	0	0.000	0	0.000
Rivers	8	0.028	-79	-0.283
Wells	0	0.000	-27	-0.097
Recharge	167	0.595	0	0.000
Evapotranspiration	0	0.000	-74	-0.265
Total Source/Sink	175	0.623	-181	-0.645
Zone Flow				
Top	0	0.000	0	0.000
Bottom	0	0.000	0	0.000
Left	3	0.010	-1	-0.005
Right	6	0.021	-1	-0.005
Front	0	0.001	-3	-0.012
Back	4	0.014	-1	-0.002
Total Zone Flow	13	0.046	-7	-0.024
Total Flow	188	0.670	-188	-0.670

Table 31: Modbil water balance of the Pyrgos pilot catchment (Area: 38.4 km²; 10/1987-09/1997). Secondary Evapotranspiration (Sec. ET) is described in detail in Chapter 4.1.3.2.

	mm/a	m³/s
Precipitation	594	0.723
Groundwater Recharge	138	0.168
Interflow	27	0.033
Actual ET	471	0.574
Sec. ET	38	0.046
Sec. ET irrigated areas/settlements	0	0.000
Sec. ET moist areas/waters	38	0.046
Total Runoff modelled	127	0.155
Total Runoff gauged	130	0.158

Table 32: Modflow flow budget of the Pyrgos pilot catchment (Area: 38.4 km²; 10/1987-09/1997).

	In		Out	
	mm/a	m³/s	mm/a	m³/s
Constant heads	0	0.000	0	0.000
Drains	0	0.000	0	0.000
General heads	0	0.000	0	0.000
Rivers	4	0.005	-103	-0.126
Wells	0	0.000	0	-0.001
Recharge	137	0.167	0	0.000
Evapotranspiration	0	0.000	-40	-0.049
Total Source/Sink	141	0.172	-144	-0.175
Zone Flow				
Top	0	0.000	0	0.000
Bottom	0	0.000	0	0.000
Left	7	0.008	-1	-0.001
Right	0	0.000	-8	-0.010
Front	5	0.006	-1	-0.002
Back	4	0.004	-3	-0.003
Total Zone Flow	16	0.019	-13	-0.016
Total Flow	157	0.191	-157	-0.191

Table 33: Modbil water balance of the Kargotis pilot catchment (Area: 86 km²; 10/1987-09/1997). Secondary Evapotranspiration (Sec. ET) is described in detail in Chapter 4.1.3.2.

	mm/a	m³/s
Precipitation	621	1.693
Groundwater Recharge	139	0.379
Interflow	59	0.161
Actual ET	535	1.459
Sec. ET	108	0.295
Sec. ET irrigated areas/settlements	49	0.133
Sec. ET moist areas/waters	60	0.163
Total Runoff modelled	90	0.245
Total Runoff gauged	80	0.218

Table 34: Modflow flow budget of the Kargotis pilot catchment (Area: 86 km²; 10/1987-09/1997).

	IN		OUT	
	mm/a	m³/s	mm/a	m³/s
Constant heads	0	0.000	0	0.000
Drains	0	0.000	-6	-0.016
General heads	0	0.000	0	0.000
Rivers	10	0.027	-64	-0.175
Wells	0	0.000	-15	-0.041
Recharge	139	0.378	0	0.000
Evapotranspiration	0	0.000	-60	-0.163
Total Source/Sink	149	0.405	-145	-0.395
Zone Flow				
Top	0	0.000	0	0.000
Bottom	0	0.000	0	0.000
Left	7	0.020	-5	-0.013
Right	6	0.016	-2	-0.007
Front	5	0.015	-1	-0.001
Back	0	0.001	-15	-0.040
Total Zone Flow	19	0.051	-22	-0.061
Total Flow	167	0.456	-167	-0.456

Table 35: Modbil water balance of the well-region Troodos NW (Area: 567 km²; 10/1987-09/1997). Secondary Evapotranspiration (Sec. ET) is described in detail in Chapter 4.1.3.2.

	mm/a	m³/s
Precipitation	519	9.331
Groundwater Recharge	113	2.032
Interflow	18	0.324
Actual ET	455	8.181
Sec. ET	63	1.133
Sec. ET irrigated areas/settlements	11	0.198
Sec. ET moist areas/waters	52	0.935
Total Runoff modelled	68	1.223

Table 36: Modflow flow budget of the well-region Troodos NW (Area: 567 km²; 10/1987-09/1997).

	In		Out	
	mm/a	m³/s	mm/a	m³/s
Constant heads	2	0.028	-13	-0.237
Drains	0	0.000	-5	-0.086
General heads	0	0.000	0	0.000
Rivers	20	0.364	-62	-1.118
Wells	0	0.000	-10	-0.179
Recharge	112	2.021	0	0.000
Evapotranspiration	0	0.000	-49	-0.880
Total Source/Sink	134	2.413	-139	-2.500
Zone Flow				
Top	0	0.000	0	0.000
Bottom	0	0.000	0	0.000
Left	0	0.008	0	-0.002
Right	2	0.043	0	-0.005
Front	3	0.061	0	-0.002
Back	0	0.000	-1	-0.016
Total Zone Flow	6	0.112	-1	-0.025
Total Flow	140	2.525	-140	-2.525

Table 37: Modbil water balance of the well-region Troodos SW (Area: 407 km²; 10/1987-09/1997). Secondary Evapotranspiration (Sec. ET) is described in detail in Chapter 4.1.3.2.

	mm/a	m³/s
Precipitation	633	8.169
Groundwater Recharge	154	1.988
Interflow	41	0.529
Actual ET	490	6.324
Sec. ET	47	0.607
Sec. ET irrigated areas/settlements	6	0.077
Sec. ET moist areas/waters	41	0.529
Total Runoff modelled	148	1.910

Table 38: Modflow flow budget of the well-region Troodos SW (Area: 407 km²; 10/1987-09/1997).

	In		Out	
	mm/a	m³/s	mm/a	m³/s
Constant heads	0	0.000	0	0.000
Drains	0	0.000	0	-0.004
General heads	0	0.000	0	0.000
Rivers	5	0.060	-109	-1.407
Wells	0	0.000	-6	-0.076
Recharge	155	1.999	0	0.000
Evapotranspiration	0	0.000	-40	-0.520
Total Source/Sink	160	2.059	-156	-2.007
Zone Flow				
Top	0	0.000	0	0.000
Bottom	0	0.000	0	0.000
Left	0	0.004	-2	-0.030
Right	3	0.037	-1	-0.009
Front	1	0.017	-1	-0.014
Back	0	0.001	-4	-0.057
Total Zone Flow	5	0.059	-9	-0.110
Total Flow	164	2.118	-164	-2.118

Table 39: Modbil water balance of the well-region Troodos Central (Area: 1036 km²; 10/1987-09/1997). Secondary Evapotranspiration (Sec. ET) is described in detail in Chapter 4.1.3.2.

	mm/a	m³/s
Precipitation	540	17.740
Groundwater Recharge	124	4.074
Interflow	35	1.150
Actual ET	462	15.177
Sec. ET	76	2.497
Sec. ET irrigated areas/settlements	22	0.723
Sec. ET moist areas/waters	54	1.774
Total Runoff modelled	83	2.727

Table 40: Modflow flow budget of the well-region Troodos Central (Area: 1036 km²; 10/1987-09/1997).

	In		Out	
	mm/a	m³/s	mm/a	m³/s
Constant heads	0	0.000	-1	-0.023
Drains	0	0.000	-1	-0.041
General heads	0	0.000	0	0.000
Rivers	11	0.368	-59	-1.951
Wells	0	0.000	-22	-0.709
Recharge	125	4.110	0	0.000
Evapotranspiration	0	0.000	-52	-1.706
Total Source/Sink	136	4.477	-135	-4.429
Zone Flow				
Top	0	0.000	0	0.000
Bottom	0	0.000	0	0.000
Left	0	0.006	-2	-0.053
Right	1	0.025	-1	-0.027
Front	1	0.024	-1	-0.020
Back	0	0.010	0	-0.013
Total Zone Flow	2	0.065	-3	-0.113
Total Flow	138	4.542	-138	-4.542

Table 41: Modbil water balance of the well-region Troodos NE (Area: 433 km²; 10/1987-09/1997). Secondary Evapotranspiration (Sec. ET) is described in detail in Chapter 4.1.3.2.

	mm/a	m³/s
Precipitation	436	5.986
Groundwater Recharge	82	1.126
Interflow	16	0.220
Actual ET	420	5.767
Sec. ET	80	1.098
Sec. ET irrigated areas/settlements	22	0.302
Sec. ET moist areas/waters	58	0.796
Total Runoff modelled	18	0.247

Table 42: Modflow flow budget of the well-region Troodos NE (Area: 433 km²; 10/1987-09/1997).

	In		Out	
	mm/a	m³/s	mm/a	m³/s
Constant heads	0	0.000	0	0.000
Drains	0	0.000	-6	-0.016
General heads	0	0.000	0	0.000
Rivers	10	0.027	-64	-0.175
Wells	0	0.000	-15	-0.041
Recharge	139	0.378	0	0.000
Evapotranspiration	0	0.000	-60	-0.163
Total Source/Sink	149	0.405	-145	-0.395
Zone Flow				
Top	0	0.000	0	0.000
Bottom	0	0.000	0	0.000
Left	7	0.020	-5	-0.013
Right	6	0.016	-2	-0.007
Front	5	0.015	-1	-0.001
Back	0	0.001	-15	-0.040
Total Zone Flow	19	0.051	-22	-0.061
Total Flow	167	0.456	-167	-0.456

Table 43: Modbil water balance of the well-region Troodos SE (Area: 481 km²; 10/1987-09/1997). Secondary Evapotranspiration (Sec.ET) is described in detail in Chapter 4.1.3.2.

	mm/a	m³/s
Precipitation	534	8.145
Groundwater Recharge	103	1.571
Interflow	34	0.519
Actual ET	465	7.092
Sec. ET	69	1.052
Sec. ET irrigated areas/settlements	20	0.305
Sec. ET moist areas/waters	49	0.747
Total Runoff modelled	68	1.037

Table 44: Modflow flow budget of the well-region Troodos SE (Area: 481 km²; 10/1987-09/1997).

	In		Out	
	mm/a	m³/s	mm/a	m³/s
Constant heads	0	0.000	-3	-0.051
Drains	0	0.000	-7	-0.105
General heads	1	0.017	0	-0.005
Rivers	8	0.117	-45	-0.681
Wells	0	0.000	-18	-0.279
Recharge	106	1.610	0	0.000
Evapotranspiration	0	0.000	-41	-0.622
Total Source/Sink	114	1.744	-114	-1.743
Zone Flow				
Top	0	0.000	0	0.000
Bottom	0	0.000	0	0.000
Left	0	0.005	-2	-0.024
Right	0	0.002	0	-0.007
Front	0	0.000	0	-0.001
Back	2	0.026	0	-0.003
Total Zone Flow	2	0.032	-2	-0.035
Total Flow	116	1.776	-117	-1.778